ENGINEERING A THREE-DIMENSIONAL CULTURE SYSTEM FOR THE DIRECTED DIFFERENTIATION OF PLURIPOTENT STEM CELLS TOWARD A HEPATOCYTE-LIKE CELL FATE

A DISSERTATION

SUBMITTED TO THE FACULTY OF THE GRADUATE SCHOOL

OF THE UNIVERSITY OF MINNESOTA

BY

Derek Jason Owens

IN PARTIAL FULFILLMENT OF THE REQUIREMENTS

FOR THE DEGREE OF

DOCTOR OF PHILOSOPHY

Advisers: Wei-Shou Hu and Catherine Verfaillie

November 2012

© Derek Jason Owens 2012

ACKNOWLEDGEMENTS

My graduate career, which has culminated in the preparation of this thesis, has been anything but an individual effort. I cannot possibly thank all the folks who have helped me over the past six years, but I shall try.

First and foremost, I would like to extend the utmost gratitude to my advisers, Dr. Wei-Shou Hu and Dr. Catherine Verfaillie, for their intellectual and personal guidance, support, and encouragement throughout my graduate career. While it has been an honor and privilege to work with two of the most well-respected researchers in their fields, their collaborative approach to scientific inquiry and the freedom with which our groups share ideas and information has been nothing short of inspiring. I will be forever grateful to my advisers.

I would also like to thank the other members of my thesis committee for their patience and valuable feedback. They are Dr. Efie Kokkoli and Dr. Robert Tranquillo of the Department of Chemical Engineering and Materials Science and Dr. Clifford Steer of the Department of Medicine.

I would like to extend special thanks to current and former members of the Hu group: Kartik Subramanian, Yonsil Park, Ravali Raju, Shikha Sharma, Andrew Yongky, Dong-Seong Cho, David Chau, Siguang Sui, Huong Le, Bhanu Chandra Mulukutla, Salim Charaniya, Kathryn Johnson, Anne Kantardjieff, Marlene Castro, Nitya Jacob, Nandita Vishwanathan, Anushree Chatterjee, Katie Wlaschin, Karthik Jayapal, Fernando Ulloa-Montoya, CM Cameron, and our wonderful undergraduate for the past two years Liang Zhang. It has been a pleasure to be a member of such a diverse and highly regarded group, and each of you have been instrumental to my ability to achieve success and work through adversity. More than that, many of you have also become fantastic friends.

The Stem Cell Institute provides a collaborative atmosphere in which groups from multiple disciplines with a common thread of stem cell research share resources, ideas, and countless hours together. The following members of the Stem Cell Institute or other

affiliated groups helped me immensely throughout my years, enabling success at every turn: Jesse Browers, Beth Lindborgh, Lucas Greder, Ersine Akinci, Natarajan Bhanu, Dr. Susan Keirstead, Dr. James Dutton, Kelsey Mosser, Windy Torgerud, Kristin Voltzke, Saswati Mahapatra, Dr. Nobuaki Kikyo, and any others whom I may have left off this list. I would also like to thank members of the Verfaillie group in Belgium with whom I have collaborated or shared ideas: Phillip Roelandt, Pau Sancho, Martin Geraerts, and Abhishek Sohni.

I would also like to extend special gratitude to the many wonderful friends that have supported and encouraged me throughout the past six years: Mark Huberty, Gopal Chakrabarti, Grayce Theryo, Raghuram Thiagarajan, Jeremy Wright, Mary Zatochill, Erin Maddy, Jeffery Sugandi, Nicholas Menth, Dawud Tan, Shawn Dodds, Brian Habersberger, Jaime Medina, Derek Schnell, Andrew Payne, Rachel Koenig, Kathleen Crawford, the numerous close friends already mentioned in the paragraphs above, and countless others to whom I apologize for leaving out.

Finally, and most importantly, I would like to thank my family for their unconditional support, unyielding belief in me, undying love, and at times guidance. To my beautiful wife Kathy, who postponed the start of her medical career and moved to Minnesota so we could build our lives together, I thank you a thousand times over; you have been the foundation of my strength and my best friend and companion. To my parents, Sandra and Derek Owens, who have supported me and guided me with nearly daily phone conversations, I thank you for "raising me right" in an environment that fostered academic inquiry and a culture of learning, in addition to always being willing to help Kathy and me in any way possible at any time. I owe my successes and the life that Kathy and I have been able to build in many ways to your love, support, and the values you instilled in me from an early age. Lastly, to my brother Joel, who is currently pursuing his doctorate in accounting at the University of South Carolina, I thank you for being a good brother, brother-in-law to Kathy, and son to our parents. You have served as a source of encouragement, advice, and often reason, and have been instrumental in all my successes.

DEDICATION

To my wife Kathy and my parents Sandra and Derek

ABSTRACT

Because stem cells have the ability to self-renew and differentiate into more specialized cell types, they hold enormous potential in the fields of regenerative and personalized medicine as well as providing a model system for studying development *in vitro*. Stem cells with the capacity to differentiate to hepatocytes, the functional cells of the liver, have potential applications in the pharmaceutical industry in high-throughput drug toxicity screening and in clinical settings in bioartificial liver devices or as candidates for transplantation to treat end-stage liver disease. However, these applications rely on the ability to generate and differentiate the stem cells to functionally mature hepatocytes in a robust and reproducible manner.

We have recently optimized a multistage directed differentiation protocol for guiding human embryonic stem (hES) cells and rat multipotent adult progenitor cells (rMAPCs), among other stem cell types, toward a hepatic fate. We also recently showed that rMAPCs, which are isolated from the bone marrow of post-natal rats and exhibit the ability to self-renew and differentiate to all three lineages, can be cultured as three-dimensional aggregates without losing their potency or self-renewal capacity. In this study, we report three-dimensional aggregate-based culture systems that enhance the differentiation of rMAPCs and hES cells to hepatocyte-like cells.

rMAPCs were allowed to self-assemble into undifferentiated aggregates before being differentiated via the four-step directed differentiation protocol. Compared to adherent monolayer cultures, differentiation as aggregates resulted in significantly higher expression of liver-specific transcripts, including *albumin*, and increased secretion of albumin and urea. The differentiated cell aggregates also demonstrated functional activities of primary hepatocytes, as demonstrated by pentoxyresorufin O-dealkylation (PROD) and ethoxyresorufin O-dealkylation (EROD), and ultrastructural features of hepatocytes by electron microscopy.

A similar three-dimensional culture system likewise enhanced the differentiation of hES cells. HSF6 cells differentiated as a monolayer culture were dissociated and allowed to self-assemble into three-dimensional spheroids in an extended differentiation culture. Compared cells maintained in the monolayer culture, cells within the spheroids exhibited significantly higher expression levels of liver-enriched transcripts and proteins, including Albuming, PEPCK, and ASGPR-1. Cells in the spheroids demonstrated hepatic functions EROD, PROD, and biliary accumulation of fluorescein diacetate metabolite and ultrastructural characteristics of hepatocytes by electron microscopy.

Finally, whole-genome transcriptome analysis was performed to investigate the expression profile of liver-specific sets of genes, including the hepatocyte nuclear factors (HNFs), cytochrome P450s (CYP450s), and UDP-glucuronosyltransferases (UGTs), during differentiation. Cells in the spheroid were shown to have overall increased expression levels of most of the genes in these families, although the expression levels were still lower than in adult liver. The transcriptome analysis was also used to identify genes that change during establishment of the spheroid culture that may play a role in the enhanced differentiation status of the cells; multiple members of the aldo/keto reductase (AKR) and metallothionein (MT) families were found to have much higher expression in spheroids than in monolayer culture.

These studies demonstrate the ability of three-dimensional, scalable culture systems to enhance the differentiation of pluripotent stem cells toward a hepatic fate and to maintain the differentiated phenotype for extended culture. With modifications to further enhance the maturity of stem cell-derived hepatocyte-like cells, these systems may facilitate the translation of stem cell generated tissues to technology.

TABLE OF CONTENTS

TABLE OF FIGURES

TABLE OF ABBREVIATIONS

ADH	Alcohol dehydrogenase
AFP	Alpha-fetoprotein
AKR	Aldo/keto reductase
AL	Adult liver sample
Alb	Albumin
ALDH	Aldehyde dehydrogenase
AP	Alkaline phosphatase
AP	Anterior-posterior
Arg	Arginase
ASC	Adult stem cell
ASGPR	Asialoglycoprotein receptor
BEC	Biliary epithelial cell
bFGF	Basic FGF
βME	β-mercaptoethanol
BMGC	Biomedical Genomics Center
BMP	Bone morphogenetic protein
BMPR	BMP receptor
BNF	β-Naphthoflavone
BSA	Bovine serum albumin
cDNA	Complementary DNA
CK	Cytokeratin
cRNA	Complementary RNA
Ct	Threshold cycle number
CX	Connexin
CYC	Cyclopamine
CYP450	Cytochrome P450
D0	Day 0 undifferentiated hES sample

D20	Day 20 monolayer sample
D32	Day 32 spheroid sample
DMEM	Dulbecco's modified eagle medium
DMEM-LG	DMEM low glucose
DMSO	Dimethyl sulfoxide
DNA	Deoxyribonucleic acid
EB	Embryoid body
EDTA	Ethylenediaminetetraacetic acid
EGF	Epidermal growth factor
ER	Ethoxyresorufin
ERK	Extracellular signal-regulated protein kinase
EROD	Ethoxyresorufin O-dealkylation
ESC	Embryonic stem cell
ExE	Extra-embryonic ectoderm
FACS	Fluorescence activated cell sorting
Fah	Fumarylacetoacetate hydrolase
FBS	Fetal bovine serum
FCS	Fetal calf serum
FDA	Fluorescein diacetate
FGF	Fibroblast growth factor
Flk-1	Vascular endothelial growth factor receptor 2
FMO	Flavin-containing monooxygenase
FN	Fibronectin
GFP	Green fluorescent protein
Gsc	Goosecoid
GSK	Glycogen-synthase kinase
GST	Glutathione-S-transferase
HGF	Hepatocyte growth factor

HNF	Hepatocyte nuclear factor
HSC	Hematopoietic stem cell
ICM	Inner cell mass
Id	Inhibitors of differentiation
IGF	Insulin-like growth factor
IHBD	Intrahepatic bile duct
iPS	Induced pluripotent stem
ITS	Insulin, transferrin, selenium
JAK	Nonreceptor tyrosine kinase Janus
LA-BSA	Linoleic acid - BSA
LIF	Leukemia inhibitory factor
LIFR	LIF receptor
MAO	Monoamine oxidase
MAPC	Multipotent adult progenitor cell
MAPK	Mitogen-activated protein kinase
MEF	Mouse embryonic fibroblast
MIAMI	Marrow-isolated adult multilineage inducible
mRNA	Messenger RNA
MRPC	Multipotent renal progenitor cell
MSC	Mesenchymal stem cell
MT	Metallothionein
Ngn	Neurogenin
NOD	Non-obese diabetic
NSC	Neural stem cell
OSM	Oncostatin M
Pax	Paired box gene
PB	Phenobarbital
PBS	Phosphate buffered saline

PC	Principle component
PCA	Principle component analysis
PDGF	Platelet-derived growth factor
Pdx	Pancreatic and duodenal homeobox
Pen/Strep	Penicillin / Streptomycin
PEPCK	Phosphoenolpyruvate carboxykinase
PR	Pentoxyresorufin
PRF	Phenol red free
PROD	Pentoxyresorufin O-dealkylation
qRT-PCR	Quantitative real-time polymerase chain reaction
RA	Retinoic acid
RIF	Rifampicin
rMAPC	Rat MAPC
RNA	Ribonucleic acid
scid	Severe combined immunodeficient
Shh	Sonic hedgehog
SMAD	Small mothers against decapentaplegic
SSEA	Stage-specific embryonic antigen
STAT	Signal transducer and activator of transcription
STM	Septum transversum mesenchyme
SZO	Streptozoticin
TGF	Transforming growth factor
TIK	Antiphosphotyrosine immunoreactive kinase
TTR	Transthyretin
UGT	UDP-glucuronosyltransferase
UIC	University Imaging Center
ULA	Ultra low attachment
USSC	Unrestricted somatic stem cell

VE	Visceral endoderm
VEGF	Vascular endothelial growth factor
VSEL	Very small embryonic like
WNT	Wingless type

CHAPTER 1: INTRODUCTION

1.1 Introduction

Advances in biological sciences and medicine have drastically improved life over the past century. Pharmaceuticals, from simple molecules such as penicillin to simple proteins such as insulin to complicated, heavily glycosylated proteins such as erythropoietin, are readily available for treatment of myriad clinical ailments, many of which were characterized by high morbidity in the past half century. Vaccinations against diseases such as polio, influenza, smallpox, and others have virtually eliminated the instances of some of these diseases, including complete eradication of smallpox, a disease with an estimated 50 million cases per year as late as the 1950s (World Health Organization 2001). Combined with advances in surgical techniques and medical specialties allowing physicians to become experts in a small subset of medicine, these advances have culminated in life expectancy nearly doubling in the past century from approximately 47 years in 1900 (Kinsella 1992) to 78.7 years in 2010 (Murphy, Xu et al. 2012).

Many of the advances in pharmaceuticals over the past few decades have been a direct result in the advances of recombinant DNA technology, in which the coding sequence for nearly any protein can be inserted into an appropriate host cell, such as bacteria cells, yeast cells, or mammalian cells, resulting in expression of the protein within the host cell through its native machinery. The recombinant protein is then purified and can be used for myriad applications, such as therapeutics, as exogenous signaling molecules such as cytokines and growth factors, etc. Indeed, the recombinant protein market was expected to have succeeded $50 billion (USD) per year by 2010 (Besley and Pavlou 2005). Although the field of cell culture technology thus far has largely focused on cells as producers of products, a new branch of cell culture technology is on the horizon that has the potential to revolutionize medicine: stem cell technology.

Stem cells are a unique cell type that are characterized by two main features: the ability to self-renew and the ability to differentiate into more specialized cell types (Weissman

2000). Self-renewal refers to the ability of stem cells to proliferate while maintaining their phenotype, specifically in maintaining their ability to self-renew and differentiate. The differentiation potential of a stem cell, which is referred to as its potency, is a description of how many different cell types it can differentiate into. Although the naming conventions are not well-defined, potency generally is described as four classes: unipotent stem cells, which can give rise to only one specialized cell type that is distinct from the stem cell state; multipotent stem cells, which can give rise to at least two but potentially thousands of cell types; pluripotent stem cells, which can give rise to all the cell types of the adult organism from which they are derived; and totipotent stem cells, which can give rise to all the cell types of the adult organism as well as extraembryonic tissue such as the yolk sack. The zygote is virtually the only example of a totipotent stem cell, which has not been established in culture. The quintessential stem cells, embryonic stem cells, are derived from the inner cell mass of the blastocyst and exhibit pluripotency and virtually unlimited self-renewal in culture. A number of less potent stem cell populations have been identified, as stem cell populations of various potency and self-renewal capability apparently reside in nearly every tissue in the adult organism. Stem cells derived from adult tissue are termed adult stem cells and typically exhibit less potency and self-renewal capability as compared to embryonic stem cells. Recently, another classification of stem cells has evolved as researchers have developed the ability to reprogram terminally differentiated somatic cells into pluripotent stem cells by forced expression of certain important transcription factors and culture in appropriate environment; these cells are termed induced pluripotent stem cells (Takahashi and Yamanaka 2006).

The ability of stem cells to self-renew and differentiate to specialized cell types holds vast potential in the field of medicine, and the ability to generate patient-specific induced pluripotent stem cells has made the possibility of individualized medicine seem more attainable. Theoretically, pluripotent stem cells could be used to generate large numbers of any given cell type for transplantation if the signaling pathways are understood well enough to guide the cells through the correct lineage fate determinations. Indeed, when combined with advances in tissue engineering of scaffolds and support matrices, it is not

out of the realm of possibility that stem cells may eventually be capable of generating sections of tissues or organs if given proper cues and patterning. In this study, we focus specifically on the ability of stem cells to differentiate toward hepatocytes, which are the functional cell type of the liver.

The liver is the largest internal organ and the largest gland organ in the body and is responsible for myriad functions including detoxification and drug metabolism, synthesis of proteins, synthesis of chemicals necessary for digestion, plays a major role in metabolism, and generally performs functions necessary for homeostasis. Although the liver displays extraordinary regenerative capacity, a number of diseases are capable of irreversibly damaging the liver to the point where it is unable to maintain function or regenerate. Such diseases, such as cirrhosis of the liver, Hepatitis B, Hepatitis C, and others are described as end stage liver disease or failure and often result in death since the liver plays such crucial roles in homeostasis and in supporting the function of other diseases.

Treatments for end stage liver failure are largely dependent on liver organ transplantation and limited by shortages of donor organs and the cost and complexities associated with the procedure (Seaman 2001; Olsen and Brown 2008). Hepatocyte cell transplantation has proven to be a viable alternative particularly in patients with liver-based congenital and metabolic disorders (Grompe 2001; Horslen, McCowan et al. 2003; Horslen and Fox 2004), although the use of isolated primary hepatocytes is restricted by their scarce availability, limited proliferation and inability to retain viability and function over long periods *ex-vivo*. Thus, enormous interest in stem cell differentiation to hepatocytes has developed over the years, primarily driven by the possible access to a renewable source of cells (Santoro, Mancini et al. 2007; Enns and Millan 2008; Haridass, Narain et al. 2008; Navarro-Alvarez, Soto-Gutierrez et al. 2009; Ogawa and Miyagawa 2009). In addition to cell-based therapies and bioartificial liver devices, stem cell derived hepatocytes may also have applications in modeling human disease and for studying drug toxicity and metabolism (Sartipy, Bjorquist et al. 2007; Dalgetty, Medine et al. 2009; Jensen, Hyllner et al. 2009). Advantages of pluripotent human stem cell-derived

hepatocytes for drug toxicity screening include the virtually unlimited availability of cells derived from particular pluripotent stem cell lines, minimizing donor-donor variability and facilitating high-throughput screening of drug candidates over a period of time, and in obtaining hepatocytes from pluripotent stem cell lines representing myriad genetic backgrounds, allowing screening specific for various disease or other genetics-induced modalities. This transition of stem cell related technology to clinical application is critically dependent on directed and controlled differentiation to functional hepatocytes (Sancho-Bru, Najimi et al. 2009).

1.2 Research Objectives

The goal of this study was to engineer a three-dimensional culture system that enhances the differentiation of rat multipotent adult progenitor cells and human embryonic stem cells to hepatocyte-like cells. This goal consisted of the following individual objectives:

Objective 1: To engineer a three-dimensional culture system for the enhancement of differentiation from rat multipotent adult progenitor cells to a hepatocyte-like cell.

Objective 2: To engineer a three-dimensional culture system for the enhancement of differentiation from human embryonic stem cells to a hepatocyte-like cell and to maintain the differentiated state for extended culture.

Objective 3: To use whole genome expression data to explore the changes in expression of genes in classes relevant to the hepatocyte fate and to discover genes or families of genes as candidates for investigation into the mechanisms of the differentiation enhancement.

1.3 Scope of Thesis

A literature review is given in Chapter 2. The first portion of Chapter 2 gives an overview on the field of stem cells, including the specific unique properties of stem cells, a description of a number of different types of stem cells, and a brief introduction to several

important signaling networks responsible for stem cell self renewal, potency, and differentiation. The second portion of Chapter 2 involves a detailed look at the *in vivo* specification of liver from fertilization of the egg to birth, mostly in the context of mouse development. After a brief introduction to the structure and function of the adult liver, a number of different strategies for generating hepatocyte-like cells either from stem cells or from transdifferentiation of other somatic cells is provided.

Chapter 3 contains a detailed description of the materials and methods used throughout each part of this study. Chapter 4 describes the three-dimensional aggregate culture system established to enhance the differentiation of rMAPC toward the hepatocyte fate and provides a comparison of that enhanced differentiation to the standard monolayer differentiation. Chapter 5 describes the three-dimensional spheroid culture system established to enhance the differentiation of hES cells after twenty days of monolayer differentiation culture and how that system is capable of not only enhancing the differentiation status of the cells but also in maintaining that differentiated state for extended cultures. In Chapter 6, a whole-genome microarray analysis is presented in which a number of gene classes expected to be expressed in hepatocytes are examined for their expression levels and changes of expression levels between the monolayer culture and the enhanced spheroid differentiation culture. Also, other gene families and genes that were identified as potentially important for the observed phenomenon were identified for investigation into the mechanisms governing the differentiation or potentially as targets for increasing the maturity of cells derived from the differentiation assay. Finally, in Chapter 7, a summary of the findings from each research objective is presented, the relevance of this work is discussed, and potential areas for further investigation are discussed.

CHAPTER 2: BACKGROUND

2.1 Overview of Stem Cells

Stem cells are a unique group of cells characterized by their capability to self-renew, to differentiate into more specialized cell types, and to functionally reconstitute tissue *in vivo* (Weissman 2000). Because of these special properties, stem cells lend themselves to a variety of natural research fields and questions. Major focuses of stem cell research include elucidating the mechanisms of regulation for self-renewal and maintenance of differentiation potential, directing differentiation of stem cell populations along defined pathways to generate desired cell types, and using cells derived from stem cell differentiation as *in vitro* models for drug testing, among others. Enhanced knowledge of the mechanisms regulating self-renewal and potency will greatly enhance the ability of scientists to isolate stem cells, identify new and unique stem cell populations, and ultimately better control the stem cell system.

The potential of stem cells to differentiate to various cell types presents major implications for stem cell therapy in a wide array of clinical applications, from treatment of degenerative diseases such as diabetes and liver disease to the regeneration of tissues or cells to replace those damaged in accidents. Theoretically, stem cells with the greatest differentiation potential should be able to generate any tissue or cell type present in the adult organism, thus providing a viable option for any implantation or replacement need. Additionally, different populations of stem cells, although exhibiting similar differentiation potential, may prove better for particular applications than others in terms of efficiency, functional maturity, and ease of manipulation along particular lineages. However, the realization of such clinical applications requires a greatly enhanced knowledge of the process of differentiation toward a mature, specialized cell fate. The advancement of knowledge in the process of differentiation will, in all likelihood, mirror research in the field of developmental biology. Major discoveries in the regulation of development of organisms will allow for a better understanding of the requirements for differentiation of stem cells, while discoveries enhancing differentiation of stem cells can

provide a basis for asking questions about the developmental process. Thus, stem cell research provides a model for studying developmental biology outside of an embryo while also benefiting from the advancement of the developmental field, or in other words, the two fields are mutually beneficial and should advance simultaneously as each fuels the other.

The ability to form mature, specialized cells and tissues *in vitro* will allow not only for therapeutic applications such as implantation, but also pharmaceutical applications such as drug screening. A tissue developed in the lab from stem cells can serve as a disease model in which various drugs can be tested for treatment of that disease. A stem cell-derived tissue can also be used to investigate the toxicity of a drug or how it will interact with various cell types without relying solely on animal models. Thus, stem cells and their differentiated cell types may help to alleviate the ethical issues surrounding animal testing and clinical trials, although it should be noted that stem cell technologies would work along with these practices, not in lieu of them.

Stem cell technology clearly has the opportunity to make an enormous impact on the world, both as a tool for pure research and the advancement of knowledge, and in the pharmaceutical industry as therapeutic applications as well as serving a role in drug screening. However, these lofty expectations for the role of stem cells in the future rely heavily on a much better understanding of the biology regulating stem cells, an understanding that is a prerequisite to controlling stem cell systems tightly enough to realize these applications. In this section, we will review first the special properties of stem cells, the ability to self-renew and the ability to differentiate, that separate them from other cell types. We will also discuss the classification of stem cells based on their origin of isolation, culture, and potency. Finally, we will explore the transcriptional and signaling regulatory networks believed to be involved in maintaining self-renewal and imparting potency (the ability to differentiate) and examine the implications of these networks on inducing normal somatic cells to become stem cells.

2.1.1 Properties of Stem Cells

The requirements for a cell to be designated as a stem cell are generally taken as three functional characteristics: self-renewal, the potential to differentiate to more specialized cell types, and *in vivo* reconstitution of particular tissues. In this section, we will explore the first two properties, focusing on what is currently known about each as well as the likely implications of each property on science and society in the future. However, it should be noted that such a functional definition is vague and actually creates a problem sometimes referred to as the stem cell conundrum: it is impossible to know that a cell is a stem cell until it is no longer a stem cell. In other words, the only way to show a particular cell is a stem cell is to allow it to self-renew, and then to differentiate it to another cell type: by the time it has been proven to be a stem cell, it no longer exists as a stem cell. The best one can do is to establish a stem cell line believed to be homogeneous, demonstrate self-renewal, and then use a portion of the progeny to demonstrate differentiation potential. However, designating the remaining line as a stem cell line requires absolute self-renewal, or assurance that generation after generation of the cell line are identical in phenotype, including differentiation potential.

Currently, there are no defined sets of markers that are unanimously accepted as defining a stem cell or distinguishing stem cell lines from normal somatic cell lines, and there may in fact not be a single, unique stem cell state. Although the existence of such a state is controversial, defining 'stemness' is a major research focus, and as the pathways and networks regulating self-renewal and differentiation potential become better understood, perhaps a set or sets of markers will emerge that are sufficient for designating stem cells. Only then can the definition of stem cells shift from a functional definition, imparting a great deal of uncertainty on the starting cell population of any given experiment, to a more rigorous and quantifiable definition, perhaps allowing a stem cell to be identified *in vitro* with a high level of certainty prior to beginning differentiation. Such rigor in identifying the initial stem cell population will become necessary as stem cell technology develops toward therapeutic applications.

2.1.1.1 Self-Renewal

Self-renewal, or the ability to maintain potency through large numbers of cell divisions, is the first special property defining a stem cell. Normal somatic cells are able to undergo only a very limited number of cell divisions before they enter a state known as senescence, where the cells are no longer able to divide further. Senescence of somatic cells is usually associated with deterioration in the structure and function of the cell, followed ultimately by cell death. Stem cells distinguish themselves from these normal somatic cells partially by the fact that they are able to escape this senescence and continue to divide, with each generation maintaining the same differentiation potential as the parent cells. Although the mechanisms regulating self-renewal remain a subject of heavy investigation, it is believed that activation of an enzyme known as telomerase, which is responsible for maintaining telomere length after DNA replication, may play an important role. Likewise, telomere shortening in the absence of telomerase activity is thought to invoke senescence in normal somatic cells. It should be noted that the activation of telomerase activity is a necessary step in the onset of cancer. Thus, investigations into the mechanisms regulating self-renewal of stem cells may also provide some insight into the mechanisms involved in the onset of cancer and vice-versa. A better understanding of the regulatory networks will also greatly enhance the ability to scale-up stem cell growth conditions to obtain the number of cells necessary for large-scale stem cell applications, such as those previously discussed.

2.1.1.2 Differentiation Potential (Potency)

The second unique property defining a stem cell is its ability to differentiate to more specialized cell types. The differentiation potential of a given cell is termed its potency, which is generally a designation of the number of cell types to which the stem cell may give rise. There are currently four categories of potency: totipotent, pluripotent, multipotent, and unipotent. The designation tititpotent refers to a cell that is capable of differentiating to all cell types found in the embryo as well as extra-embryonic cell types. A zygote, formed from the fusion of a sperm and an egg, as well as the daughter cells

from the first cell divisions of the zygote, are the best examples of totipotent stem cells. The designation of pluripotent refers to a stem cell that is capable of differentiating to all the cell types of all three germ layers. Pluripotent is distinct from totipotent in that the ability to differentiate to extra-embryonic cell types is lost. Embryonic stem cells are the best-characterized examples of pluripotent stem cells. Most stem cells derived from adult tissue are characterized as multipotent or unipotent stem cells. Multipotent stem cells possess the ability to differentiate only to particular closely related cell types and are generally restricted to the tissue from which the stem cell was isolated. For example, neural stem cells (NSCs), which exist in and are isolated from the brain, are capable of giving rise to neurons, astrocytes, and oligodendrocytes, the three main neuronal cell types in the brain (Gage 2000). Similarly, hematopoietic stem cells (HSCs) are isolated from the bone marrow and give rise to all the various blood types. The least potent of categorical stem cells are unipotent stem cells, which give rise only to one particular specialized cell type.

Although these four categories provide the conventional classification of stem cells based on differentiation potential, a number of recent studies suggest that the line between pluripotency and multipotency may not be as distinct as once thought. The term 'plasticity' has recently been used to describe a phenomenon in which adult stem cells have shown the ability to differentiate to lineages outside of their tissue of origin. This plasticity of adult stem cells seems to be contradictory to the established concept of lineage restriction during organogenesis. Indeed, if these more potent adult stem cells exist in adult tissues, as is one possibility, it certainly is in direct contradiction of lineage restriction during organogenesis. One explanation may be that the cells are actually residual pluripotent cells that persisted throughout embryonic development and escaped the lineage restriction at later stages of development. However, the increased potency of an adult stem cell line does not necessarily correlate to the presence of stem cells of equivalent differentiation capability in the tissue from which the lines were derived. In other words, the stem cell may become more potent during the process of isolation and culture, resulting in a pluripotent stem cell that did not exist in that pluripotent state *in vivo*.

Another classification of cells that are often considered in conjunction with stem cells is progenitor cells. A progenitor cell is a cell with differentiation capability, typically either unipotent or multipotent, and with limited self-renewal capability. This limited self-renewal is the principle distinguishing factor between progenitor cells and stem cells. However, the terms "progenitor cells" and "stem cells" are commonly used somewhat interchangeably, and indeed many of the adult stem cell populations identified to date would more appropriately be labeled progenitor cells based on the strict requirement of unlimited self-renewal for a stem cell.

2.1.2 Types of Tissue-Derived Stem Cells

One classification for stem cells is based on their origin, and the majority of stem cells fall into two such groups: embryonic stem cells and adult stem cells. Embryonic stem cells are isolated, as the name implies, from the embryo during early embryonic development. Adult stem cells indicate stem cells that are isolated from any animal after birth and include well-studied examples such as hematopoietic stem cells (HSCs) and mesenchymal stem cells (MSCs), both of which are isolated from bone marrow, and neural stem cells (NSCs) isolated from the brain.

2.1.2.1 Embryonic Stem Cells

Embryonic stem cells (ESCs) are pluripotent stem cells derived from the inner cell mass (ICM) of early embryos at the blastocyst stage of development. Since the ICM is responsible for generation of the adult organism, but not extra-embryonic structures, ESCs retain the ability to differentiate to all tissues of the adult organism. Kaufman et al. derived the first ESCs from mouse embryos in 1981, while human ESCs were not successfully derived from human blastocysts until 1998 by Thomson et al. (Evans and Kaufman 1981; Thomson, Itskovitz-Eldor et al. 1998). Besides self-renewal and pluripotency, another characteristic of mouse ESCs is the ability to re-enter embryogenesis after injection into a pre-implantation embryo and functionally contribute to all the tissues and organs of the resulting adult mouse (Smith 2001). Although human ESCs should be capable of re-entering embryogenesis as well, this aspect of human ESCs

has not been studied for obvious ethical reasons. Both human and mouse ESCs have been shown to form teratomas, which are tumors consisting of various types of tissues with representatives from all three germ layers, including skin, hair, bone, nerve, blood vessels, and muscle, when transplanted into post-natal animal models (Wobus, Holzhausen et al. 1984; Reubinoff, Pera et al. 2000). ESCs have also been differentiated *in vitro* to cells of each of the three somatic lines, although the culture is typically comprised of a mixture of many different cell types. Figure 1 shows a summary of the derivation and differentiation of ESCs (Ulloa-Montoya, Verfaillie et al. 2005).

Both human and mouse ESCs were initially isolated and are still routinely cultured with a 'feeder layer' consistent of irradiated mouse embryonic fibroblasts (MEFs) in the presence of serum. Attempts have been made to replace MEFs, serum, or both, measures that will prove necessary for clinical applications, with defined media conditions including serum replacements, various cytokines, MEF-conditioned media, or other sources of feeder layers, such as human feeders derived from fetal skin or muscle fibroblasts or adult marrow cells (Chase and Firpo 2007). Undifferentiated ESCs typically grow in small colonies with well-defined boundaries and are defined morphologically by small cell size, high nucleus to cytoplasm ratio, and compactness of the colonies. They are further characterized phenotypically by expression of the transcription factors Oct4, Nanog, Sox2, and Rex1 and the surface markers SSEA-1 in mouse ESCs and SSEA-3, SSEA-4, TRA-1-60, and TRA-1-81 in human ESCs. The quality of ESCs over time is demonstrated by karyotypic stability and the lack of chromosomal abnormalities over large numbers of passages (Ulloa-Montoya, Verfaillie et al. 2005).

Embryonic stem cells are typically differentiated either in three-dimensional aggregates known as embryoid bodies (EBs) on non-adherent plates or as a monolayer in tissue culture dishes plated on either extra-cellular matrix replacements like Matrigel or on a cell support layer such as stromal cells. Various techniques have been employed to differentiate ESCs to desired cell types. One strategy is to allow the ESCs to spontaneously differentiate and select for the desired cell types by sorting, trapping, or other selection techniques. However, the percentage of any given cell type in a

spontaneously generated heterogeneous culture is typically quite low. Thus, strategies of directed differentiation to promote particular cell fate choices at different stages involve the addition of various combinations of cytokines or biologically active molecules to the media, co-culture with certain cell types, and enrichment of lineages, which can be accomplished by sorting based on specific surface markers or selection based on drug-resistance or fluorescence driven by transcription of a particular gene. Perhaps the most challenging aspect of differentiation from ESCs is the purification of the desired cell type, as the percentage of cells in the heterogeneous population is typically fairly low, the cells are relatively fragile and may have low viability after selection or sorting, and the absolute need to eliminate any residual stem cells from the population due to the ability of ESCs to form teratomas after implantation even at the single cell level. Thus, while ESCs have the potential for wide-spread clinical use as a virtually infinite population of pluripotent cells, numerous obstacles must be overcome before clinical therapies can be realized. Adult stem cells, although typically possessing less differentiation potential and self-renewal ability than ESCs, may prove more useful for clinical therapeutic applications in the nearer future.

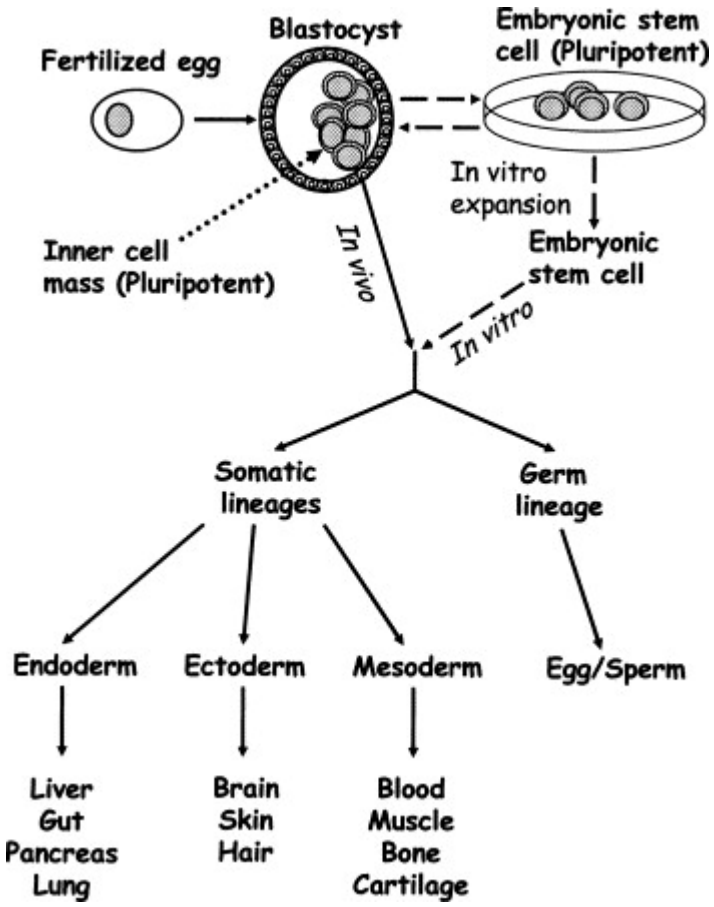

Figure 1: Summary of the derivation of differentiation of embryonic stem cells (Ulloa-Montoya, Verfaillie et al. 2005).

2.1.2.2 Adult Stem Cells

Adult stem cells (ASCs) are derived from the tissue of post-natal or adult animals and are typically characterized by a lower differentiation potential and more limited self-renewal than ESCs. To date, ASCs have been isolated from a number of tissues and organs, including bone marrow, peripheral blood, cord blood, blood vessels, the brain, skeletal muscle, liver, and others. ASCs are thought to exist in very low numbers in a particular well-defined microenvironment, often referred to as the stem cell 'niche,' within the tissue. Further, the cells are quiescent *in vivo*, existing for long periods of time without dividing. These properties, although not well understood mechanistically, are fairly intuitive considering the main purpose of adult stem cells in tissue is to replenish the cell population of the particular tissue after cell death, and therefore likely exist in a relatively inactive state until activated.

A number of the best-studied ASCs have been isolated from the bone marrow, including hematopoietic stem cells (HSCs), mesenchymal stem cells (MSCs), and multipotent adult progenitor cells (MAPCs; discussed in detail in the next section). HSCs are the quintessential ASC and are, as a matter of course, the best studied. HSCs are isolated from the bone marrow and are capable of limited self-renewal and differentiation to all the types of blood cells. HSCs are also capable of repopulating the entire hematopoietic system in an ablated recipient and are the cells responsible for this function in current bone marrow transplant procedures. MSCs are isolated from a second fraction of the bone marrow and give rise to a number of mesenchymal cell types, including bone, cartilage cells, fat cells, and other connective tissues. Neural stem cells (NSCs), another type of well-studied ASC, are isolated from the brain and give rise to neurons, astrocytes, and oligodendrocytes, the three types of neural cells. A number of other, tissue-specific stem cells have also been identified.

2.1.2.3 Multipotent Adult Progenitor Cells (MAPCs)

In 2002, a novel adult stem cell was isolated from the bone marrow of postnatal rats, mice, and humans that possessed a higher level of differentiation potential than traditionally believed possible. These cells, termed multipotent adult progenitor cells (MAPCs), demonstrated the ability to differentiate to cells of all three germ layers *in vitro* and to contribute to nearly every somatic cell type when injected, as a single cell, into a preimplantation embryo. Further, after transplantation in a non-irradiated or minimally irradiated host, MAPCs demonstrated engraftment and differentiation not only to the hematopoietic lineage, but also to the epithelium of liver, lung, and gut. MAPCs were also shown to proliferate for numerous population doublings without losing their differentiation potential and without obvious senescence or telomere shortening, thus demonstrating the capability for self-renewal (Jiang, Jahagirdar et al. 2002). After the initial isolation of MAPCs from the bone marrow, it was later shown that MAPCs could be isolated from other tissues as well, namely the brain and muscle (Jiang, Vaessen et al. 2002). Although MAPCs demonstrate a higher potency than traditional adult-derived stem cells, the nature of this potency remains an open question; further investigation is necessary to determine whether MAPCs exist as such in adult tissue, or if the increased potency is a culture-induced phenomenon, perhaps involving the de-differentiation of one or more endogenous adult stem cell populations.

2.1.2.3.1 Isolation and Culture of MAPCs

The media and culture conditions in which MAPCs are isolated and maintained seems to be quite important. The standard MAPC media contains 60% DMEM-LG, 40% MCDB-201, 1X ITS, 0.5X LA-BSA, 0.1 mM ascorbic acid 2-phosphate, 100 U of penicillin, 1000 U of streptomycin, 10 ng/ml of human PDGF and EGF, 2% FBS, and leukemia inhibitory factor (LIF). While most MAPC isolation and culture is performed in the original formulation, with the modification of the addition of dexamethasone, slight modifications have shown modest improvement in the isolation of mouse MAPCs. The changes included replacing ITS with SITE, the addition of chemically defined lipids, and

removal of dexamethasone. MAPCs are routinely isolated and cultured on fibronectin-coated tissue culture dishes. MAPCs were originally isolated and cultured at 37°C in 21% O_2 (normoxic) and 6% CO_2 conditions. However, it was later shown that isolation and culture in 5% O_2 (hypoxic) conditions resulted in clones with enhanced phenotypic and genotypic stability over longer periods of culture time (Breyer, Estharabadi et al. 2006). The modified conditions also led to the isolation of new clones that expressed relatively high levels of Oct4, a transcription factor shown to be important for the maintenance of pluripotency in ESCs (see section 2.1.3). These high Oct4 clones have also been shown to be less sensitive to high density passaging when compared to the original low Oct4 clones, maintaining potency and the ability to self-renew even when maintained at higher densities. However, high Oct4 MAPCs do not express Nanog or Sox2 and, based on studies to date, do not form teratomas upon transplantation into a host organism, all of which are characteristic of ESCs.

The protocol for isolating MAPCs from bone marrow involves harvesting the bone marrow from post-natal or adult animals and plating the cells at high density on fibronectin-coated tissue culture dishes, typically on 6-well plates. The cells are then maintained in MAPC media and culture conditions for a period of four weeks. During the first week, media is only added to the dishes, as some cells take a long time to initially attach to the plates and may be lost if media was removed. During the second week, half of the media is removed and replaced with fresh media every 2-3 days. During the third and fourth weeks, media changes continue as in the second week, but the cells are passaged upon reaching confluency and replated at 60-70% confluency. After four weeks, the cells are column depleted by magnetic removal of $CD45^+$ and $Ter119^+$ cells, followed by plating at clonal densities of 5-10 cells/well in 96-well tissue culture plates. MAPC clones are then selected and expanded based on morphology and further characterized by qRT-PCR, FACS analysis, immunohistochemistry, *in vitro* differentiation, and periodic karyotyping.

2.1.2.3.2 MAPC Characteristics (Phenotype and Transcriptome Analysis)

Although the definition of MAPCs is mostly functional in nature, the phenotypes of MAPCs seem to be fairly reproducible and distinct. The phenotype of mouse MAPCs is B220, CD3, CD15, CD31, CD34, CD44, CD45, CD105, Thy1.1, Sca-1, E-Cadherin, and MHC class I and II negative and $EPCAM^{low}$ and c-kit, VLA-6, and CD9 positive. The phenotype of rat MAPCs is CD44, CD45, and MHC class I and II negative and CD31 positive.

Recently, a comparative transcriptome analysis was performed between MAPCs, ESCs, and MSCs in an effort to compare the similarities between these populations of stem cells and, more importantly, to ascertain the differences that confer varying levels of potency to each line (Ulloa-Montoya, Kidder et al. 2007). Although, as discussed earlier, high Oct4 MAPCs do not express Nanog or Sox2, the analysis revealed that a number of other genes believed to be involved, directly or indirectly, in the maintenance of pluripotency in ESCs were also expressed in MAPCs, including Klf4, Mycn, Tbx3, Dppa4, Sall4, and a number of additional Ecat. Also, MAPCs were found to express a number of transcription factors known to interact with Nanog target genes, suggesting a possible mechanism to compensate for the lack of Nanog expression, although further analysis is required to draw any definitive conclusions. Further, principle component analysis (PCA), a multivariate analysis technique, was used to examine how closely related each of the cell lines were to one another. Interestingly, a plot in two-dimensional PCA space (PC 1 vs PC 2) revealed that rat and mouse MAPC clustered together, but these clusters were distinct from both ESCs and MSCs, which were also distinctly located. This analysis definitively demonstrated that MAPCs are quite distinct from both ESCS and MSCs despite sharing overlapping gene expression with both. Further, MSCs cultured in MAPC conditions did not acquire MAPC characteristics, suggesting that the enhanced potency of MAPCs may not be culture-induced. However, the MSCs were cultured in MAPC conditions for relatively short periods of time, and recent studies on induced pluripotent stem cells (see Section 2.1.4) indicate that reprogramming of somatic cells to a pluripotent state by force expression of transduced genes takes on the order of four weeks. Thus, repeating the experiment for a longer culture period could help to further answer the question of the origin of MAPCs.

2.1.2.3.3 Differentiation of MAPCs to Specific Lineages

MAPCs are currently being investigated for their ability to generate various cell types both *in vitro* and *in vivo* using various differentiation techniques. Indeed, the potential clinical therapeutic applications of MAPCs rely not only on the ability to reproducibly isolate MAPCs, but also on the ability to generate desired cell types in a rigorous and efficient manner. Published reports have demonstrated the ability of MAPCs to differentiate to neuroectodermal cells, hepatocyte-like cells, arterial and venous endothelium, smooth muscle cells, and hematopoietic stem cells (Reyes, Dudek et al. 2002; Schwartz, Reyes et al. 2002; Jiang, Henderson et al. 2003; Ross, Hong et al. 2006; Aranguren, Luttun et al. 2007). Additionally, studies are currently underway to investigate the directed differentiation of MAPCs to bone and insulin-producing β-cells, among other cell and tissue types. Further, the differentiation protocols for each cell type are continually analyzed and refined to improve yield, efficiency, and reproducibility. Besides producing clinically relevant cell types, these differentiation protocols also provide a platform for studying interesting developmental processes governing lineage fate choices, self-renewal, and the regulation of potency. Indeed, lessons learned in the differentiation of MAPCs can be applied to advance developmental knowledge and, demonstrating reciprocity, advances in developmental knowledge can lead to improvements in differentiation protocols.

2.1.2.4 Other Adult Stem Cells with Enhanced Differentiation Potential

Although MAPCs were the first population of adult stem cells reported to have enhanced differentiation potential, a number of additional adult stem cells have recently been reported with similar potency. Such adult stem cells include marrow isolated adult multilineage inducible (MIAMI) cells, multipotent renal progenitor cells (MRPCs), unrestricted somatic stem cells (USSCs), and very small embryonic-like cells (VSELs). The ability to isolate these stem cells may provide evidence for an *in vivo* presence of stem cells with enhanced potency, or may simply demonstrate the reproducibility of de-differentiation *in vitro*, as many of the stem cell lines are isolated under similar

conditions to MAPC. Indeed, a thorough investigation into the origin of more potent adult stem cells should provide answers to numerous questions, and a comparative transcriptome analysis, similar to that discussed earlier between MAPCs, ESCs, and MSCs, could help to quantify the similarities and differences between each of these adult stem cell populations.

MIAMI cells were isolated by collecting the total bone marrow from the vertebrae of recently deceased humans and plating on fibronectin-coated tissue culture dishes in media made up of DMEM-LG, 5% FBS, 100 U/ml of penicillin, and 1 mg/ml of streptomycin. The cells were kept in 3% O_2 and 5% CO_2 at 37°C with media changes once or twice per week and at less than 30% confluence. The MIAMI cells were shown to self-renew for greater than 30 population doublings and to differentiate to bone cells, chondrocytes, fat cells, islet-like clusters, and neural-like cells (D'Ippolito, Diabira et al. 2004).

MRPCs were isolated by harvesting kidney cells from 2 to 4 week old rats and subsequent culture in MAPC media and culture conditions. The isolation protocol was similar to MAPC isolation except that column depletion was not performed. MRPC clones were generated by plating at clonal density and subsequently picking colonies using cloning rings. MRPCs demonstrated the ability to self-renew for over 200 doublings without obvious senescence or telomere shortening and differentiate to endothelial, hepatic, and neuronal lineages (Gupta, Verfaillie et al. 2006).

USSCs were isolated from umbilical cord blood by plating in culture flasks in either myelocult medium (StemCell Technologies) or DMEM-LG supplemented with 30% FCS, dexamethasone, penicillin, streptomycin, and ultraglutamine. The cells were incubated in 37°C at 5% CO_2 and were kept at less than 80% confluency during isolation. The cells were expanded in the supplemented DMEM-LG media (with lower concentrations or in the absence of dexamethasone) for greater than 40 population doublings without loss of differentiation potential or telomere length. They were further

shown to differentiate to neural cells, bone cells, cartilage cells, fat cells, hematopoietic cells, myocardial cells, and hepatic cells (Kogler, Sensken et al. 2004).

VSELs were isolated from murine bone marrow, and later from human cord blood, by removal of erythrocytes in hypotonic solution followed by multiparametric sorting for $Lin^-/Sca\text{-}1^+/CD45^-$ or $Lin^-/Sca\text{-}1^+/CD45^+$ populations. They showed that the $Lin^-/Sca\text{-}1^+/CD45^-$ population were very small in size, demonstrated a high nucleus to cytoplasm ratio, and had euchromatin characteristics of ESCs. Further, they demonstrated that the VSELs express Oct4, Nanog, Rex1, SSEA (1 for mouse, 4 for humans), and Dppa3, all of which are characteristic ESC markers. They also demonstrated the ability of VSELs to differentiate to cardiomyocytes, neural cells, and pancreas cells (Kucia, Reca et al. 2006; Kucia, Halasa et al. 2007).

The recent reports of these populations of adult stem cells exhibiting enhanced differentiation potential raises many more questions about the nature of stem cells *in vivo* and the regulatory networks responsible for maintenance of potency and self-renewal capabilities. Although much research has focused on answering the question of whether these highly potent adult stem cells exist *in vivo* or are the result of *in vitro* culture phenomena, it has proven quite difficult to resolve the issue. While studies to further enhance the characterization, isolation, maintenance, and directed differentiation of these and other adult stem cell populations is ongoing, parallel studies are being conducted to try to elucidate the mechanisms regulating potency and self-renewal, as an enhanced understanding of these processes will likely lead to a greater understanding of the stem cell niche in adult tissues, among many other benefits.

2.1.3 Regulatory Networks in Embryonic Stem Cells

As has been previously discussed, stem cells are defined by their special abilities to self-renew and to differentiate to different cell types. Although considerable progress has been made in the ability to isolate stem cells, maintain them *in vitro* for extended periods of time, and even manipulate their differentiation to specific cell types, the mechanisms

regulating these properties remain fairly elusive. The identification of a gene or a set of genes invoking stem cell properties on the cells in which they are expressed has been a major focus of research in recent years. Indeed, a detailed understanding of the genetic networks involved in maintaining self-renewal and promoting potency would greatly accelerate progress in isolation, culture, and differentiation of stem cells. Additionally, due to the recent identification of "cancer stem cells," which also exhibit the properties of self-renewal and differentiation potential and are thought to cause many types of cancers in humans, understanding the regulatory mechanisms of self-renewal and differentiation may have an impact in the treatment of cancer as well (Reya, Morrison et al. 2001). In this section, the progress of elucidating such mechanisms to date will be reviewed.

The potency of embryonic stem cells (ESCs), isolated from the inner cell mass of early embryos, and adult stem cells, isolated from various tissues of post-natal or adult animals, is such an important property for survival that a number of redundant regulatory pathways have probably evolved over time. Clearly, the pluripotency of the inner cell mass is absolutely essential for development and survival of the organism, while adult stem cells existing in tissues are responsible for maintaining tissue function and homeostasis by repopulating the cell population after damage or other cell death. Thus, without the differentiation potential of adult stem cells, the life span of most animals would likely be significantly reduced. This presents the possibility that various populations of stem cells may retain different mechanisms for regulating potency, as well as self-renewal, each of which may be a subset of the full complement of redundant networks. Since pluripotency represents the highest level of potency in cultured stem cell lines, it makes sense to begin the examination of the regulatory networks involved by examining the systems in ESCs. Self-renewal in stem cell lines implies the maintenance of potency over successive cell divisions, so the regulation of self-renewal and potency are likely to be highly interconnected.

Although the whole picture of pluripotency and self-renewal is not yet understood, considerable progress has been made in identifying numerous signal transduction networks important for maintaining pluripotency *in vivo* and *in vitro*. Sato et al.

compared the transcriptome of undifferentiated and differentiated hESCs using Affymetrix microarray chips to identify the genes upregulated or downregulated in the undifferentiated, pluripotent state (Sato, Sanjuan et al. 2003). The authors reported 918 genes enriched in the undifferentiated population, of which 28% are unknown genes, while 17% correspond to genes involved in signal transduction pathways, indicating a large role of these relatively well-understood networks in the maintenance of pluripotency. The signal transduction networks implicated include the fibroblast growth factor (FGF) pathway, the transforming growth factor (TGF)-β/bone morphogenetic protein (BMP) pathway, the Nodal pathway, and the Wingless type (WNT) pathway. Additionally, a number of transcription factors are known to play an important role in maintaining pluripotency, including Oct4, Sox2, and Nanog (Johnson, Rathjen et al. 2006). The interactions between these transcription factors and pathways have been a major focus of research, especially in mouse and human ESCs, over the past years, and considerable progress has been made toward understanding their roles. Figure 2 and Figure 3 show a summary of the combinatorial effects of these pathways and transcription factors on maintaining pluripotency both *in vitro* and in the developing embryo and the ability to derive ESCs from it in the mouse (Boiani and Scholer 2005).

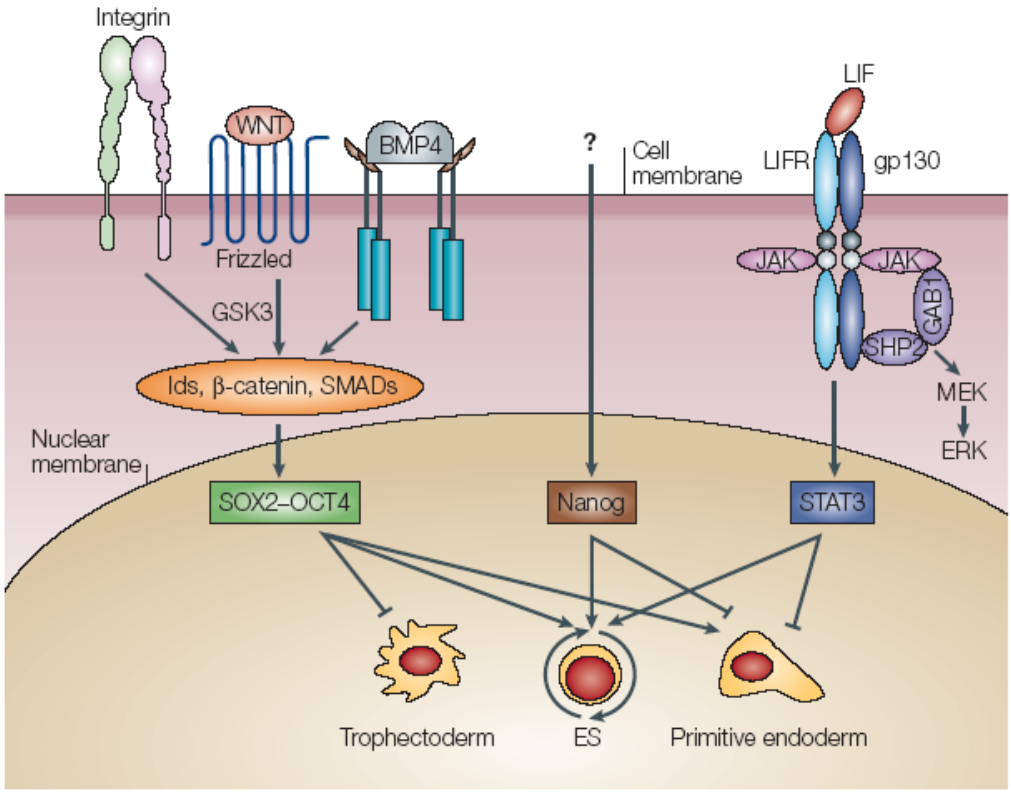

Figure 2: Signaling pathways involved in maintaining pluripotency in mouse ESCs (Boiani and Scholer 2005).

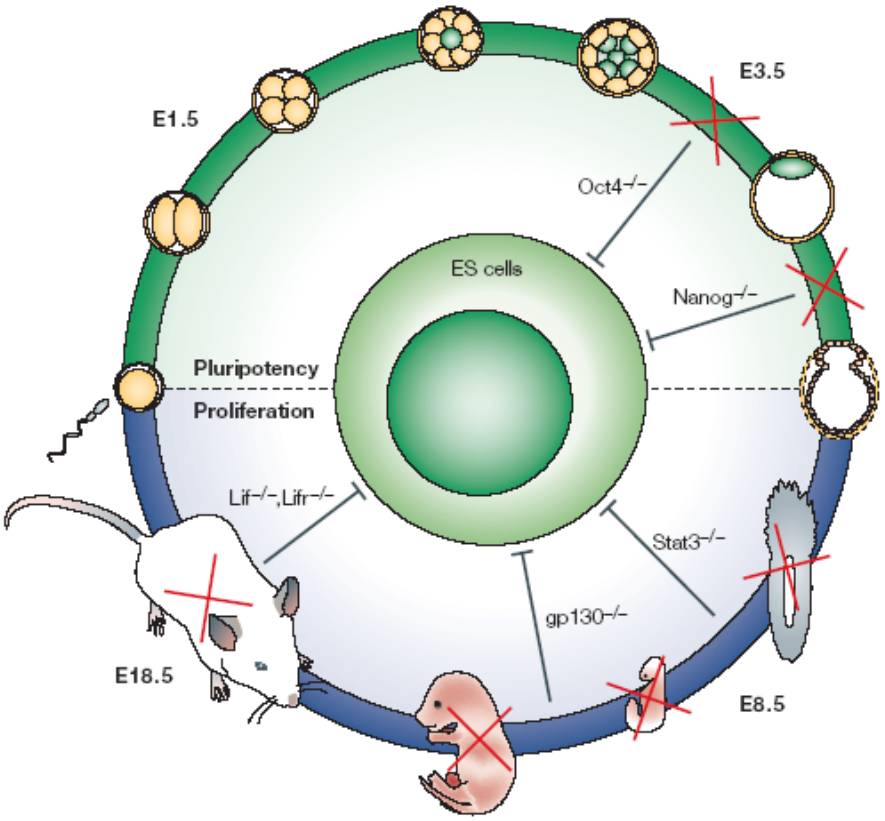

Figure 3: The developmental effects of loss of genes thought to be involved in maintenance of pluripotency at the physiologically relevant stage of development (Boiani and Scholer 2005).

2.1.3.1 Wnt Signaling

Wingless type (Wnt) signaling, so named because it was initially identified in drosophila flies lacking wings, is actually quite diverse, functioning through several distinct pathways and is responsible for a wide array of functions ranging from embryogenesis and organogenesis to normal physiological processes and even cancer in adult organisms. The best understood Wnt signaling pathway is known as the canonical Wnt pathway, as it was also the first discovered. In this pathway, WNT, a secreted glycoprotein, binds to the receptor complex comprised of Frizzled, LRP, and many other proteins, on the surface of the cell membrane. Upon binding by extracellular WNT ligands, the transmembrane receptor complex activates Dishevelled in the cytoplasm, which then disrupts the complex formed by glycogen-synthase kinase-3 (GSK3) and Axin by recruiting Axin to the transmembrane recptor complex. The GSK3/Axin complex regulates the concentration of β-catenin by actively marking it for degradation; thus, disruption of the GSK3/Axin complex by Dishevelled results in the accumulation of β-catenin, which is then translocated into the nucleus where it interacts with various transcription factors to promote the transcription of downstream target genes (Gilbert 2006).

Although the Wnt signaling pathway has potentially hundreds of target genes, its specific role in maintaining pluripotency is currently not understood. Nonetheless, it has been shown that activation of the canonical Wnt pathway helps to maintain ESCs in an undifferentiated state, either by, or in addition to, maintaining the expression of Oct4, Nanog, and Rex1 (Sato, Meijer et al. 2004). Thus, Wnt appears to have some role in self-renewal and maintaining potency, although that role is not well understood.

2.1.3.2 LIF Signaling

The leukemia inhibitory factor (LIF) is required for maintenance of undifferentiated mouse, but not human, ESCs in the presence of serum. In the mouse ESC system, LIF acts by binding to LIF receptor (LIFR) – gp130 heterodimer complex on the surface of the cell membrane, thereby activating via phosphorylation the signal transducer and

activator of transcription-3 (STAT3), a transcription factor that locates to the nucleus and promotes transcription of downstream targets upon activation. Despite its necessity in cultured mouse ESCs, LIF-deficient mouse embryos develop well beyond the blastocyst stage, where pluripotent stem cells are abundant, suggesting the presence of redundant signaling pathways (Boiani and Scholer 2005). In addition to activating STAT-3, LIF may also act through a number of other signaling cascades in mouse ESCs, including activation of the nonreceptor tyrosine kinase Janus (JAK), which activates other members of the STAT family via the JAK/STAT signaling cascade, recruitment of the antiphosphotyrosine immunoreactive kinase (TIK), activation of the extracellular signal-regulated protein kinases 1 and 2 (ERK1 and ERK2), and upregulation of the mitogen-activated protein kinase (MAPK) signaling cascade, although many of these activities have been shown to be not required for maintenance of ESC pluripotency (Boeuf, Hauss et al. 1997; Burdon, Stracey et al. 1999; Auernhammer, Bousquet et al. 2000). Further, the inability of LIF to inhibit differentiation in human ESCs suggests that the activity of LIF signaling in maintaining the potency of ESCs is not universal (Humphrey, Beattie et al. 2004). Thus, further investigation is required to determine the mechanisms underlying the differences between LIF signaling in human and mouse ESCs.

2.1.3.3 BMP4 Signaling

Although the mechanisms of bone morphogenetic protein (BMP), of the transforming growth factor beta (TGF-β) superfamily, signaling involved in the maintenance of ESC pluripotency is quite poorly understood, it has been shown that the presence of BMP4 inhibits differentiation of ESCs to neuronal fates, acting in concert with the LIF signaling cascade to prevent differentiation (Ying, Nichols et al. 2003). BMP acts through BMP receptors (BMPR) on the surface of the cell membrane to activate transcription of a member of the small mothers against decapentaplegic (SMAD) family, SMAD4, which subsequently activates transcription of members of the inhibition of differentiation (Id) family. A recent study also provided evidence that BMP proteins may be downstream targets of the Wnt signaling cascade, possibly providing a connection to the previously discussed pathway (Haegele, Ingold et al. 2003). However, further investigation is

required to elucidate the mechanisms by which BMP4 promotes maintenance of pluripotency.

2.1.3.4 OCT4 Activity

The transcription factor OCT4, a POU-domain transcription factor, is essential for the maintenance of pluripotency in both human and mouse ESCs as well as in pluripotent cells of the developing embryo. Embryos lacking the Oct4 gene fail to form true blastocysts, as the cells located where the inner cell mass should be are actually trophoectodermal and cannot give rise to ESC lines (Nichols, Zevnik et al. 1998). Furthermore, Oct4 transcription is generally downregulated as cells undergo differentiation to most lineages, excepting perhaps neuronal differentiation. Although Oct4 has been shown as essential for maintenance of pluripotency, it is not sufficient, indicating that it acts in concert with other transcription factors or signaling cascades in pluripotent cells (Johnson, Rathjen et al. 2006). Thus, the downstream targets of OCT4, as well as its potential interaction with other signaling molecules, is a major focus of ongoing research.

2.1.3.5 SOX2 Activity

SOX2, a member of the HMG-domain DNA-binding-protein family, may serve dual roles in maintaining pluripotency in ESCs as a transcription factor and in maintaining the organization of chromatin in pluripotent cells (Pevny and Lovell-Badge 1997). Indeed, SOX2 has been shown to complex with OCT4, allowing the complex to bind to the enhancer sequences of the Fgf4 gene, indicating a direct role in the maintenance of pluripotency via direct interaction with OCT4 (Yuan, Corbi et al. 1995). Loss of SOX2 activity in the developing embryo results in fatal defects in the pluripotency of the epiblast, providing further evidence for a role in the maintenance of pluripotency (Avilion, Nicolis et al. 2003). Thus, SOX2 plays a major role in the establishment and maintenance of pluripotency and acts synergistically with OCT4 in upregulating FGF4 protein. The possibility of other members of the SOX family acting similarly, along with

the possibility of specific interactions of SOX2 with other transcription factors remains to be further investigated.

2.1.3.6 Nanog Activity

Nanog is a homeodomain-containing transcription factor that is expressed in both mouse and human ESCs and is thought to be responsible for the maintenance of primitive ectoderm in the developing embryo (Boiani and Scholer 2005). Additionally, overexpression of Nanog in mouse ESCs can compensate the absence of LIF in maintaining the undifferentiated state, although physiological levels of Nanog are insufficient to do so. Thus, Nanog is one of many factors, including those previously discussed, that plays an active role in maintaining pluripotency and promoting self-renewal.

Indeed, the signaling pathways promoting pluripotency appears to contain both redundancies as well as combinatorial effects from a number of signaling cascades and transcription factors. However, the full complement of functions invoking pluripotency in stem cell lines is far from understood and must continue to be investigated. Increased knowledge of these regulatory networks will enable much better control of undifferentiated pluripotent stem cells in culture, differentiation of these cells along desired paths, and perhaps even the induction of pluripotency in non-pluripotent precursor populations, as is discussed in the next section.

2.1.4 Induced Pluripotent Stem (iPS) Cells

In 2006, Shinya Yamanaka and Kazutoshi Takahashi reported the successful reprogramming of mouse embryonic and adult fibroblasts to pluripotent cells resembling embryonic stem cells by transfecting the fibroblasts with a combination of four genes (Takahashi and Yamanaka 2006). The authors began by identifying a set of 24 candidate genes, each of which was believed to be associated with imparting pluripotency and self-renewal on embryonic stem cells and introduced the genes into mouse embryonic fibroblasts by retroviral transduction. They selected for induced cells via neomycin resistance imparted by endogenous expression of the *Fbx15* gene, which is expressed in embryonic stem cells but is known to be dispensable for pluripotency. By selecting induced cells based on neomycin resistance and morphology, the authors picked nine clones and expanded them under selection. These clones were shown to have properties similar to embryonic stem cells including morphology, growth rate, teratoma formation and differentiation, expression of specific markers, and formation of embryoid bodies. However, the methylation profiles of Nanog and Oct3/4 promoters contained methylation patterns different from embryonic stem cells, indicating that the induced cells are not identical to ES cells. The authors termed these reprogrammed cells "induced pluripotent stem" (iPS) cells. Next, they systematically narrowed down the transfected genes required to induce pluripotency, ultimately defining a minimal set of four genes: Oct3/4, Sox2, c-Myc, and Klf4. To show that the reprogramming was not a unique ability of embryonic fibroblasts, the authors repeated the induction process with tail-tip fibroblasts of 7-week old mice with similar results.

In late 2007, two separate groups published the ability to form iPS cells from human somatic cells. Yamanaka's group reported the successful reprogramming of adult human dermal fibroblasts (skin cells) to iPS cells by retroviral transduction of the same four genes they previously used in mice: Oct3/4, Sox2, c-Myc, and Klf4 (Takahashi, Tanabe et al. 2007). Simultaneously, James Thomson's group reported the ability to reprogram adult fibroblasts using a lentiviral transfection system expressing four genes: Oct4, Sox2, Nanog, and LIN28 (Yu, Vodyanik et al. 2007). Importantly, this reprogramming used a

different set of genes, although a minimum of four genes still needed to be expressed. Also importantly, this system eliminated the use of c-Myc, an oncogene associated with numerous types of cancer (Fearon and Dang 1999). In both cases, the iPS cells were capable of self-renewal and differentiation to cell types of all three germ layers in addition to exhibiting similar morphogenic properties, surface markers, and gene expression to embryonic stem cells.

The implications of iPS cells are tremendous. One important political implication is that the ability to induce formation of pluripotent stem cells from adult fibroblasts may eliminate the need for oocytes and embryos used to create embryonic stem cell lines. Given the ethical debates around the sacrifice of embryos, the use of reprogrammed adult cell lines would circumvent the current federal limitations placed on human embryonic stem cell research. The possible therapeutic implications include using the patient's own cells to generate histocompatible iPS cells, which could then be differentiated to tissues or cells for implantation. Since the differentiated cells are derived from the patient's cells, these cells would be genetically identical to the patient's cells, or histocompatible, thus reducing immune response rejection typical of implantations. Indeed, it was recently shown that iPS cells could be generated from the tail tip fibroblasts of mice suffering from sickle cell anemia, corrected of sickle cell anemia by gene targeting, differentiated into hematopoietic progenitor cells, and implanted back into the sickle cell mice to cure the disease (Hanna, Wernig et al. 2007). Such autologous treatment with iPS cells is very attractive clinically. However, numerous obstacles must first be overcome before such treatments would become feasible. Obviously, the ability to differentiate the cells to the desired cell or tissue type must be shown with high efficiency. However, this aspect of stem cell research is ongoing in all types of stem cells, and the differentiation techniques demonstrated in embryonic stem cells and other stem cell types will likely eventually be applicable to iPS cells. More importantly, the use of lentiviral or retroviral systems for transfecting the inducing genes should eventually be eliminated. In other words, induction of fully differentiated somatic cells to pluripotent stem cells should be achieved without the use of transfected gene expression, instead utilizing the endogenous genome for the induction procedure. Further, as with embryonic stem cells, iPS cells are capable

of forming teratomas from the single-cell level, necessitating the complete removal of all undifferentiated iPS cells from the culture before transplantation.

Unfortunately, the process of reprogramming is still very poorly understood, as the field of iPS cells is still in the earliest stages of infancy. Indeed, a thorough understanding of the mechanisms of reprogramming must be achieved before one can realistically hope to achieve induction to the pluripotent state without transgene expression. To this end, several papers were recently published investigating the timing of endogenous gene expression during reprogramming using a doxycycline-inducible transgene expression system and either Oct4-GFP or Nanog-GFP mice. The dox-inducible vector contained the coding regions for Oct4, Sox2, c-Myc, and Klf4, thus allowing for tight temporal control of the expression of the four transgenes. Using this system, Brambrink et al. investigated the timing of endogenous activation of several pluripotency genes to determine the mechanism of reprogramming to iPS cells (Brambrink, Foreman et al. 2008). The pluripotency markers they selected were stage-specific embryonic antigen 1 (SSEA1), alkaline phosphatase (AP), Oct4, and Nanog. They determined that reprogramming of MEFs to iPS occurs through a series of stages marked by activation of endogenous gene expression and showed that intermediates could be detected at various stages, some of which were stable populations. They showed that the first step of reprogramming was the activation of endogenous AP, occurring at approximately day 3. By the end of the 26-day protocol, nearly 80% of the entire population was AP^+. Out of the cells expressing AP, a subpopulation of cells began to also express SSEA1 starting at day 9. By the end of the protocol, approximately 15% of the culture was $AP^+/SSEA1^+$. Finally, a subpopulation of the $SSEA1^+/AP^+$ cells began to express endogenous Oct4 and Nanog by day 16, indicating successful reprogramming to iPS. Thus, they presented a pathway of reprogramming from MEF to iPS in which cells initially acquire expression of AP, followed by SSEA1, and finally Oct4 and Nanog upon complete reprogramming. Interestingly, the study also determined that the minimum amount of time that cells required transgene expression to become reprogrammed was only 12 days. Thus, even before cells begin to express Oct4 and Nanog, they acquire the ability to continue the path to reprogramming on their own, without the aid of transgene expression. Naturally,

longer expression of the transgenes resulted in increased numbers of iPS cells, indicating that the induction does not occur simultaneously for all cells, but instead that there is a distribution of lag phases before reprogramming begins.

Induced pluripotent stem (iPS) cells will continue be a major focus of research studies worldwide. As the mechanism of reprogramming and the full potential of these cells become better understood, the timeline of possible applications should become clearer. More recently, a great effort has been made to effect reprogramming without integrating transgenes. Such approaches include expressing the reprogramming factors via non-integrating vector systems such as episomal vectors or Sindai virus. Additionally, a number of groups are investigating reprogramming via small molecule signaling in lieu of viral expression. Advancement in these areas hold the potential to make iPS derived cell products available for therapeutic uses in the not-too-distant future.

2.2 Liver Organogenesis

2.2.1 Formation of the Blastocyst

After fertilization, the zygote undergoes a series of asymmetric and asynchronous cell divisions resulting in cells known individually as blastomeres. At the 8-cell stage, the blastomeres begin producing cell adhesion proteins and come together in a process known as compaction to form a tightly sealed spherical ball of blastomeres. The 16 blastomeres resulting from the next division are known collectively as the morula and are arranged in two groups, with one group surrounding the other. Most of the external cells of the morula contribute to the trophoblast, which ultimately incorporates with the placenta and supports the developing embryo by facilitating the transfer of oxygen and nutrients from the mother and suppressing immunorejection of the fetus. The inner cells of the morula, along with a few supplemental cells from the external cells, form the inner cell mass (ICM), which eventually gives rise to the entire adult organism. Over the next few cell divisions, the trophoblast cells promote the formation of an inner cavity, known as the blastocoel, by pumping sodium ions to the interior of the embryo, thus drawing in

water via osmosis. Meanwhile, the inner cells of the morula continue to divide and become positioned on one side of the cavity, resulting in what is known as the blastocyst. Figure 4 shows both a high resolution photograph and a drawing of a blastocyst, indicating the ICM, the blastocoel, the trophoblast, and the zona pellucida, which is a glycoprotein membrane surrounding the developing membrane that prevents premature attachment of the egg (www.embryology.ch).

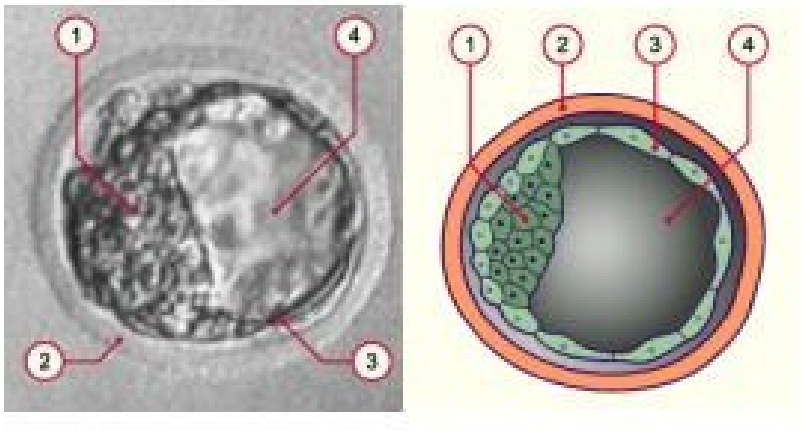

Figure 4: High resolution photo (left) and drawing (right) of a blastocyst: 1) inner cell mas; 2) zona pellucida; 3) trophoblast; 4) blastocoel. (http:www.embryology.ch)

The blastocyst is an important milestone in development and has special significance in stem cell biology. The specification of the trophoblast and the inner cell mass represents the first lineage-restricting differentiation of embryonic development. Prior to this differentiation, all the blastomeres are totipotent, able to form all the cell types of the organism as well as the extra-embryonic structures, such as the trophoblast. However, the inner cell mass of the blastocyst stage is pluripotent, having lost the ability to develop into the extra-embryonic structures, but maintaining the ability to develop into the entire adult organism. The ICM is characterized by the expression of Oct4, Nanog, and Stat3, which are believed to promote pluripotency by maintaining the undifferentiated stage.

The trophoblast cells, however, express Cdx2, which downregulates Oct4 and Nanog, and eomesodermin, a T-box transcription factor that activates the production of trophoblast-specific proteins. Importantly, embryonic stem cells are derived by collecting these pluripotent cells from the ICM and culturing them in conditions that promote undifferentiated expansion by preservation of the expression of Oct4, Nanog, and Stat3, as was previously discussed (Gilbert 2006).

2.2.2 Endoderm Specification from the Blastocyst

The three germ layers, the endoderm, the ectoderm, and the mesoderm, all arise from the inner cell mass of the blastocyst through a process known as gastrulation. The first lineage choice involves patterning the bilaminar germ disc from the cells in the ICM; the lower cells become the visceral endoderm (VE), which is also known as the primitive endoderm or hypoblast, while the cells above the VE form the epiblast. The visceral endoderm eventually forms the yolk sac, while the cells of the epiblast become further specified into the embryonic epiblast and the amnionic ectoderm. The embryonic epiblast is the precursor of all the cells of the organism, while the amnionic ectoderm form a lining of an amnionic cavity. The anterior-posterior (AP) axis is specified in the VE by signaling from the extra-embryonic ectoderm (ExE) on the presumptive posterior side of the embryo. It has been suggested that Wnt signaling in the posterior portion of the epiblast and/or VE promotes formation of the node and, subsequently, the primitive streak, thereby specifying the beginning of gastrulation (Tam, Loebel et al. 2006). The endoderm and mesoderm are formed during migration and simultaneous differentiation through the primitive streak. The cells migrating through the anterior portion of the primitive streak are induced to form the endoderm, although the mechanisms regulating the choice between endoderm and mesoderm are currently unknown (Wells and Melton 1999). Definitive endoderm can be identified by the expression of goosecoid, Foxa2, CXCR4, Sox17, and E-cadherins, among other markers. Mesoderm does not express Sox17, and visceral endoderm does not express goosecoid.

2.2.3 Gut Tube Formation

Immediately after gastrulation in the mouse embryo, at approximately day E7.5, the endoderm exists as a layer of approximately 500 cells on the outside of the mesoderm and endoderm in a cup-shape orientation. Fate-mapping has led to the designation of four distinct regions of the definitive endoderm, as shown in Figure 5. Region I, the anterior most region, gives rise to the yolk sac and the ventral foregut, which later gives rise to liver, ventral pancreas, lungs, and thyroid. Region II gives rise to the dorsal foregut, which gives rise to the esophagus, stomach, dorsal pancreas, and duodenum. Regions III and IV give rise to the small intestine and the large intestine, respectively (Wells and Melton 1999). During the following day of development, this two-dimensional layer of cells undergoes a series of migrations and folds that results in formation of the primitive gut tube in which the areas of formation of various organs are already specified. However, further instruction is required during organogenesis to pattern individual organs.

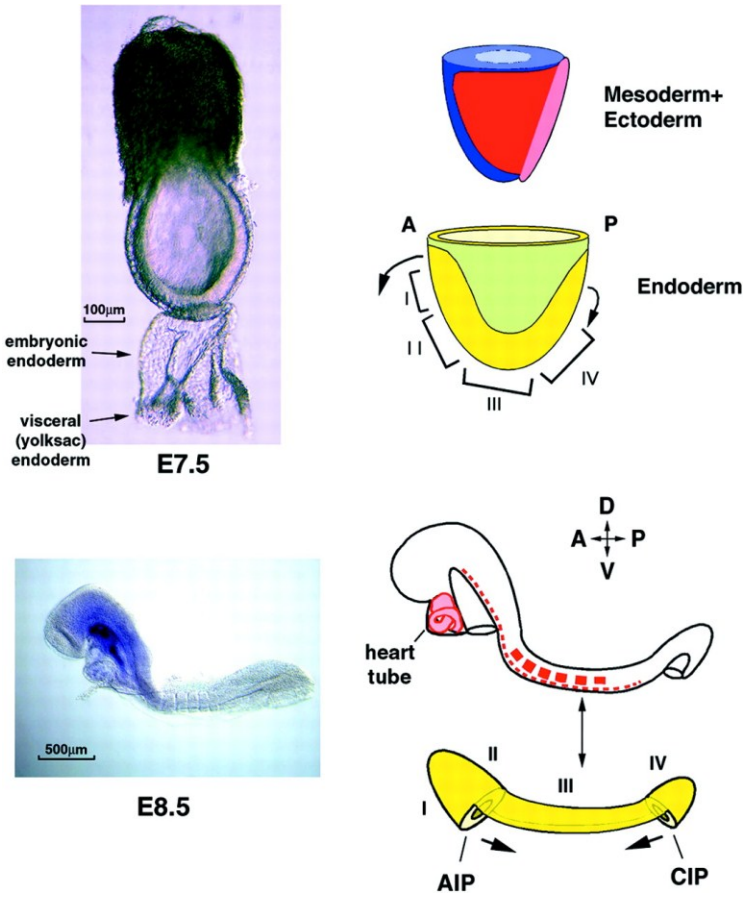

Figure 5: Formation of the three-dimensional gut tube from the definitive endoderm, depicting Regions I, II, III, and IV indicating future sites of organogenesis (Wells and Melton 1999).

2.2.4 Specification of Hepatic Endoderm and Liver Morphogenesis

A portion of Region I of the gut tube becomes the ventral foregut endoderm which gives rise to liver, ventral pancreas, lungs, and thyroid, with pancreas being the default fate

state of this tissue (Deutsch, Jung et al. 2001). Blocking of the pancreatic fate and induction of the hepatic fate is effected by FGF1 and FGF2 signaling from the adjacent cardiac mesoderm (Jung, Zheng et al. 1999) in combination with BMP signaling from the septum transversum mesenchyme (Rossi, Dunn et al. 2001). This FGF and BMP signaling activates the early transcriptional network, including expression of AFP, Albumin, HNF4α, and TTR. These hepatic endoderm cells then thicken to form bipotential hepatoblasts in the early liver bud, which expand by additional signaling from mesenchymal tissue, including hepatic mesenchyme stellate cells which form from the STM. The factors and cytokines secreted by the mesenchymal tissue include FGF, BMP, HGF, Wnt, TGFβ, and retinoic acid (RA), which promote hepatoblast proliferation, survival by anti-apoptosis signaling, and eventually migration into the STM where the liver architecture begins to form. A brief summary of this process is depicted in Figure 6. As the liver architectures is being established in the developing liver bud, angiogenesis begins to occur from a population of neighboring angioblasts, although the source of these cells, their potential role in specification of relevant cell types, and the mechanisms by which they interlace with the developing liver, are all questions that are still being investigated. During this stage of liver bud growth, which occurs from about E9.5 to E15, the developing liver bud functions as the primary site of fetal hematopoiesis.

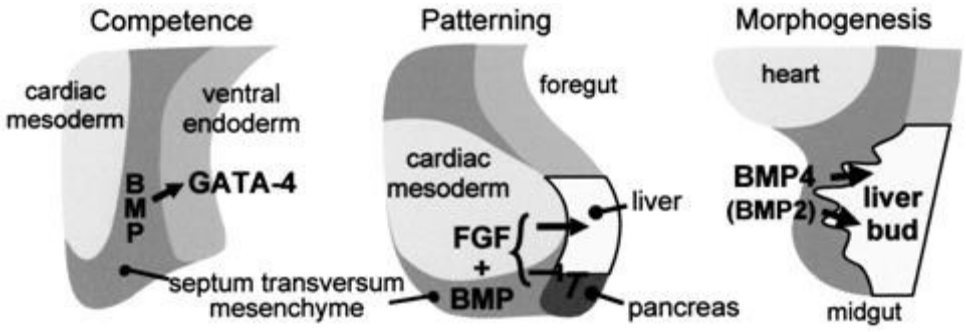

Figure 6: Model of specification of hepatic endoderm and liver bud formation by BMP signaling from the STM and FGF signaling from cardiac mesoderm (Rossi, Dunn et al. 2001).

The bipotential hepatoblasts of the developing liver give rise to the two main cell types of the liver, hepatocytes and biliary epithelial cells (BEC), also known as biliary duct cells or cholangiocytes, beginning around E13. The bipotential hepatoblasts, which express the fetal liver marker AFP along with hepatocyte markers such as HNF4α and albumin along with BEC markers such as cytokeratin-19 (CK19), differentiate according to their location in the developing liver. The cells around the portal vein undergo a process called ductal plate remodeling from E17 through birth in which a bilayer of cells around the portal vein differentiate and remodel to form the intrahepatic bile duct (IHBD) (Lemaigre 2003). During this process, the hepatoblasts upregulate expression of CK19 and lose expression of the hepatic genes. The majority of the hepatoblasts, which are not in contact with the portal vein, differentiate into hepatocytes by signaling from the secreted factors Oncostatin M (OSM), HGF, Wnt, and glucocorticoid hormones, which effect the expression of the hepatocyte nuclear factors (HNF) including HNF1α, HNF3α (FOXA1), HNF3β (FOXA2), and HNF3γ (FOXA3) along with other liver-enriched transcription factors such as C/EBPα (Kyrmizi, Hatzis et al. 2006). During this differentiation of hepatoblasts to hepatocytes, the cells begin to adopt a polarized cuboidal epithelial morphology and lose their hematopoietic activity as they gain their hepatic functions. A summary of the full fate decisions and signaling molecules is shown in Figure 7.

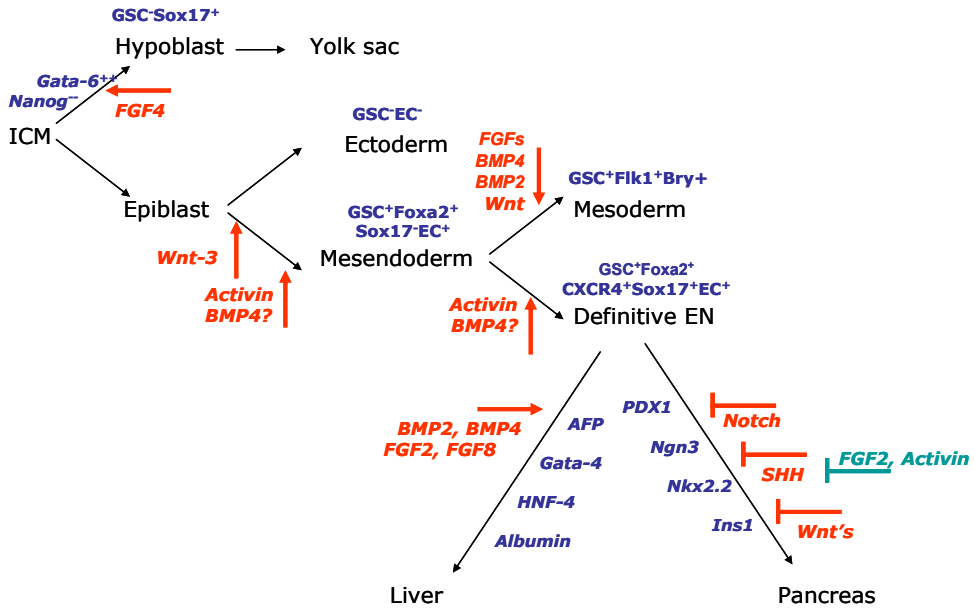

Figure 7: Lineage choices, expression profiles, and signaling molecules during specification of the liver and pancreas from the inner cell mass (prepared by Catherine Verfaillie and Meri Firpo).

2.2.5 The Adult Liver

After birth, the liver grows along with the animal until reaching its full size by adulthood. In humans, the liver weighs approximately 3.5 pounds and is divided into two or four lobes depending on the criteria chosen. Hepatocytes are responsible for most functions of the liver and make up approximately 80% of the liver by volume. These functions include protein synthesis and storage, carbohydrate metabolism, cholesterol, bile salts, and phospholipids synthesis, and detoxification and secretion of potentially toxic substances. Although all hepatocytes of the liver appear virtually indistinguishable, they are specialized in function based on their location in the liver, a phenomenon known as hepatocyte zonation. The zones and their functions, which are often complementary in

adjacent sections, seem to be a function of position in relation to the portal triad, which is comprised of the portal vein, the biliary duct, and the hepatic artery. Thus, the functions are likely organized based on availability of nutrients, oxygen, and the ability to secrete hepatic products.

Detoxification of toxic substances is a critical function to preserve the viability of any organism. Although most tissues are capable of limited detoxification functions, the liver is responsible for the majority of detoxification in the adult body. Drug metabolism, which can toxify or detoxify, is primarily carried out in the endoplasmic reticulum (ER) of hepatocytes. There are two stages of drug metabolism: Phase I, or nonsynthetic reactions, and Phase II, or conjugation reactions. Phase I reactions typically involve oxidation, reduction, or hydrolysis reactions carried out by a variety of oxidases including the Cytochrome P450 monooxygenases, flavin-containing monooxygenases, alcohol dehydrogenases, aldehyde dehydrogenases, monoamine oxidases, peroxidases, esterases, amidases, or epoxide hydrolases. Although some polar products of Phase I reactions may be directly excreted, many must be further metabolised by a Phase II conjugation reaction to facilitate elimination. Conjugation reactions include methylation by methyltransferases, sulphation by sulfotransferases, acetylation by N-acetyltransferases, glucuronidation by UDP-glucuronosyltransferases (UGTs), glutathione conjugation by glutathione S-transferases, and glycine conjugation by acetyl Co-enzyme As.

2.3 Strategies for Forming Hepatocyte-Like Cells

Currently, the only viable treatment option for end-stage liver disease is transplant of a whole or partial liver. Due to the limited availability of donor livers and the necessity of immunosuppressant medications upon liver transplantation, considerable effort has been made in attempting to identify a suitable alternative cell source capable of mimicking liver function. In addition to potential therapeutic uses in transplantation, renewable sources of hepatocyte-like cells have potential uses in high-throughput drug-toxicity screening for pharmaceutical discovery or populating bioartificial liver devices which could be used to temporarily bridge patients awaiting a viable transplant or recovering

from a transplantation procedure. A number of strategies have been identified with the potential to generate cells with some phenotypic and functional similarities to hepatocytes, although none have yet fully recapitulated the *in vivo* hepatocyte function. In this section, we will review a number of different such strategies, mostly including differentiation from various stem cell populations.

2.3.1 Differentiation from ES and iPS cells

ES cells have long been regarded as the quintessential pluripotent stem cell due to their ability to differentiate into every cell type of the adult organism. The earliest identification of ES cells differentiating into cells of the hepatic lineage resulted from spontaneous, or undirected, differentiation in which the ES cells are removed from the microenvironment sustaining self-renewal and pluripotency and allowing them to spontaneously generate more specified cell types. In one such study, Chinzei et al demonstrated that mES cells cultured as embryoid bodies (EBs) in the absence of LIF expressed detectable levels of AFP mRNA after 9 days, Albumin mRNA after 12 days, and secreted albumin after 15 days (Chinzei, Tanaka et al. 2002). They also demonstrated the ability to inject D9 EB cells into the portal vein and identify ES-derived cells in the liver after four weeks. However, spontaneous differentiation strategies result in extraordinarily low numbers of cells of the hepatic lineage interspersed with myriad other cell types.

Differentiation strategies quickly evolved to include signaling of relevant molecules by addition of exogenous factors to media. In an early study from our group, Schwartz et al demonstrated morphological and phenotypic characteristics of hepatocytes after 7 days of FBS-mediated differentiation of hES cells as EBs followed by attachment on type I collagen and an additional 14 days of culture in the presence of FGF4 and HGF (Schwartz, Linehan et al. 2005).

This and other similar studies eventually gave rise to a directed differentiation strategy in which the cells are guided through discrete stages of development by addition of relevant

signaling molecules to the media in an effort to recapitulate the sequence of cell fate decisions followed during *in vivo* development. We recently described an optimized four-step protocol that yields 20-30% hepatocyte-like cells from mouse and human ES and iPS cells (Roelandt, Pauwelyn et al. 2010). In this protocol, which is described in detail in the next chapter, cells are differentiated as a monolayer on Matrigel first to a definitive endoderm fate by addition of Activin A and Wnt3a, then to a hepatic endoderm fate by addition of bFGF and BMP4, then to a bipotential hepatoblast state by the FGF cocktail of aFGF, FGF4b, and FGF8, and finally to a hepatocyte-like cell fate by addition of HGF and Follistatin. This protocol results in high expression of a number of liver-enriched genes and transcription factors and cells exhibiting hepatic functions such as albumin and urea secretion.

A number of recent studies present multistep differentiation protocols similar to ours; Asgari et al, Nakamura et al, and Chen et al have all recently developed three-step, five-step, and three-step, respectively, protocols to generate cells of the hepatic lineage from hES and/or hiPS cells (Asgari, Moslem et al. 2011; Chen, Tseng et al. 2012; Nakamura, Saeki et al. 2012). Similar to our method, each of these protocols involves endoderm formation by a combination of Activin A and/or Wnt3a, a middle stage or stages to push toward hepatic endoderm lineage, and a final stage of hepatic maturation. The maturation stage for each of these involves treatment with Oncostatin M and Dexamethasone. More recently, Takayama et al have shown that a multi-step differentiation protocol very similar to ours can be enhanced by transient ectopic expression of FOXA2 and HNF1α at various stages of differentiation (Takayama, Inamura et al. 2012). In all of these studies, similar levels and extents of differentiation were achieved. Unfortunately, the expression and level of function of the differentiated cells fall well short of primary or *in vivo* hepatocytes, indicating that additional strategies must be developed to push terminal differentiation to a clinically relevant level.

2.3.2 Differentiation of bipotential hepatoblasts to hepatocytes

Perhaps the most intuitive starting cell population for hepatocyte differentiation is the bipotential hepatoblasts which are one cell fate decision removed from adult hepatocytes in the developing liver. Indeed, the liver is populated almost entirely of bipotential hepatoblasts as late as E15 to E16 in the mouse before nearly all of them terminally differentiate into hepatocytes, with the balance differentiating into the biliary tract lineage, as discussed in Section 2.2.4. Furthermore, since hepatoblasts undergo massive expansion as the liver bud forms and grows, a population of hepatoblasts could presumably be expanded in vitro to large numbers prior to a single-stage, highly efficient differentiation to mature hepatocytes. Conversely, hepatoblasts are present only in the fetal liver, so primary human hepatoblasts are virtually unavailable. If hepatoblasts could be generated from a more potent starting population, however, such as hES or hiPS cells, and purified and expanded as hepatoblasts, this system could be highly useful for generating clinically relevant hepatocytes. Indeed, ongoing studies in our group are focusing on this question.

Nevertheless, a number of groups have investigated the ability to isolate or generate bipotential hepatoblasts, proliferate them, and terminally differentiate them to hepatocytes with varying degrees of success. Suzuki et al purified a population of apparent hepatocyte progenitor cells from E11.5 and E13.5 fetal mouse liver cells by sorting a c-Kit-CD49f^{+}CD29^{+}CD45^{-}TER119^{-} population (Suzuki, Zheng et al. 2000). These cells exhibited proliferative capacity when cultured at low density in the presence of HGF and demonstrated bipotential differentiation to two discrete populations of cells after 21 days: one population expressing Albumin; and one population expressing CK19. Similarly, working with human fetal liver tissue, Lazaro et al dissociated first- and second-trimester fetal liver tissue into single cell suspensions and selected hepatoblasts by culturing on collagen-coated tissue culture plates with EGF (Lazaro, Croager et al. 2003). These cells exhibited an ability to proliferate in culture and differentiate to hepatocyte-like cells upon treatment with Oncostatin-M (OSM). Interesting, after extended culture for a month, a population of smaller cells clustered together became

apparent and were termed blast cells; upon further analysis these cells seemed to have some characteristics of oval cells.

Li et al recently demonstrated the ability to purify a population of hepatoblast-like cells from differentiated mES cells by selection for a $EpCAM^{+}c\text{-}Kit^{-}$ population of cells after a multistep differentiation protocol (Li, Liu et al. 2010). Although the resulting cells exhibited long-term expansion in culture and the ability to repopulate damaged liver tissue, the cells were limited in their ability to differentiate into hepatocytes in vitro, and evidence of unspecified definitive endoderm cells in the sorted population was observed. Nevertheless, this study demonstrates a proof of principle that, while still requiring optimization in selection, culture conditions, and differentiation strategy, the approach of generating hepatoblasts from pluripotent cells before expansion and differentiation to hepatocytes may be a good approach for reproducibly generating clinically significant numbers of hepatocyte-like cells from myriad genetic backgrounds.

2.3.3 Differentiation of bone marrow derived stem cells to hepatocytes

Although traditional bone marrow derived stem cell populations are lineage restricted, a number of reports have indicated the ability of certain bone marrow derived stem cell populations to differentiate toward the hepatic fate. We recently demonstrated the ability to differentiate multipotent adult progenitor cells (MAPCs), which were described extensively in Section 2.1.2.3, efficiently toward hepatocyte-like cells using our four-step directed differentiation protocol (Roelandt, Pauwelyn et al. 2010). Although rMAPC cannot be isolated directly from the bone marrow, they do arise from culture of bone marrow cells after 10-11 weeks, as we recently described (Subramanian, Geraerts et al. 2010). However, other cell populations from the bone marrow have also been described as having the plasticity to generate hepatic tissue.

Avital et al have reported the ability to isolate a population of bone marrow-derived hepatocyte stem cells (BDHSC) by sorting for $\beta_2m^{-}/Thy\text{-}1^{+}$ cells in freshly harvested bone marrow from rat and human (Avital, Inderbitzin et al. 2001). This cells exhibited

positive staining for albumin, AFP, CK8, and C/EBPα. These cells were found to secrete urea when co-cultured with primary rat hepatocytes and to be capable of proliferation and differentiation to more mature hepatocytes. However, the level of function of these BDHSC-derived hepatocytes was still far lower than that observed in primary hepatocytes. This study and other similar studies demonstrating the ability of certain bone marrow-derived stem cell populations to differentiate toward the hepatic fate suggests that the bone marrow may be a potential renewable source of hepatocyte-like cells. However, this area needs far more characterization and advancement in isolation, culture, and differentiation techniques to reproducibly yield high quality functional hepatocytes.

2.3.4 Transdifferentiation of other cell types to hepatocytes

Differentiating stem cell populations of various origins and potencies toward hepatocyte-like cells has proven limited success, and indeed utilizing the inherent mechanisms of cell fate determination is likely to be the most viable option for developing hepatocytes for therapeutic applications. However, an alternative approach similar to the generation of iPS cells through reprogramming is to generate hepatocytes or hepatocyte-like cells by transdifferentiation of other cell populations. The starting cell population may be another terminally differentiated cell type, such as pancreas cells, or stem cell populations with or without the potential to differentiate into hepatocytes.

Transdifferentiation may occur naturally in some instances from closely related cell types. As an example, it has been observed for more than twenty years that pancreas cells or pancreatic cancer cells, under specialized conditions, can give rise to hepatocyte or hepatocyte-like cells (for a review see Shen et al) (Shen, Horb et al. 2003). As discussed in previous sections, pancreas and liver tissues develop from adjacent regions of the foregut endoderm during embryonic development, with pancreas being the default program and liver being specified by specific signaling from the cardiac mesenchyme and other mesenchymal cells. So it is not surprising that, given appropriate specific cues,

some small fraction of pancreatic cells are capable of transdifferentiating to liver cells. While this phenomenon may be interesting from an academic perspective for studying the mechanisms underlying transdifferentiation, it is unlikely to have any clinical relevance given that pancreatic tissue is even more scarce than liver donors and that any pancreatic tissue available for transplant is likely to be used for the treatment of diabetes by harvest and transplantation of islets.

A recent study demonstrated the ability to directly reprogram fibrosblasts, which are much more readily available than pancreatic tissue, to hepatocyte-like cells, which they termed induced hepatocytes (iHep) by the forced expression of HNF4a in combination with either FOXA1, FOXA2, or FOXA3 (Sekiya and Suzuki 2011). The resulting cells exhibited gene expression and function characteristic of hepatocytes, although at levels much lower than primary hepatocytes, and demonstrated the ability to reconstitute hepatic tissue in fumarylacetoacetate hydrolase (*Fah*)-deficient ($Fah^{-/-}$) mice. Although this study used mouse fibroblasts, the principle is likely to be applicable in human cells with some modifications, as was the case in generating iPS cells.

Transdifferentiation has also been demonstrated from stem cell populations with limited or, at best, controversial differentiation capacity to the hepatic lineage. A number of studies have claimed the ability to transdifferentiate hematopoietic stem cells (HSCs) to hepatocyte-like cells. Khurana et al first demonstrated in 2008 the ability to generate hepatocyte-like cells from hematopoietic stem cells by culturing a specific fraction of HSCs ($Lin^{-}OSMRb^{+}$ bone marrow cells) in serum obtained from mice with induced liver-damage, presumably enriched with hepatic regenerative factors (Khurana and Mukhopadhyay 2008). These cells demonstrated some characteristics of hepatocyte-like cells including gene expression, microstructural characteristics, and some cytochrome P450 function. They subsequently showed that forced expression of HNF4a was capable of inducing transdifferentiation of this population of HSCs in a more efficient manner (Khurana, Jaiswal et al. 2010). Advantages of using HSCs as a starting population include ready availability of bone marrow for transplant and that bone marrow transplant has had FDA approval for a number of years, although this approach requires overcoming

the same hurdles as iPS differentiations, namely achieving physiologically relevant levels of hepatic function and eliminating viral expression systems used for transdifferentiation.

CHAPTER 3: MATERIALS AND METHODS

3.1 Rat Multipotent Adult Progenitor Cell (rMAPC) Culture

3.1.1 rMAPC Medium

Rat multipotent adult progenitor cells (rMAPCs) are expanded in rMAPC medium as previously described (Breyer, Estharabadi et al. 2006). rMAPC medium contains 60% low glucose Dulbecco's Modified Eagle Media (DMEM-LG; Gibco), 40% MCDB 201 Medium (Sigma), 1X insulin-transferrin-selenium (ITS; Sigma), 1X linoleic acid from bovine serum albumin (LA-BSA; Sigma), $5x10^{-8}$ M dexamethasone (Sigma), 10^{-4} M ascorbic acid 3-phosphate (Sigma), 100 units of penicillin, 1000 units of streptomycin (Pen/Strep; Cellgro), 2% fetal bovine serum (FBS; Hyclone), 10 ng/ml mouse epidermal growth factor (mEGF; Sigma), 10 ng/ml human platelet-derived growth factor (PDGF; R&D Systems), 1X β-mercaptoethanol (βME, Sigma), and 1000 units/ml mouse leukemia inhibitory factor (LIF, ESGRO; Chemicon). MCDB is prepared fresh by dissolving 17.7 grams (one bottle) in 1000 ml of purified, distilled water and adjusting the pH to 7.2 by addition of sodium hydroxide tablets. The MCDB is then vacuum-sterilized using a 0.22 μm filter and stored for up to one week at 4°C. All rMAPC medium components, with the exception of βME, are mixed together and vacuum-sterilized using a 0.22 mm filter and stored for up to four weeks at 4°C. βME is added fresh immediately prior to use, and the media is kept for only one week at 4°C after the addition of βME.

3.1.2 rMAPC Expansion

Routine rMAPC expansion and maintenance is carried out at low density on ten centimeter tissue culture dishes (Nunc) coated with 100 ng/ml rat fibronectin (FN; Sigma) in phosphate-buffered saline without calcium or magnesium (PBS, 1X, without calcium or magnesium; Cellgro). Prior to passaging, the dishes are coated with approximately 3 ml FN in PBS. The dishes are swirled gently to insure full covering of

the culture surface, and the coating is carried out for one hour at 37°C, two hours at room temperature, or overnight at 4°C.

rMAPCs are expanded in a climate-controlled incubator at 37°C with 5% oxygen (O_2) and 5.5-6% carbon dioxide (CO_2) and are kept at low density via passaging every two days. Media is aspirated from the dish and retained in a 15 or 50 ml Falcon tube for later use. The dish is then washed once by the addition of 5 ml PBS, gentle swirling, and aspirating the PBS. The rMAPCs are then removed from the surface of the dish via trypsinization by the addition of 1 ml 0.05% trypsin-EDTA (Cellgro, 25-052-Cl). To minimize the exposure to trypsin, the dishes are gently tapped to dislodge the cells. Once detachment is confirmed by microscopy, the trypsin is neutralized with 5 ml rMAPC media (containing 2% FBS). This media can be either recycled (the media retained in the Falcon tube) or fresh depending on preference and situation. The cells are then collected in the 15 or 50 ml Falcon tube and centrifuged at 1800 rpm and 4°C for 6 minutes. The supernatant is aspirated off, and the pellet is resuspended in fresh rMAPC media. Cells are counted using a hemacytometer and are plated at 250-350 cells/cm^2, or about 20,000 cells/dish. Prior to passaging, the dishes are coated with FN as previously described, and fresh rMAPC media is prewarmed for at least 20 minutes in the climate-controlled expansion incubator. FN is aspirated from the culture dish and replaced immediately with 6 ml prewarmed rMAPC media. The appropriate number of cells are pipetted onto the dish, and the dish is rocked gently to spread the cells out on the dish.

3.1.3 Freezing and Thawing of rMAPC

Freezing of early passage and/or karyotypically normal rMAPCs is carried out via a two-step process. Cells are collected from tissue culture dishes as described in the previous section, centrifuged, resuspended in fresh rMAPC media, and counted. The cells are then centrifuged again and the rMAPC media (supernatant) is aspirated off. The pellet is resuspended in 500 µl of step 1 freezing media, consisting of 80% rMAPC media and 20% FBS, for every 5-6x10^5 cells present in the pellet. The equivalent volume of step 2 freezing media, consisting of 60% rMAPC media, 20% FBS, and 20% dimethyl

sulphoxide (DMSO; Sigma, D2650), is added dropwise with constant swirling or tapping between drops. The suspension is then distributed into 1 ml cryovials, 1 ml per vial, and the cryovials are immediately transfered into an isopropanol jacket and placed in a –80°C freezer. The vials are kept in the –80°C freezer for 6 to 24 hours before being transferred to a liquid nitrogen storage tank.

Thawing is carried out quickly in order to remove the cells from DMSO, which is toxic to the cells, as quickly as possible. Vials are removed from the liquid nitrogen tank and transferred to a bucket containing dry ice. The vials are then swirled gently in a 37°C water bath until the suspension is about half frozen. The half-frozen suspension is then transferred into a 15 ml Falcon tube containing 10 ml fresh, cold (4°C) rMAPC media. This suspension is then centrifuged at 1000 rpm and 4°C for 8 minutes and the supernatant is aspirated and discarded. The pellet of cells is then resuspended in fresh, prewarmed rMAPC media and distributed onto one or two FN-coated tissue culture dishes in 6 ml rMAPC media, as was previously described for rMAPC expansion.

3.1.4 Isolation of rMAPC Lines

Rat MAPCs are isolated from either the entire hind limbs of newborn rats or the tibia and femurs of 3-4 week old rats, as described (Breyer, Estharabadi et al. 2006). Based on previous isolations, it appears that the probability of a successful isolation is inversely proportional to the age of the rodent; the younger the rat, the higher the likelihood of isolating rMAPC clones. Rats are euthanized using CO_2, and all steps are carried out in sterile conditions.

For newborn rats, the entire hind limbs are minced into very small pieces, followed by digestion with 0.2% collagenase in Media 199 (1X; Gibco, 11150059) by shaking at 37°C for approximately one hour on a shaker. For older rats, 3-4 weeks old, the tibia and femur are removed from each hind limb with special care to keep the heads of the bones intact, and the muscle and connective tissues are carefully removed. The bones are then flushed vigorously with 15 to 20 ml of Media 199 into a tissue culture dish using a 23-

guage needle until the bones appear transparent. If necessary, the very tip of the bone may be cut away from each side to allow for proper flushing; however, it is hypothesized that the cells of interest reside near the growth plates and endosteum at the end of the bone, so special care should be exercised to cut away minimal amounts of bone. For both procedures, cells are then triturated several times using a 23-guage needle until a single-cell suspension is observed. The suspension is then passed through a 40 μm nylon mesh strainer and collected in a Falcon tube. For newborn rats, the collagenase must then be neutralized with 10% FBS. The suspension is then centrifuged at 1800 rpm and 4°C for 6 minutes and washed two to three times with PBS or rMAPC media.

After washing, the pellet is suspended in fresh, prewarmed rMAPC media, counted, and approximately $6x10^6$ cells are transferred into each well of fibronectin-coated 6-well plates (Corning) in 2 ml rMAPC media. The plates are incubated at 37°C in 5% O_2 and 5.5-6% CO_2, the same conditions used for expansion of rMAPCs. On the third day, and every second day thereafter, an additional 1 ml of fresh, prewarmed rMAPC media is added to each well. After the first week, the majority of cells have attached to the plate, and half of the media is replaced with fresh, prewarmed rMAPC media every second day to maintain a volume of 4 ml media per well. From the second week to the end of the fourth week, the cells are monitored and, upon reaching confluence, are replated at approximately 70% confluence (i.e., split 2 to 3). After four weeks, column depletion is performed to remove $CD45^+$ and $Terr119^+$ cells in a CS column with magnetic microbeads specific for CD45 and Terr119. Cells collected from the column are centrifuged, suspended in fresh rMAPC media, and counted. They are then plated into fibronectin-coated 96-well plates (Corning) at a density of 10 cells/well in 50 μl of media. Half of the media is changed every 2-3 days, and the wells are monitored for two to three weeks until small colonies of 20-30 cells appear in the wells. Colonies morphologically resembling MAPCs (small round cells that are mostly nuclear) are selected and the contents of each selected well are transferred to one well of a fibronectin-coated 24 well plates. These individual 'clones' are expanded as necessary to maintain low cell density, avoiding cell-to-cell contact, and transferring to progressively

larger plates and dishes. Clones are constantly monitored and scored based on morphological resemblance to MAPCs. When the clones have grown to sufficient numbers, they are characterized using qRT-PCR for Oct-4 and Rex-1, flow cytometry for Oct-4, CD45 and CD41, karyotyping, G-banding, and differentiation potential. Cell lines are labeled as MAPCs based on phenotype and differentiation potential. It should be noted that, since cells are plated at 10 cells/well after column depletion, subcloning must be performed at some later time before the cell line can be rigorously labeled as a MAPC clone.

3.1.5 Formation of Three-Dimensional rMAPC Aggregates

Aggregates were formed from single cell suspensions of MAPCs using the forced aggregation method (Ng, Davis et al. 2005). Briefly, cells in suspension were seeded in each well of ultra-low attachment round bottomed 96 well plates (Corning) at 1000 cells/well in 100 μl of media, and centrifugal force (1500 rpm, 4 min) was applied to settle them to the bottom of the well thus facilitating agglomeration. The plates were subsequently incubated in a 37°C incubator at 5% oxygen and aggregates formed with time.

3.1.6 Differentiation of rMAPC to the Hepatic Lineage

For the monolayer differentiation, rMAPCs were plated in 24 or 12 well plates, pre-coated with 2% matrigel (BD Biosciences) at a starting cell density of 25,000 – 50,000 cells/cm^2 in rMAPC medium and maintained in a 5% O_2, 5.8% CO_2 incubator until 80-90% confluency was reached. For the aggregate differentiation, aggregates were allowed to form for four days after forced aggregation, as previously described (Subramanian, Park et al. 2011), and differentiation was continued in the 96 well U-bottom plates with one aggregate/well. To initiate differentiation, maintenance media was removed, the wells were rinsed with PBS, and the differentiation medium was added. During differentiation, the cells were maintained in a 21% O_2, 5% CO_2 environment. The basal medium for hepatic differentiation was similar to MAPC medium except for the

following: ITS and LA-BSA were at 25% of the level in MAPC medium, dexamethasone was at 0.4 μg/ml, and the three growth factors and serum were absent. Differentiations were carried out in four stages for a total of twenty days. On D0, D6, D10, and D14, complete media was replaced with fresh medium with the following growth factor supplements: (i) D0: Activin A at 100 ng/ml and Wnt3a at 50 ng/ml (Note: on D2.5 and D4, in 50% medium exchange, fresh medium containing only Activin A was added), (ii) D6: bFGF at 10 ng/ml and BMP4 at 50 ng/ml, (iii) D10: FGF8b at 25 ng/ml, aFGF at 50 ng/ml and FGF4 at 10 ng/ml, (iv) D14: HGF at 20 ng/ml and Follistatin at 100 ng/ml. During each stage, 50% of medium was exchanged every two days. The differentiation protocol is briefly summarized in Figure 8.

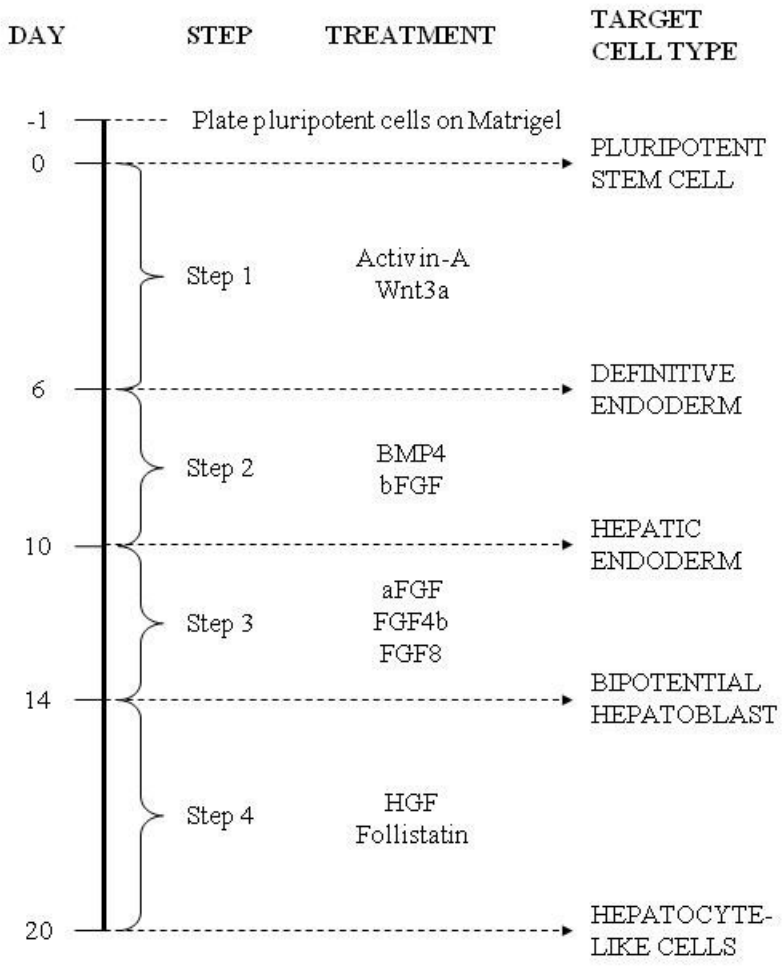

Figure 8: Schematic of monolayer hepatic differentiation protocol

3.2 Mouse Embryonic Fibroblast (MEF) Isolation and Culture

MEF cells were used as feeder cells to support the culture of human embryonic stem cells during expansion and routine maintenance. Due to the cost and variability of commercially available MEF for use as feeder cells for hESC culture, we derived, expanded, irradiated, and banked MEF cells in-house for use with hESC culture.

3.2.1 MEF Medium

MEF were maintained in a medium consisting of 90% (v/v) DMEM High Glucose (Invitrogen), 10% (v/v) fetal bovine serum (Hyclone), and 2 mM L-glutamine (Invitrogen).

3.2.2 MEF Isolation

MEF were isolated from pregnant mice at E13 or E14 of gestation as previous described (Bodnar, Meneses et al. 2004). Briefly, pregnant CF-1 mice (Charles River Laboratory) were obtained at E13 or E14 of pregnancy and sacrificed by cervical dislocation or CO_2 overdose. Immediately upon expiring, the abdomen of the mouse was sprayed with 70% ethanol, followed by exposure of the abdominal cavity by vertical midline incision. The uterine horns were removed and transferred to a tissue culture dish with DPBS prechilled to 4°C.

Working quickly, the individual fetuses were counted and removed from the uterus, followed by removal of the head and visceral tissues by manipulation with surgical scissors and forceps. Tissue was transferred to fresh dishes of prechilled DPBS as needed. Finally, the remaining fibroblastic tissue was transferred into a 10-cm tissue culture dish containing 4 ml of 0.25% (w/v) trypsin-EDTA (Invitrogen) and finely minced with two disposable surgical scalpels. When a single cell slurry suspension was achieved, or when the tissue had been in trypsin for a maximum of 10 minutes, the

trypsin was inactivated by addition of MEF culture medium containing 10% FBS which inactivates trypsin activity. The cell suspension was then washed twice in MEF culture medium by centrifugation at 1000 rpm at 4°C before being distributed at to T-175 culture flasks (Falcon) that were precoated with Embryomax 0.1% (w/v) gelatin solution (Millipore) at a density of two fetuses per flask. These MEF are defined as p0 (passage 0).

3.2.3 MEF Passaging

MEF were maintained and expanded in MEF medium on gelatin-coated T-175 flasks in a 37°C incubator until confluent. Upon reaching confluency, MEF were passaged by trypsinization. Briefly, the cells were rinsed with 10 ml PBS followed by addition of 1 ml 0.05% (w/v) trypsin EDTA to each flask. To insure coverage of the flask with a film of trypsin, 5 ml of trypsin was added to the flask, spread around by gentle shaking, and then 4 ml of trypsin was removed. This process was performed serially in up to 8 flasks per batch processing. The flasks were then incubated at 37°C for 3-5 minutes, followed by gentle tapping of each place to dislodge a single cell suspension. The trypsin was inactivated by addition of 5 ml MEF media per flask. The suspension was then pelleted by centrifugation at 1000 rpm and 4°C for 5 minutes, followed by cryopreservation (Section 3.2.4), irradiation (Section 3.2.5), or passaging into new gelatin-coated T-175 flasks.

Depending on the expansion rate of MEF, the cells were passaged at a ratio of 1:3 or 1:4. Generally, the first two passages (p0 to p1 and p1 to p2) were passaged at a ratio of 1:4 and the third passage was passaged at a ratio of 1:3.

3.2.4 MEF Cryopreservation

MEF were cryopreserved via a two-step freezing protocol. Briefly, MEF were harvested as a single-cell suspension by trypsinization as with MEF passaging (Section 3.2.3). The number of vials to be frozen was estimated based on cell density within the culture dish. In general, MEF were cultured until confluent, and the desired plating density upon thaw

was 60%, and a correction for surface area was included. Subsequent to centrifugation, the cell pellet was resuspended in 0.5 ml of MEF medium for each vial to be frozen. Finally, 0.5 ml of 2X freezing medium was added to the suspension, the suspension was mixed by gentle pipetting and then distributed at 1 ml per cryovial. The concentrated freezing medium consisted of MEF medium supplemented with an additional 30% (v/v) FBS and 20% (v/v) DMSO. The vials were frozen slowly to -80°C in a Mr. Frosty and transferred to liquid nitrogen after 12-24 hours.

MEF thawing was performed by removing the vial from the liquid nitrogen, briefly venting the cap to relieve pressure within the vial, and thawing quickly in a 37°C water bath with gentle swirling until a very small crystal of frozen cells was observed. The vial was the transferred to the cell culture hood, mixed by gentle pipetting, and added to 9 ml chilled MEF medium (9 ml medium + 1 ml cell suspension). The suspension was mixed by gentle swirling and centrifuged at 1000 rpm and 4°C for 5 min. The supernatent was discarded, and the pellet was resuspended in MEF medium to the desired volume, followed by seeding into the appropriate tissue culture dish precoated with 0.1% gelatin.

3.2.5 MEF Irradiation

Passage 3 (p3) MEF were non-lethally irradiated before being used as a feeder layer for human embryonic stem cell culture. Briefly, a batch of p3 MEF were harvested simultaneously (as described in Section 3.2.3), and after centrifugation were pooled together into a single 50-ml Falcon conical tube. The cell suspension was then exposed to 3000R of radiation. The irradiated cells were then centrifuged again and frozen into the desired number of vials as described in Section 3.2.4.

3.2.6 Plating MEF as Feeder Layer for hES Culture

As previously described, MEF were isolated from E13 to E14 pregnant mice and cultured to passage 3 prior to irradiation for use as a feeder layer. Approximately 24 hours prior to passaging human embryonic stem cells, MEF were thawed and plated on a gelatin-coated tissue culture dish to serve as a feeder layer for the ES cells. Although the number of

vials banked in each batch of irradiated MEF was determined based on a calculation of a desired density of 60% after thawing, variance in the survival and attachment of MEF varied between batches. Thus, each batch was first tested at various seeding densities to determine the appropriate distribution for vials from that batch.

The process for a typical batch is described. The p3 MEF were grown to confluency in T-175 tissue culture flasks. To calculate the number of vials to freeze per flask, a desired plating density of 60% was used with an assumed recovery of 50% and a desired distribution to 6 wells of a 6-well dish (approximately 60 cm^2). Therefore, the number of vials per flask was estimated to be 2.4 (0.5 * 175 cm^2 / 60 cm^2 / 0.6 = 2.43 vials). However, the recovery was often significantly better than 50%, resulting in higher cell density if only 6 wells were plated. Thus, for the first vial, the cells were distributed at densities corresponding to 4 wells, 6 wells, 10 wells, and 12 wells per vial to determine the optimum number of wells for distribution. All vials from that batch were then distributed to the determined number of wells after thawing.

3.3 Human Embryonic Stem (hES) Cell Culture

The hES cell line HSF6 was used for all experiments described in the hES sections of this study. However, it should be noted that there are many different hES lines, and correspondingly many methods of culturing hES cells. Therefore, all methods described in this section are specific for the cell line HSF6 unless otherwise noted.

3.3.1 hES Medium

HSF6 were maintained in a basal medium consisting of 80% (v/v) Knockout Dubelcco's modified Eagle medium (KO-DMEM) (Gibco) and 20% (v/v) Knockout Serum Replacer (Gibco) with 2 mM L-glutamine (Gibco), 0.1 μM nonessential amino acids (Gibco), and 0.1 μM β-mercaptoethanol (Invitrogen). The hES Basal Medium was filter sterilized and kept for up to 4 weeks at 4°C, and the hES Culture Medium was prepared by adding

FGF-2 to the hES Basal Medium and was stored at 4°C and used within one week of growth factor addition.

3.3.2 hES Expansion

HSF6 were passaged every 4-7 days depending on the size and density of the colony and impending differentiation of larger colonies, with full media replacement every day between passages. Daily inspection of the culture was necessary to determine the optimal time to passage the cells. Irradiated MEF p3 were plated (see Section 573.2.6) the day prior to HSF6 passaging. At any day during HSF6 culture, irregular colonies, such as those with significant differentiation, feeder clump integration, raised center, or lost boundaries, were removed prior to the media change by marking the colony under microscopy with a colony marking objective, removing the spent culture media, minimally covering the well with DPBS, and scraping the marked area with a sterile 200 µl pipette tip. The well was then rinsed again with DPBS, insuring the scraped colony was removed, and adding fresh culture media or collagenase.

To passage HSF6, the spent media was removed followed by a brief rinse with PBS. Subsequently, 0.1% (w/v) Collagenase Type IV (Gibco) in hES Basal Medium was added to the culture dish. The collagenase solution was made fresh and used within one week. The cells were then incubated at 37°C for 8-10 minutes followed by gentle scraping. Each well or plate was inspected for complete scraping by slightly tilting the plate and checking the light refractivity within the well; areas of the surface requiring further scraping were evident based on the light refraction. Furthermore, culture of HSF6 was generally limited to the corner wells (4 wells) of 6-well tissue culture plates to minimize the risk of contamination due to plate manipulation, and scraping was performed from two angles by rotating the dish 90°, allowing for nearly complete lid covering during the passaging process.

After scraping, the colonies were dissociated into numerous smaller colonies of 20-50 cells per colony by applying repeated sheer force on cell suspension. Generally, up to 4

wells of a 6-well tissue culture dish were combined into one well and sheer stress was applied by passing the cells through a 5-ml pipette tip pressed firmly against the bottom of the well at an angle just past flush. For small starting colony sizes, the cell suspension was sheered 4-5 times until feeder clumps were visibly dissociated; however, for larger colony sizes, the cell suspension was sheered 5-8 times until the small colonies reached appropriate sizes of 20-50 cells per colony as determined by inspection under microscopy.

The cell suspension was then collected into a 15-ml or 50-ml Falcon conical tube, and hES Basal Medium was added at 1.5 times the volume of the collagenase suspension. The cell suspension was centrifuged at 1000 rpm and 4°C for 5 minutes. The supernatant was removed, the pellet was loosened by gentle flicking of the tube, and another equal volume of hES Basal Medium was added with gentle pipetting to distribute the colonies evenly. The suspension was centrifuged a second time before being resuspended in hES Culture Medium and distributed to fresh wells containing an established MEF feeder layer. The MEF feeder layer was rinsed once with hES Basal Medium prior to seeding HSF6 to remove residual FBS from the MEF medium. Typically, HSF6 were passaged at a ratio of 1:3 to 1:6 depending on colony size and density, and 2.5 ml of hES Culture Medium was added to each well of a 6-well culture dish.

3.3.3 hES Cryopreservation

hES were cryopreserved by slow freezing in FBS supplemented with 10% DMSO. hES colonies were passaged as described in Section 3.3.2, except that the colonies were not broken up into as small of colonies; instead, shear stress was applied as described only until feeder clumps were no longer observable by visible inspection. Thus, slightly larger colonies were used for cryopreservation than for routine passaging and maintenance. After washing twice with hES Basal Media, as described, the cells were gently resuspended in 1 ml FBS+DMSO for each vial to be banked. Generally, colony densities were selected such that each vial would thaw into two wells of a 6-well tissue culture dish, assuming a 67% survival rate. Thus, for every three wells to be passaged into, one

vial was frozen. The vials were placed in a Mr. Frosty freezing container at -80°C for 16-24 hours before being transferred to liquid nitrogen for extended cryopreservation.

The day prior to thawing cryopreserved vial of hES, MEF feeder layers were plated as described in Section 3.2.6. hES thawing was performed by removing the vial from the liquid nitrogen, briefly venting the cap to relieve pressure within the vial, and thawing quickly in a 37°C water bath with gentle swirling until a very small crystal of frozen cells was observed. The vial was the transferred to the cell culture hood, mixed by gentle pipetting, and added to a 15-ml Falcon centrifuge tube. 9 ml chilled hES Basal Medium was then added to the tube slowly by adding one drop at a time to the wall of the tube and letting it run down, gently swirling to mix as the media was added. The suspension was mixed by gentle swirling and centrifuged at 1000 rpm and 4°C for 5 min. While centrifuging the hES cells, the MEF feeder layer was prepared by removing the supernatent from each well and briefly rinsing with 1 ml hES Basal Medium. 1.5 ml hES Medium was then added to each well. When centrifugation was complete, the supernatent was discarded, and the pellet was resuspended in hES Medium to the desired volume of 1 ml per well to be plated. The hES cells were then distributed to the wells for a total media volume of 2.5 ml per well of a 6-well tissue culture dish. Complete media was exchanged between 16-24 hours after thawing and every one or two days, depending on the acidity level, thereafter.

3.3.4 hES Monolayer Differentiation to Hepatic Lineage

Monolayer differentiation of HSF6 hES cells to the hepatic lineage was typically carried out in 12-well tissue culture dishes. Prior to passaging, the 12-well tissue culture dishes were precoated with 2% Matrigel (BD Biosciences). Briefly a 200 μl aliquot of Matrigel was thawed on ice for 15 minutes in a 4°C room followed by 15 minutes at room temperature but still on ice. The Matrigel was then combined with 10 ml KO-DMEM and sterile-filtered with a syringe-driven filter. The diluted Matrigel was distributed to each well of a 12-well tissue culture plate at a volume of 800 μl per well. The plate was incubated for at least one hour at 37°C prior to seeding hES cells for differentiation.

HSF6 in routine maintenance were carefully selected for differentiation based on growth characteristics in the passages before differentiation and by monitoring Oct4 and Sox2 expression levels by qPCR periodically. Colonies that were ready for differentiation were typically larger, well-defined colonies growing at a reasonably high colony density (~35-40% colony confluency within each well of a 6-well plate), and approximately four wells of a 6-well plate were used to seed a 12-well Matrigel-coated plate. Cells were passaged as described in Section 3.3.2, except colonies were allowed to remain larger by applying less shear stress. After the second wash, the cells were suspended in 12 ml of MEF-conditioned media (CM; briefly, hES Basal Media was added to irradiated MEF for 24 hours and collected as CM) supplemented with 4 ng/ml bFGF, and the cells were distributed to the 12-well plate at 1 ml per well.

To initiate differentiation, the CM was aspirated, the cells were rinsed once with PBS, and differentiation medium was added. The differentiation basal medium consisted of a 60/40 (v/v) mixture of low glucose Dulbecco's Modified Eagle media (DMEM) (Gibco, USA) and MCDB-201 (Sigma) and supplemented with 0.026 μg/ml ascorbic acid 3-phosphate (Sigma), linoleic acid bovine serum albumin (LA-BSA, Sigma)) (final concentrations of 1 mg/ml BSA and 8.13 μg/ml linoleic acid), insulin-transferrin-selenium (ITS, Sigma) (final concentration 2.5 μg/ml insulin, 1.38 μg/ml transferrin, 1.25 ng/ml sodium selenite), 0.4 μg/ml dexamethasone (Sigma), 4.3 μg/ml β-mercaptoethanol (Hyclone), 100 IU/ml penicillin and 100 μg/ml streptomycin (Gibco) and qualified fetal bovine serum (2% (v/v) for the first six days and 0.5% (v/v) for the subsequent time period). In addition, cytokines and growth factor supplements were added to the basal medium as follows: (i) D0: Activin A at 100 ng/ml and Wnt3a at 50 ng/ml (ii) D6: bFGF at 10 ng/ml and BMP4 at 50 ng/ml (iii) D10: FGF8b at 25 ng/ml, aFGF at 50 ng/ml and FGF4 at 10 ng/ml (iv) D14: HGF at 20 ng/ml and Follistatin at 100 ng/ml. Differentiations were carried out for twenty days with 50% media change, corresponding to the differentiation stage, every two days. On D0, D6, D10, and D14, complete medium was replaced with fresh medium with supplements for the ensuing differentiation stage after a brief rinse with PBS.

3.3.5 Harvesting Cells from Monolayer Differentiations

Cells were washed with PBS and then incubated with 0.1% (w/v) Collagenase Type IV (Invitrogen) for 15-20 minutes in the 37°C incubator. The cells were scraped gently using a cell scraper and transferred to a 15 ml conical tube. The cell suspension was centrifuged at 1000 rpm for 5 min and the supernatant was discarded. The cell pellet was incubated with 0.05% (w/v) trypsin-EDTA with 2% (v/v) chicken serum in a 37°C water bath for an additional 10 min with pipetting every 2 or 3 min. If single cells were not yet liberated, the cell suspension was gently triturated with an 18G syringe 3-5 times and then passed through a 100 um nylon mesh to obtain a single cell suspension. Cells were counted and viability was estimated using Trypan Blue exclusion.

3.3.6 Formation of Hepatic spheroids

Spheroids were formed using the forced aggregation method (Ng, Davis et al. 2005) with the cells harvested on D20 of hES differentiation. Briefly, in the forced aggregation method, cell suspension of approximately 8000 cells in 100 µl of differentiation basal medium supplemented with HGF (20 ng/ml) and Follistatin (100 ng/ml) was added to each well of an ultra-low attachment round bottomed 96 well plate (Corning) and centrifugal force (1500 rpm, 4 min) was applied to settle them to the bottom of the well, thereby forcing agglomeration. The plates were subsequently incubated in a 37°C incubator at 21% O_2 and 3D spheroids formed with time.

3.4 Primary Rat Hepatocyte Harvest and Spheroid Culture

Hepatocytes were harvested from 4-5 week old female Sprague-Dawley rats weighing 200-250 g using the two-step collagenase perfusion procedure (Seglen 1976). The isolated hepatocytes were plated in Williams E medium (Sigma) supplemented with 2.2 g/l sodium bicarbonate (Sigma), 20 ng/ml epidermal growth factor (EGF, Sigma), 10^{-7} M dexamethasone, 1X ITS (Sigma), 10^{-4} M L-Ascorbic Acid, and 100 IU/ml Penicillin and 100 µg/ml Streptomycin (Gibco) on 35 mm Falcon Primaria dishes (Becton Dickinson) at

approximately 10^6 cells/plate and kept in a 21% O_2, 5.8% CO_2 incubator to form the spheroids.

3.5 Quantitative Real-Time Polymerase Chain Reaction (qRT-PCR)

Total RNA is collected from undifferentiated rMAPCs, cells undergoing differentiation, and directly from pancreatic tissue using the Qiagen RNeasy microkit (Qiagen). Cells in culture are lysed directly on the tissue culture dish surface or in a 15 ml Falcon tube for cells not attached. The lysing procedure involves aspirating the media, rinsing the cells once in PBS, and finally lysing the cells using RLT lysis buffer + 1% βME, as prescribed by Qiagen. Each sample is collected in 350 μl of lysis buffer, vortexed for 30 second to homogenize the sample, and finally stored in a –80°C freezer for later processing.

Primary pancreas is surgically removed from the three-week old rats at the same time as rMAPC isolation. The pancreas is instantaneously frozen using the snap-freeze method in which the pancreas is placed into a vial and quickly submerged into an ethanol-dry ice slurry before being transferred to a –80°C freezer. Total RNA is collected from the tissue by dissociation and lysis in RLT lysis buffer + 1% βME at a volume of 350 μl lysis buffer per 5 mg tissue. The frozen tissue is submerged in the lysis buffer, and the tissue is triturated by vigorously passing it through a 20-guage needle until a single-cell suspension is observed. To quicken the process, the tissue can be placed directly into a 10 ml syringe, with the lysis buffer, and passed through a 20-guage needle several times. Once sufficiently triturated, the suspension is then transfered to a Qiagen Shredder column and centrifuged at 13200 rpm for three minutes. The supernatant contains the total RNA from the tissue and is processed downstream along with other sources of RNA.

Quantitative real-time polymerase chain reaction (qRT-PCR) is performed using the total RNA lysate as starting material. Messenger RNA (mRNA) is separated from the total lysate using the Qiagen RNeasy isolation procedure described elsewhere. DNA contaminants are eliminated by treatment with Turbo DNase free (Ambion, AM1907) at

37°C for 30 minutes. First-strand complementary DNA (cDNA) synthesis is performed using Superscript III reverse transcriptase (Invitrogen). The cDNA is then amplified over 40 cycles using an Eppendorf MasterCycler (*realplex*^{2} module), and the Ct value for each gene is defined as the cycle number at which the DNA concentration, synthesized using a primer specific for the gene of interest and quantified using SYBR Green (Invitrogen) fluorescense, crosses a threshold value positioned above the background noise contamination. Gene expression is quantified relative to a housekeeping gene, typically GAPDH, and is typically expressed as either expression relative to GAPDH, $\log_2$(expression relative to GAPDH), fold change relative to a reference, or $\log_2$(expression relative to a reference). The following formulas are used to calculate these values:

$$\Delta Ct\Big|_{t,gene} = Ct\Big|_{t,gene} - Ct\Big|_{t,GAPDH}$$

$$\text{fold change relative to GAPDH} = 2^{-\left(\Delta Ct\,|_{t,gene}\right)}$$

$$\Delta\Delta Ct\Big|_{t,gene} = \Delta Ct\Big|_{t,gene} - \Delta Ct\Big|_{t=0,gene}$$

$$\text{fold change relative to time 0} = 2^{-\left(\Delta\Delta Ct\,|_{t,gene}\right)}$$

3.6 Immunofluorescence

The presence of proteins are visualized under a fluorescent microscope by marking the proteins of interest with fluorescent dyes attached to specific antibodies or secondary antibodies that interact with primary antibodies for the proteins. Cells in culture are washed once with PBS and then fixed for 15 minutes at room temperature with 4% formalin. The cells are then permeabilized with PBST (250 µl Tween in 500 ml PBS) for 15 minutes at room temperature. The cells are then blocked against non-specific staining by treatment with 0.4% fish skin gelatin for 60 minutes at room temperature. The cells are then incubated in the presence of the specific antibody or isotype control (dilutions

chosen based on antibody, prepared to a volume of 400 μl / well of a 24-well plate) for two hours at room temperature. The cells are then washed three times with PBST and then incubated in the secondary antibody for 20 minutes. 2 ml of Hoescht 33258 for DAPI staining is then added to the well, which still contains the secondary antibody, for an additional ten minutes at room temperature. The cells are then washed three times with PBST and visualized beneath a fluorescent microscope.

3.7 Fluorescence-Activated Cell Sorting (FACS) Analysis

For each marker tested, positive and negative control cell populations are chosen. Typically, for Oct4 staining, high Oct4 rat MAPCs, in which the percentage of cells expressing Oct4 is known, are used for a positive control. In the absence of good positive controls, fluorescent beads can be used, although the size distribution (forward scatter and side scatter) will be quite different than in a cell population. For fluorescence-activated cell sorting (FACS) analysis, approximately $5x10^5$ cells are harvested for each sample being tested. Cells are trypsinized and centrifuged as in MAPC expansion. The pellets are washed twice in PBS and strained, if necessary, to create a single cell suspension. The cells are then counted and distributed into FACS tubes (Falcon) and an appropriate volume of PBS is added to result in 2 ml PBS. The cells are then centrifuged at 1400 rpm and 4°C for 6 minutes and washed twice with PBS. The cells are then washed once with 2 ml staining media. The cells are then suspended in 2 ml staining media and incubated at room temperature for one hour to block against non-specific binding. The cells are centrifuged, and the media is aspirated off. The primary antibodies and isotype controls are then added to the appropriate tubes and incubated for 30 minutes at room temperature. The cells are then washed once with staining media, and if no internal markers are being investigated, the cells are sorted using the FACS machine. If internal markers are being investigated, the cells are blocked for an additional 60 minutes at room temperature in 2 ml staining media, followed by centrifugation and permeabilization in 1ml 4% paraformaldehyde for 30 minutes at room temperature. The cells are then washed with staining media and incubated with the primary antibodies and isotype controls for the internal markers for 30 minutes at room

temperature. The cells are then washed twice in SAP Serum Buffer (0.1% saponin, 0.05% sodium azide in PBS with 10% donkey serum) and strained for cell sorting. The positive controls, negative controls, and isotype controls are used for proper gating, which sets the threshold for a positive verses negative reading for the presence of a particular marker.

3.8 Albumin Secretion Measurement by ELISA

Rat or human albumin was measured using a quantitative ELISA kit (Starters Kit Bethyl E101 and Bethyl E110-125 (rat) or E80-129 (human)) following the manufacturer's instructions. An internal standard, provided with the kit, was used to obtain a four-parametric logistic fit to enable the estimation of albumin concentration. The albumin concentration in the samples was subtracted from amount present in fresh medium to quantify the amount secreted by the cells in one day of incubation. The cell number was estimated and the albumin secretion was reported on a per cell basis.

3.9 Urea Secretion Measurement

To quantify urea secretion, cells were rinsed with PBS then grown in hepatocyte differentiation basal medium containing 1 mM ammonia-bicarbonate and 0.5% FBS for 24 hr. Supernatant was kept at -80°C until urea was measured using the QuantiChrom^{TM} Urea Assay Kit (BioAssay Systems DIUR-500). Cells were counted at D20, and urea secretion was reported on a per cell basis.

3.10 Cytochrome P450 Activity by Confocal Imaging

For drug treatment conditions, spheroids were incubated for 24 hours in differentiation media with or without 50 μM β-Naphthoflavone (BNF) or 500 μM Phenobarbital (PB) as indicated. After the treatment period, spheroids were collected and washed once with assay media (phenol red free (PRF) Williams' Medium E supplemented with 25 mM dicumarol and 2 mM probenecid at pH 7.4), followed by incubation for 10 min at 37C in assay medium. An equal volume of assay medium containing 2X ethoxyresorufin (ER,

39 μM final concentration) or 2X pentoxyresorufin (PR, 20 μM final concentration) was added to each well, and the spheroids were incubated for 30 minutes at 37C. The samples were then transferred to concavity microscope slides (Electron Microscopy Sciences), covered with a coverslip, and sealed for imaging. Confocal laser scanning microscopy was performed using an Olympus FluoView FV1000 Inverted microscope, and images were processed using ImageJ software (University Imaging Center, University of Minnesota). Briefly, z-stacks were collected using a 10X objective with step sizes of 4.36 μm with 10-15 sections for each spheroid, and the final image was prepared by projecting the maximum intensity from each z-slice into a single image. Background fluorescence was subtracted based on negative controls (samples processed identically but without ER or PR).

3.11 Intracellular staining for Albumin by flow cytometry

Cells were harvested by trypsinization, washed with PBS thrice, and suspended at 100,000 cells per tube. Cells were fixed with 4% paraformaldehyde for 15-20 min at RT then permeabilized in SAP buffer (PBS with 0.1% (w/v) saponin and 0.05% (w/v) sodium azide) for 30 min at 4°C. An incubation at 4°C with 1 μg/ml rat-albumin-specific antibody (Dako, A0001) or 1 μg/ml Rabbit IgG isotype control (Jackson Immunoresearch) in SAP buffer for 15 min was followed by three washes of SAP buffer and incubation with Cy5 labeled anti-rabbit IgG (Jackson Immunoresearch, 1:500 in SAP buffer) for 30 min in the dark. Finally, cells were washed thrice with SAP buffer, filtered, and resuspended in 500 μl PBS for flow cytometric analysis using FACS Calibur (Becton Dickinson).

3.12 Immunohistochemistry

Cells were fixed with 4% paraformaldehyde for 30 min and washed with PBS. The samples were incubated in 5% sucrose in PBS overnight and supercooled with isopentane before freezing in OCT for sectioning. H_2O_2 was used to inhibit endogenous peroxidase, and fetal bovine serum (FBS) was used to reduce non-specific binding. Cells were then

incubated with antibodies against AFP (Neomarkers, 1:75 dilution), CK18 (Abcam, 1:75 dilution), albumin (MP Biomedicals, 1:5000 dilution), or E-cadherin (BD Biosciences, 1:150 dilution). The antibody treated samples were then treated with EnVision-Peroxidase with DAB substrate (Dako) and examined under microscope. To rule out non-specific binding, samples were stained with the secondary antibodies only without primary antibodies.

3.13 Scanning Electron Microscopy

Spheroids from D30 of differentiation culture were collected and washed twice with PBS followed by fixation in 1 ml glutaraldehyde (8% glutaraldehyde in 0.2M sodium cacodylate buffer at pH 7.2) for 90 minutes at room temperature. The samples were then washed 3 times with 0.1M sodium cacodylate buffer for 5, 10, and 10 min, sequentially. Post-fixation was performed in 1 ml of 1% (w/v) osmium tetraoxide (2% (w/v) osmium tetraoxide in 0.2M sodium cacodylate buffer at pH 7.2). Samples were then rinsed three times with distilled water for 10, 15, and 15 min, sequentially. The samples were then dried by exposure to increasing concentrations of ethanol: 50% ethanol for 10 min, 75% ethanol for 15 min, 100% ethanol for 15 min, and dry ethanol twice, once for 20 min and a second time for 30 min. The samples were then mounted on aluminum stubs using double-sided carbon adhesive tabs, sputter-coated with gold-palladium, and imaged using a scanning electron microscope (S3500N; Hitachi High Technologies America, Inc.; Schaumberg, Illinois) at an accelerating voltage of 5 kV. Sample processing and imaging were performed at the Imaging Center in the College of Biological Sciences at the University of Minnesota.

3.14 Transmission Electron Microscopy

Spheroids from D30 of differentiation were harvested and washed thrice (3X 5 minutes) with 0.1M cacodylate buffer, followed by fixation in 2.5% glutaraldehyde and 0.1M sodium cacodylate buffer (pH 7.2) for 40 minutes at RT. Postfixation was performed in in 1% osmium tetroxide and 0.1M of cacodylate buffer, and the samples were

subsequently dehydrated in graded series of ethanol followed by propylene oxide treatment and embedded in epoxy resin. Ultrathin sections were cut, stained with uranyl acetate and lead citrate, and examined using a JEOL 1200 EXII electron microscope at the Characterization Facility at the University of Minnesota. Sample processing and electron microscopy was performed by Ms. Fang Zhou, Characterization Facility, University of Minnesota.

3.15 Timelapse Imaging of Spheroid Formation

Cells from D22 monolayer differentiation were harvested according to the previously described protocol and seeded for differentiation at 8000 cells/well in each well of a 96-well ultra-low attachment plate. After centrifugation, the plate was placed on a motorized stage in a climate-controlled chamber (37C, 5% CO2), and phase contrast images were collected in each of 6 wells, at 5 z-positions (separated by 10 μm each) every 7 minutes for 48 hours. Image processing was performed using ImageJ software (University Imaging Center, University of Minnesota) to generate the movie file.

3.16 Viability Stain of Forming Spheroids

Two days after seeding for spheroid formation, cells were stained for viability with Calcein-AM (5 μM final concentration), which labels viable cells only with green fluorescence (γ_{em} 490 nm, γ_{ex} 515 nm) and propidium iodide (2 μg/ml final concentration), which labels dead cells only with a red fluorescence (γ_{em} 535 nm, γ_{ex} 515 nm). The mixture was added as a 20X concentrated solution to individual wells by pipetting gently into the edge of the meniscus to prevent disturbing the spatial arrangement of cells within each well. The sample was incubated for 30 minutes at 37C before fluorescent imaging was performed. Image processing was performed using ImageJ software (University Imaging Center, University of Minnesota).

3.17 Cell Surface staining for ASGPR-1 by flow cytometry

Cells were harvested by cell dissociation protocol (described above), washed with PBS three times, counted, and distributed to 100,000 cells per FACS tube. Cells were fixed in 4% paraformaldehyde for 15-20 mins at RT. Subsequently, cells were incubated for 30 minutes with 10 μg/ml ASGPR-1 antibody (Thermoscientific) or 10 μg/ml mouse IgG_1 isotype control (R&D) diluted in a buffer (PBS with 2%(w/v) bovine-serum albumin (BSA, Sigma)). The cells were then washed with buffer and incubated with Alexa-fluor 488 labeled anti-mouse IgG_1 (Molecular Probes, 1:500 in buffer) for 30 minutes at RT in the dark. Finally, cells were washed three times with buffer, filtered, and resuspended in 500 μl PBS for flow cytometry analysis using FACS Calibur (Becton Dickinson).

3.18 PEPCK Immunofluorescence Staining and Flow Cytometry

Differentiated spheroids from D32 were harvested as whole spheroids, washed with PBS and fixed by treatment with 4% paraformaldehyde at room temperature for 20 min. After fixation, the cells were treated with 1 g/L Triton X-100 and 5% FBS at room temperature for 1 hr for blocking, and then incubated overnight at 4ºC with primary antibody anti-human PEPCK (Santa Cruz, 0.1 μg/ml in blocking solution). The samples were then washed thrice with PBS and incubated at room temperature with Alexa-fluor 488 conjugated anti-rabbit secondary antibody (Molecular Probes, 1:500 dilution) for 30 min, followed by nuclear labeling with 1mM Hoechst 33258 (Sigma) for an additional 10 min. The samples were then washed twice with PBS and transferred onto a concavity microscope slide (Electron Microscopy Sciences), covered with a coverslip, and sealed for imaging. Confocal laser scanning microscopy was performed on an Olympus FluoView FV100 Inverted microscope, and image analysis was performed using ImageJ software (University Imaging Center, University of Minnesota). Background intensities were removed based on a control sample (secondary antibody only).

For FACS analysis of PEPCK expression, differentiated spheroids were dissociated as previously described prior to fixation. Cells were labeled using PEPCK antibody as

described above for imaging, and FACS analysis was performed as described for ASGPR-1.

3.19 Biliary Excretion visualization by fluorescein staining

Biliary accumulation of cleaved fluorescein from fluorescein diacetate was observed on D32 differentiated spheroids. The spheroids were washed in phenol-red free (PRF) Williams' E medium twice followed by incubation with 3μg/ml fluorescein diacetate (FDA) (Molecular probes) in PRF William's E medium at 37°C for 40 min. The samples were then washed once with PRF Williams' E medium and transferred onto a concavity microscope slide (Electron Microscopy Sciences), covered with a coverslip, and sealed for imaging. Confocal laser scanning microscopy was performed on an Olympus FluoView FV100 Inverted microscope, and image analysis was performed using ImageJ software (University Imaging Center, University of Minnesota). Briefly, z-stacks were obtained at steps of 2 μm, and a stack of 10-15 images (20-30 μm) was selected that spanned representative sections of fluorescein accumulation. The maximum intensities of these images were projected into a single image, and the background intensities were removed based on negative control images (spheroids processed without FDA).

CHAPTER 4: ENHANCED DIFFERENTIATION OF rMAPC TO HEPATIC LINEAGE BY THREE-DIMENSIONAL AGGREGATE CULTURE

4.1 Introduction

Our group recently developed a multi-stage protocol for the directed differentiation of rat multipotent adult progenitor cells (rMAPC) as a monolayer . However, this protocol leads to a heterogeneous population with a relatively small fraction of hepatocyte-like cells. We hypothesized that further optimization of the culture system may increase the yield and functional maturity of these rMAPC-derived hepatocyte-like cells.

It has been previously demonstrated by our group and others that primary hepatocytes exhibit higher levels of hepatic-specific function, such as albumin and urea synthesis and cytochrome P450 activity, for a longer period of time *in vitro* when cultured as three-dimensional (3D) spheroids as compared to monolayer culture (Koide, Sakaguchi et al. 1990; Wu, Friend et al. 1999; Tzanakakis, Waxman et al. 2002). A number of factors such as the microenvironment, cell-cell interactions, and cellular polarization may play a positive role in sustaining liver specific functions in those hepatocyte spheroids. Thus, it is worth exploring whether such positive effects of 3D cultivation translate to the differentiation of stem cells to hepatocyte-like cells. Differentiation to the hepatic lineage in 3D culture has been attempted using both ESC (Imamura, Cui et al. 2004; Baharvand, Hashemi et al. 2006) and Mesenchymal Stem Cells (MSC) (Ong, Dai et al. 2006; Kazemnejad, Allameh et al. 2008) with encouraging results. However, those early studies were performed with single step protocols, not with the multi-step directed differentiation methods that have been employed recently with more success. Human ESCs differentiated using a multi-step directed hepatic differentiation protocol (Cai, Zhao et al. 2007) in a 3D four-compartment hollow fiber capillary membrane perfusion platform exhibited enhanced hepatic differentiation(Miki, Ring et al. 2011). However, further exploration is needed to optimize the differentiation protocol and culture

conditions to yield mature hepatocyte-like cells capable of functioning at the level of primary hepatocytes.

In this study, we applied the multi-step directed differentiation protocol, previously optimized for monolayer differentiation (Roelandt, Pauwelyn et al. 2010), to a spheroid-like aggregate culture system. We recently demonstrated that MAPCs as aggregates can be expanded 85 fold within four days of stirred spinner flask culture to reach a final cell concentration of approximately 10^6 cells/ml (Subramanian, Park et al. 2011). The propensity of differentiation of these spinner-expanded cell aggregates to 'hepatocyte-like' cells was also shown. Given the ease of scalability of the aggregates and the established ability to generate cells with hepatic functions in two-dimensional monolayer culture, we explored whether hepatic maturation would be further increased in differentiations carried out using a directed differentiation protocol on cells cultured as aggregates.

4.2 Results

4.2.1 Liver differentiation in 3D aggregates

Rat MAPC aggregates were allowed to form by the forced aggregation method for four days, yielding one cell aggregate in each well of a 96 well plate. Differentiation was initiated by the addition of 100 µl differentiation medium per well for a starting cell concentration of $1.5x10^5$ cell/ml. In addition, rMAPC differentiation to the hepatic cell lineage was also carried out in monolayer cell culture on matrigel coated plates at a similar cell concentration. Three biological replica cultures were performed for each condition. A four-step differentiation protocol designed to mimic embryonic liver development was used to direct the cells to 'hepatocyte-like' cells over a period of twenty days (Roelandt, Pauwelyn et al. 2010). The cells were treated with Activin-A and Wnt3a till D6 to induce differentiation to mesendoderm and definitive endoderm (Zhou, Sasaki et al. 1993; Lowe, Yamada et al. 2001; Rivera-Perez and Magnuson 2005; D'Amour, Bang et al. 2006; Bakre, Hoi et al. 2007). The transition through this stage was monitored

by the expression of *Goosecoid (Gsc), eomesodermin (Eomes), Mixl1,* and *Foxa2* transcripts. Next, to specify the cells to the ventral foregut endoderm/hepatoblast, FGF2 and BMP4 were supplemented to the medium from D6 to D10 (Jung, Zheng et al. 1999; Rossi, Dunn et al. 2001; Serls, Doherty et al. 2005; Zaret and Grompe 2008); expression of *Afp* and *Ttr* transcripts, typical hepatoblast markers, was evaluated. To promote proliferation of hepatoblasts and maturation to 'hepatocyte-like' cells, FGF8b, FGF1, and FGF4, were added between D10 and D14 (Sekhon, Tan et al. 2004), and HGF and Follistatin-288 from D14 to D20.

Generation of cells with mature hepatic functions was assessed by qRT-PCR for several hepatic specific genes: *albumin (Alb)*, a protein secreted by hepatoblasts and mature hepatocytes; *Arginase 1 (Arg1)* of the urea cycle; *phosphoenolpyruvate carboxykinase (Pepck) and glucose 6-phosphatase (G6pc)* of the gluconeogenesis pathway; *microsomal GST1 (mGst1)* of the glutathione-S-transferase (GST) pathway; *Factor 7 (F7)* of the coagulation factor cascade; *Mrp2,* a bile acid transporter; and *Hepatocyte nuclear factor 4a (HNF4a),* a liver enriched transcription factor.

We first assessed if MAPC aggregate cultures remained undifferentiated after four days of formation by assessing expression of *Oct4* transcript and several genes expressed early during differentiation. *Oct4* transcripts were at a similar high level in aggregate and monolayer cultures on D0 (Figure 9a,b) while levels of *Gsc, Afp, Albumin, G6pc* and *Tat* were all undetectable (data not shown). This is consistent with published data in that *Oct4* remained high after MAPC aggregate formation, while differentiation markers were low or undetectable (Subramanian, Park et al. In Press). Thus, at the start of differentiation, cells in both monolayer and aggregate cultures were undifferentiated. The expression level of *Oct4* transcripts decreased by 16-32 fold in both cultures as early as D6 and subsequently remained relatively unchanged. Transcripts for the definitive endoderm genes *Gsc, Eomes, Mixl1, and Foxa2* increased and peaked on D6 in both cultures (Figure 9c,d). A similar increase in expression of transcripts for the hepatic endoderm markers *Afp* and *Ttr* was observed on D10 in both culture systems and remained unchanged till D20 (Figure 9e,f), suggesting that cells progress through definitive

endoderm and hepatoblast stages with similar efficiencies in both monolayer and aggregate cultures.

The transcript level for *albumin*, which was similar for both conditions during the first two stages of differentiation (to D10), became more than 17 fold higher in the aggregate culture as compared to the monolayer culture on D20 (Figure 9e,f). Similarly, transcript levels of several other mature hepatic genes such as *G6pc* (11-fold), *Pepck* (69-fold), *mGst1* (8-fold), and *Hnf4a* (4-fold) were significantly higher in aggregate cultures on D20, based on p-values of less than 0.05 (Figure 9g). A trend of higher levels of transcripts was observed for several other mature hepatocyte genes, such as *Arg1* (6-fold), *Ttr* (2-fold), *Aat* (2-fold), *Tat* (2-fold), and *Mrp2* (1.4-fold), in aggregate cultures compared to monolayer cultures on D20, although the higher p-values cast doubt on the significance of the differences (Figure 9g). Therefore, although the dynamics of expression of stage-specific genes were similar between the monolayer and aggregate differentiations through D10, the expression levels of some hepatocyte specific transcripts were significantly higher in aggregate differentiation on D20. The expression levels of several non-hepatic lineage transcripts, including *pancreatic and duodenal homeobox 1 (Pdx1)*, *neurogenin-3 (Ngn3), VE-cadherin (Ve-cad)*, and *paired box gene 6 (Pax6)*, on D20 were either similar in both conditions or significantly lower in aggregate cultures (Figure 9h).

4.2.2 Albumin Expression in Hepatocyte-Like Cells

We next compared the fraction of albumin positive cells in the entire population by fluorescence-activated cell sorting (FACS) in aggregate and monolayer cultures (Figure 10). Primary hepatocytes isolated from adult rat liver were used as a positive control. rMAPC-progeny cultured for 6 days without cytokines, in which no *albumin* transcripts were detected, were used as a negative control. Gating was set such that false positives in the negative control were limited to 0.5%. With this gating, 92.3% of the primary hepatocyte population was albumin positive (Figure 10a). The data, including the samples and their isotype matched controls, are presented as histogram plots wherein the

relative abundance of cells expressing albumin protein at a particular intensity can be enumerated. In the D20 aggregate differentiation sample, 12% of the population expressed albumin protein at levels comparable to adult hepatocytes (Figure 10b). In contrast, 0.67% of the population from the D20 monolayer culture expressed albumin protein at similar levels (Figure 10c), and this population virtually overlapped with the negative control. To further investigate the fraction of cells expressing albumin in each population, data of albumin and side scattering intensities were shown as a contour plot (Figure 11). Gating on the side scatter intensity axis was set such that >99% of hepatocytes fell in the positive region (upper two quadrants). These data demonstrate that 5.9% of the cells from the aggregate culture had similar side scatter characteristics as primary hepatocytes (Figure 11a), suggesting a similar level of cell complexity and granularity between the two samples, in addition to their comparable levels of albumin expression. Only 0.3% of cells from the monolayer differentiation had similar side scatter characteristics as primary hepatocytes (Figure 11b). Thus, a larger fraction of cells from the aggregate differentiation appear to possess primary 'hepatocyte-like' features.

4.2.3 Albumin Secretion by Aggregate Progeny

We next tested whether the increased albumin transcript and protein levels in the aggregate culture were reflected in increased albumin secretion. Albumin production was measured, normalized to the number of cells, and compared to primary rat hepatocytes cultured as spheroids. The albumin secretion rate of the aggregate culture on D20 was 1.8 ± 1.0 pg/cell/day, which was at least 10 times that of the secretion in the monolayer culture (0.1 ± 0.06 pg/cell/day) (Figure 12a) and 20% of that of adult hepatocytes spheroids (8.3 ± 3.7 pg/cell/day). Considering that only 12% of aggregate-progeny contained significant amounts of albumin protein, it is possible that this small population of cells may produce albumin at levels comparable to primary hepatocytes cultured as spheroids.

4.2.4 Other Mature Hepatocyte Functions

The urea secretion rate of aggregates from D20 was measured. On a per cell basis the rate, 32 ± 12 urea pg/cell/day, was 2.5 times of the corresponding D20 monolayer culture (13 ± 5 pg/cell/day) and at a 25% level of primary hepatocyte spheroids (132 ± 20 pg/cell/day), respectively (Figure 12b). Cytochrome P450 activity in the aggregates was assessed by CYP1A (EROD) activities. The rate of resorufin generation from ethoxyresorufin and its subsequence release into the culture media was quantified on undifferentiated and differentiated cells with or without BNF treatment and compared to activity in rat hepatocyte spheroids (Figure 13). Negligible activity was observed in undifferentiated rMAPCs in both monolayer and aggregate cultures. However, on D20 of the differentiation, cells maintained in the aggregate culture exhibited higher EROD activity (1008 pmol/hr/10^6 cells) than cells from the monolayer culture (172 pmol/hr/10^6 cells). EROD activity increased in both cultures after a 24 hour treatment with BNF to 5150 and 1280 pmol/hr/10^6 cells in aggregate and monolayer cultures, respectively. These EROD activity levels corresponded to 34.5% (aggregate) and 8.6% (monolayer) of the activity observed in BNF-treated rat hepatocyte spheroids (14900 pmol/hr/10^6 cells).

We also assessed EROD and PROD activities by imaging intracellular accumulation of the fluorescent reaction product. Although the method is qualitative, it provides a more sensitive assessment than the resorufin release assay. Higher EROD and PROD induced fluorescence can be seen in the D20 differentiated aggregates as compared to D0 undifferentiated samples (Figure 14 and Figure 15). The expression of *Cyp1A1* and *Cyp2B1/2* transcripts was also investigated by RT-PCR. Expression levels of *Cyp1A1* and *Cyp2B1/2* transcripts were higher in the aggregate culture samples as compared to the monolayer cultures (Figure 16). No *Cyp1A1* or *Cyp2B1/2* transcript expression was observed in the undifferentiated samples.

4.2.5 Morphological and Structural Features in Differentiated Aggregates

The morphological and structural characteristics of the differentiated aggregates were examined by transmission electron microscopy (Figure 17). Cells in the aggregates on

D0 (Figure 17a,b) had a high nucleus to cytoplasm ratio. In differentiated aggregates, cells had developed a polygonal epithelial shape with low nucleus to cytoplasm ratio and much more complex cytoplasmic features (Figure 17c-e). Abundance of mitochondria, rough ER, canaliculi-like structures between cells delimited by tight junctions on both ends, and microvilli (Figure 17f), features indicative of a differentiated 'hepatocyte-like' cell structure (Dvir-Ginzberg, Elkayam et al. 2004), were identifiable within the cells.

Immunostaining was performed on the aggregates on D0 and D16 or D20 for AFP, CK18, E-Cadherin and Albumin (Figure 18). No AFP, CK18 or Albumin immunoreactivity was found in the aggregates on D0. On D16 of differentiation, AFP was localized to cells on the exterior of the aggregate (Figure 18a), and on D20, CK18 (Figure 18b) and albumin (Figure 18d) were also observed to localize to the cytoplasm of cells on the exterior of the aggregate. Cell-cell adhesion protein E-cadherin is seen at both D0 and D16 in the cell membranes of some cells (Figure 18c).

4.3 Discussion

In this study in which we combined directed multi-step differentiation of MAPCs toward the hepatocyte lineage with a three-dimensional aggregate culture system, we observed an enhanced level of differentiation and a higher degree of maturity of MAPC derived hepatocytes as compared to differentiation in monolayer culture. Many mature hepatocyte specific genes were expressed at higher transcript levels in the aggregate culture than in the monolayer, including members of the gluconeogenesis pathway (*Pepck, G6pc*), glutathione conjugation (*mGst1*), and liver-enriched transcription factors (*Hnf4a*).

The enhanced hepatocyte differentiation in aggregate cultures, as compared to the monolayer culture, could be attributed either to a larger fraction of 'hepatocyte-like' cells in the population with similar levels of maturation, to a higher level of maturation in a similar fraction of 'hepatocyte-like' cells within the population, or to a combination of both. It is also conceivable the aggregate culture sustains differentiated 'hepatocyte-like'

properties better and contributes to the observed higher activities. The expression levels of mesendoderm, definitive endoderm, and hepatoblast transcripts were similar between the aggregate and monolayer cultures up to the midstage of differentiation, suggesting that a similar fraction of cells were induced towards liver-endoderm in both differentiation systems. It is therefore likely that the increased hepatocyte specific transcript levels observed in the aggregate differentiation are at least partly due to an enhancement in the terminal stage of differentiation to more mature hepatocytes. The larger fraction of cells with increased maturity is indeed shown by intracellular albumin protein expression using flow cytometry. The albumin-positive cells seen in the aggregate culture, comprising 12% of the bulk population, had levels of intracellular albumin similar to primary hepatocytes. They also exhibited similar granularity and cellular complexity to primary hepatocytes as suggested by the side scatter profile. The albumin staining protocol was optimized to eliminate background staining in undifferentiated MAPCs; the substantially reduced false positive staining may have been at the expense of a lower sensitivity in identifying the positive cells, as suggested by the relatively low level of positive cells in the monolayer culture.

The relative differentiation efficiency can be estimated from the input of stem cells and the resulting hepatocyte-like cells. Using the initial seeded rMAPC density and the number of albumin positive cells on D20, the efficiency of hepatocyte-like cell generation is estimated to be 60% and 3.85% for aggregate and monolayer culture, respectively.

Overall, the results suggest that the increased transcript levels of hepatocyte specific genes in the aggregate culture is likely the result of enhanced differentiation of the hepatoblasts to cells with more mature functions in the final stages of differentiation. Indeed, the maturation of fetal liver cells into functional hepatocytes has been demonstrated in three-dimensional based systems using various cytokines, including acidic FGF, FGF4, and HGF, which are present in the late stages of our protocol (Jiang, Kojima et al. 2004; Hanada, Kojima et al. 2007). However, it is not clear if and why these growth factors are more effective in aggregate culture than in monolayer. Hepatocytes

cultured as spheroids sustain higher levels of liver specific functions over a longer period than when maintained in the conventional monolayer culture. The sustained functions are synchronous to structural and morphological characteristics of spheroids, including the existence of tight cell-cell contact, retention of cell-cell junctions, and polarization (Koide, Sakaguchi et al. 1990; Peshwa, Wu et al. 1996; Wu, Friend et al. 1999; Abu-Absi, Friend et al. 2002; Schwartz, Reyes et al. 2002; Tzanakakis, Waxman et al. 2002). Under TEM, cells in the differentiated aggregates appeared to be abundant in tight junctions at cell-cell boundaries. Bile-canaliculi-like openings possessing microvilli and delimited by tight junctions were also highly visible.

A key feature to the three-dimensional aggregate system is the extensive cell-cell contact, which may have contributed to the enhanced differentiation. E-cadherin, which plays a key role in cell polarity and junction formation, is seen at cell-cell contacts. It has been shown to regulate signaling in some systems (e.g., in Caco-2 enterocytes) by controlling the nuclear abundance of liver transcription factor Hnf4a (Peignon, Thenet et al. 2006). Using a surface deposited with different amount of E-cadherin, it was shown that hepatocytes have higher levels of albumin and urea secretion when exposed to higher concentrations of cadherin (Semler, Dasgupta et al. 2005). Similarly, mouse ESCs grown as embryoid bodies (EBs) over-expressing E-cadherin were shown to have higher transcript levels of *G6pc* in response to growth factor cocktails than EBs in which E-cadherin expression was down-regulated (Dasgupta, Hughey et al. 2005). Other than cell-cell interactions, polarization of cells in 3D configurations has been shown to help in enhancing and stabilizing the differentiated functions of hepatoyctes (Abu-Absi, Friend et al. 2002; Haouzi, Baghdiguian et al. 2005). Whether similar positive effects of 3D culture on hepatocytes are in play in enhancing differentiation of stem cell certainly requires further investigation.

In spite of the enhanced differentiation in the aggregate culture, the degree of maturation we observed still falls short of genuine hepatocytes. For many applications, further improvement in terms of the percentage of cells and their extent of differentiation will need to be demonstrated. Co-culture of hepatocytes with other non-parenchymal cells

such as endothelial cells, bone marrow cells, and fibroblasts has been shown to enhance maturation and stabilize differentiated function over a long period of time (Abu-Absi, Hansen et al. 2004; Ogawa, Tagawa et al. 2005; Shi, Zhang et al. 2009). Co-culture with non-parenchymal cells in a three-dimensional culture system and further optimizing the protocol, are worth exploring for generating organized 'liver-tissue equivalents.'

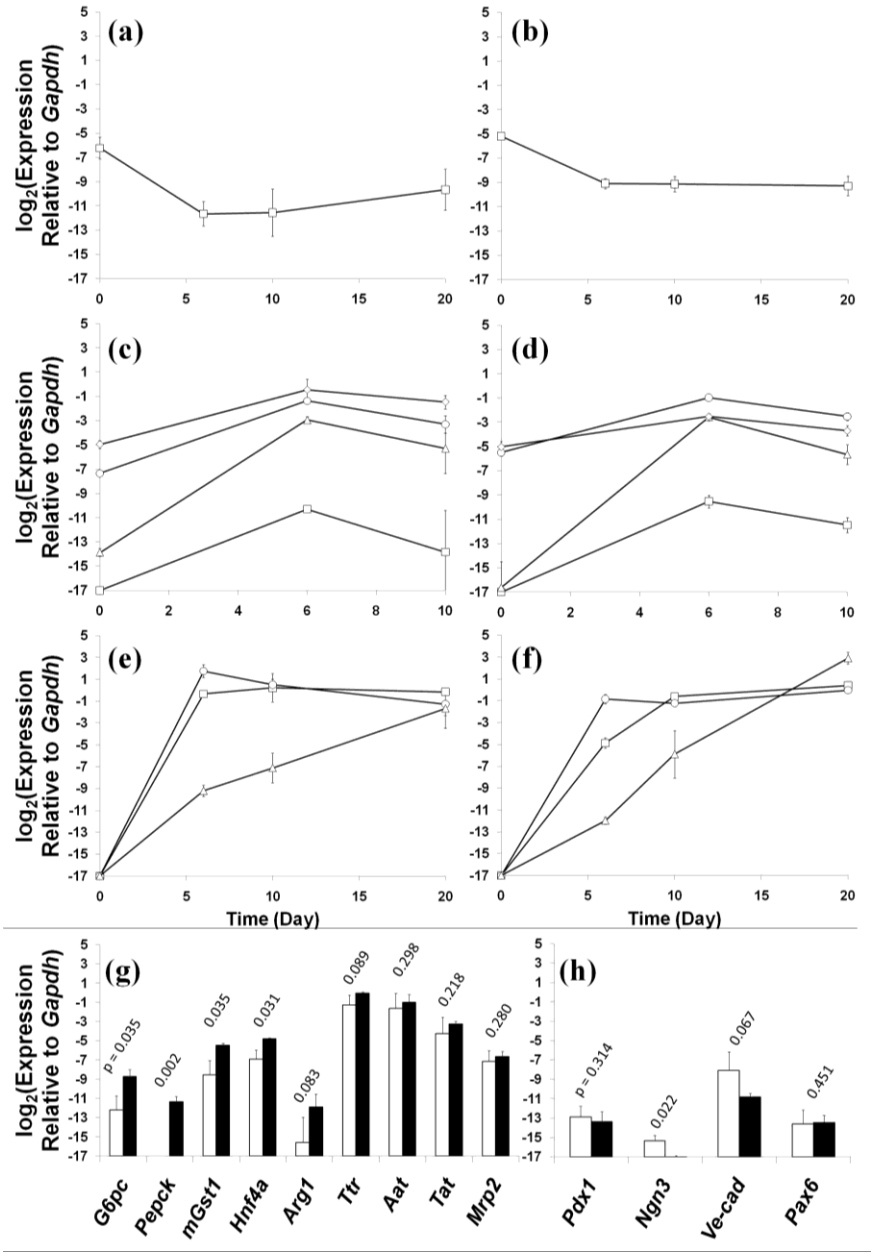

Figure 9: Gene expression during differentiation by qRT-PCR (average of n=3)

(a,b) Temporal expression of the pluripotency gene transcript Oct4 in monolayer (a) and aggregate (b) cultures; (c,d) Temporal expression of definitive endoderm gene transcripts Gsc (□), Eomes (○), Mixl1 (Δ), and Foxa2 (◇) in 2D (c) and aggregate (d) cultures; (e,f) Temporal expression of hepatic endoderm gene transcripts Afp (□) and Ttr (○) and hepatoblast/hepatocyte marker Alb (Δ) in 2D (e) and aggregate (f) cultures; (g) D20 expression of mature hepatic gene transcripts G6pc, Pepck, mGst1, Hnf4a, Arg1, Ttr, Aat, Tat, and Mrp2 in monolayer (□) and aggregate (■) cultures; (h) D20 expression of non-liver lineage gene transcripts Pdx1, Ngn3, Ve-cad, and Pax6 in monolayer (□) and aggregate (■) cultures

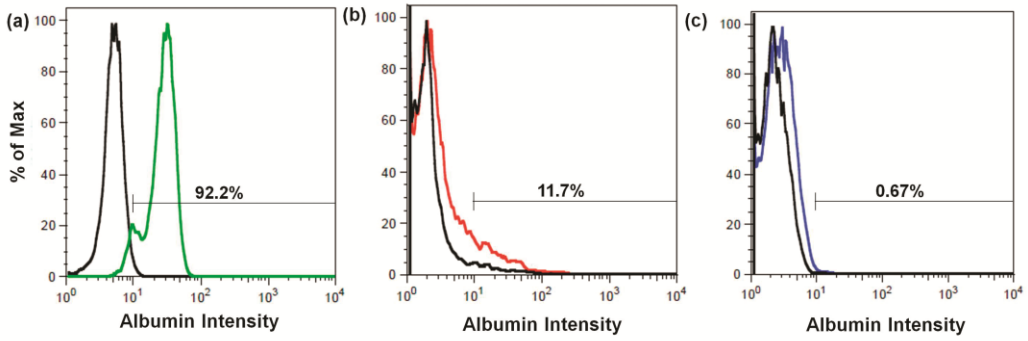

Figure 10: Expression of intracellular albumin in differentiation cultures

Flow cytometric comparison of cells expressing intracellular albumin in primary rat hepatocytes (a) and in cells differentiated in aggregate cultures (b) or monolayer cultures (c), with isotype controls. Percentages were generated from gating based on 0.5% false positive in a negative control population (not shown).

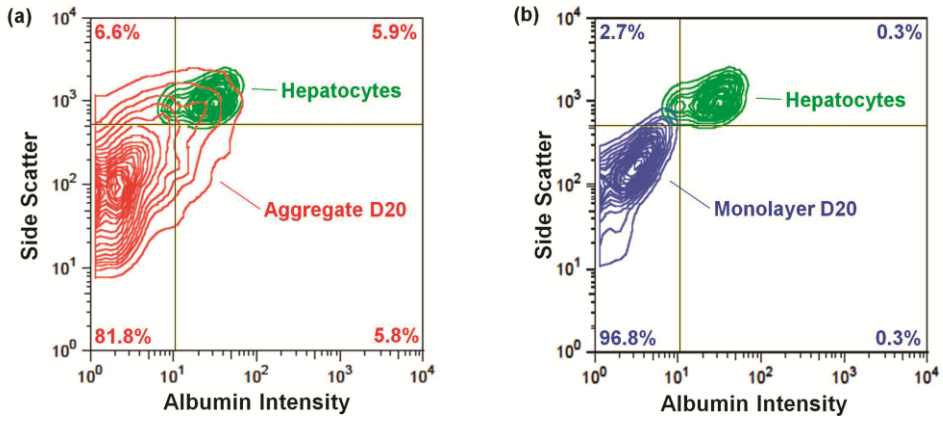

Figure 11: Side scatter versus albumin intensity in flow cytometry data

Flow cytometry data are presented as contour plots for rMAPCs differentiated in aggregate culture (a; red) or monolayer culture (b; blue) compared to primary hepatocytes (green). Cells localized to the upper right quadrant demonstrate similar albumin expression levels as well as similar levels of cellular complexity and granularity to primary rat hepatocytes; 5.9% of rMAPCs differentiated in aggregate culture possess this hepatocyte-like phenotype, as compared with only 0.3% of cells differentiated in monolayer culture. Cells localized to the lower right quadrant demonstrate similar albumin expression levels to primary rat hepatocytes but exhibit lower cell complexity and granularity, indicating a less mature phenotype; 5.8% of rMAPCs differentiated in aggregate cultures possess this immature hepatic lineage phenotype, as compared with 0.3% of cells differentiated in monolayer culture.

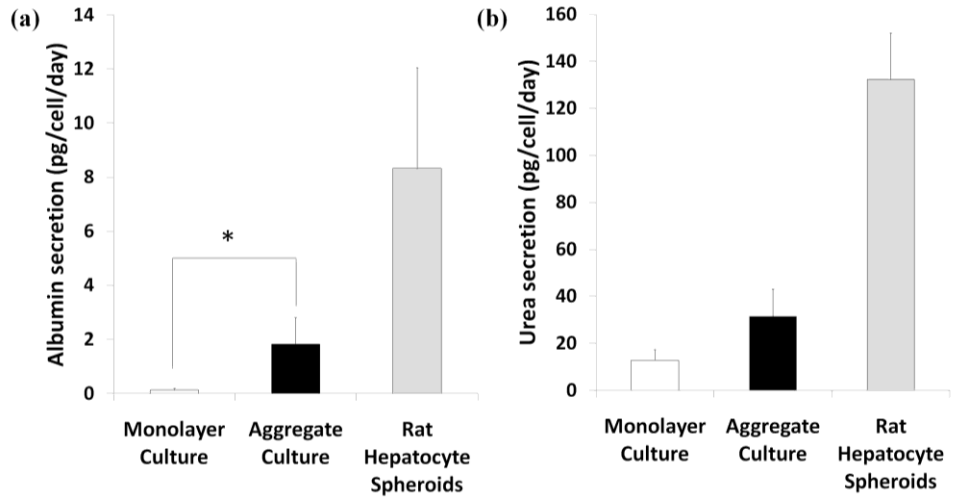

Figure 12: Functional activity in aggregate differentiation cultures

(a) Albumin secretion by ELISA and (b) urea secretion quantification in monolayer (□) and aggregate (■) cultures on D20 of differentiation and in primary rat hepatocytes spheroids (■) (average of n=3; * denotes $p < 0.05$)

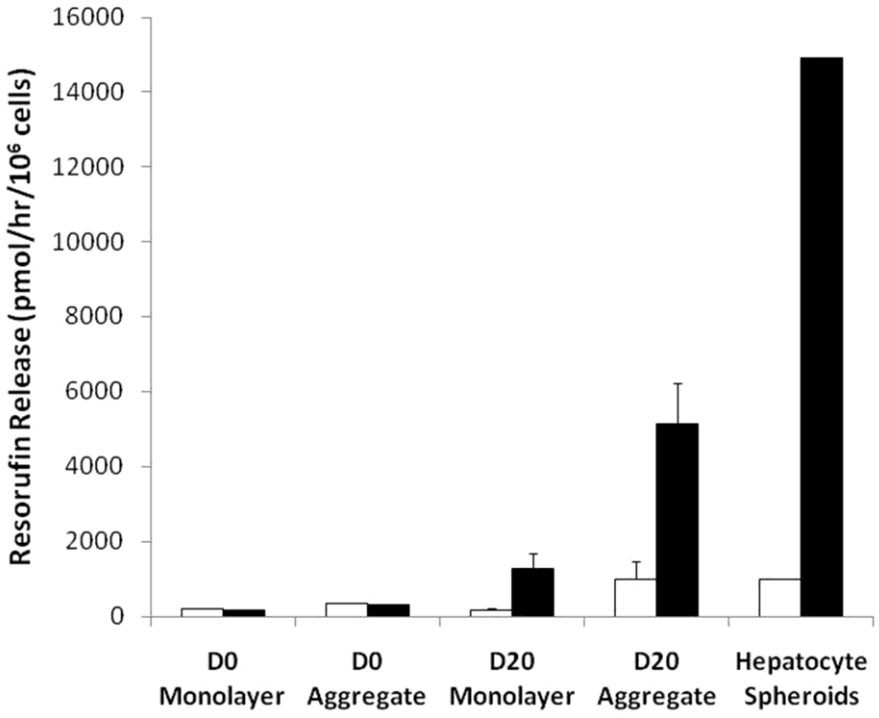

Figure 13: Release of resorufin into media by EROD activity

Kinetic measurements of resorufin release into the media without drug treatment (□) and after BNF treatment (■) in monolayer and aggregate cultures on D0 and D20 of differentiation and in primary hepatocyte spheroids (D20 samples average of n=3).

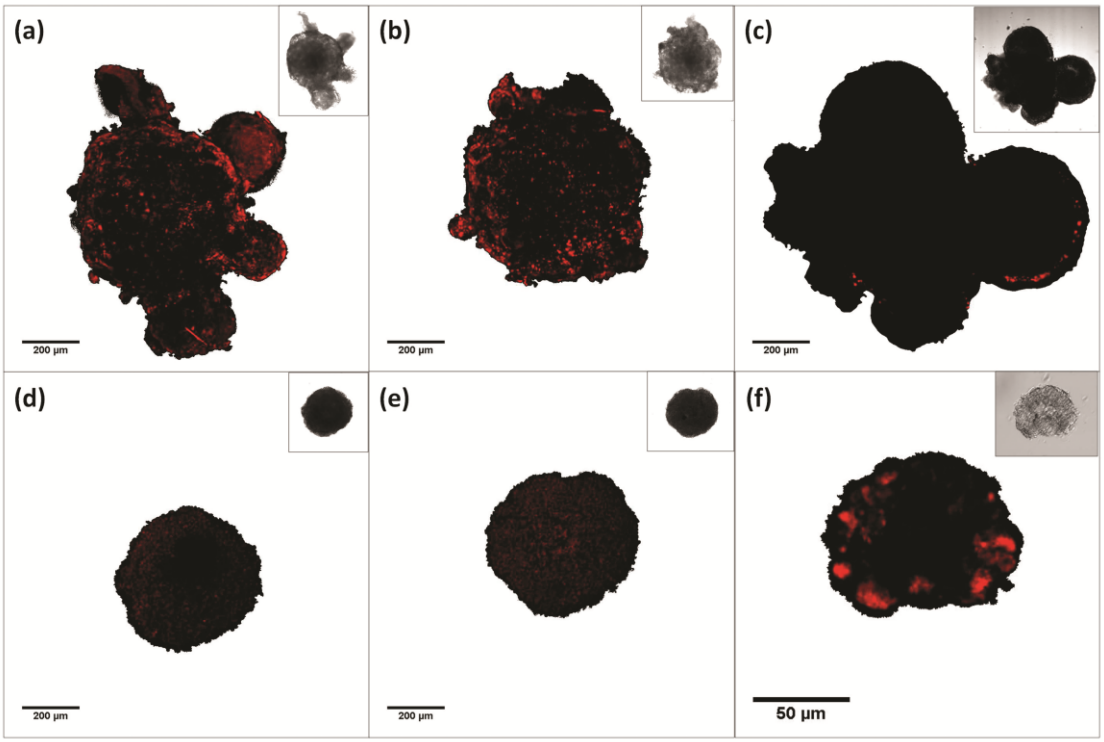

Figure 14: Intracellular accumulation of resorufin due to EROD activity in differentiated aggregates

(a) D20 differentiated aggregates after treatment with BNF demonstrate EROD activity with higher fluorescence at the exterior of the aggregate. (b) D20 differentiated aggregates without drug treatment similarly demonstrate EROD activity with higher fluorescence at the exterior of the aggregate. (c) Unstained D20 differentiated control of EROD activity without ethoxyresorufin addition demonstrates minimal background fluorescence at some aggregate edges. (d,e) Undifferentiated D0 aggregates exhibit uniform background fluorescence either with (d) or without (e) BNF drug treatment. (f) Primary hepatocytes cultured as spheroids and treated with BNF demonstrate EROD activity.

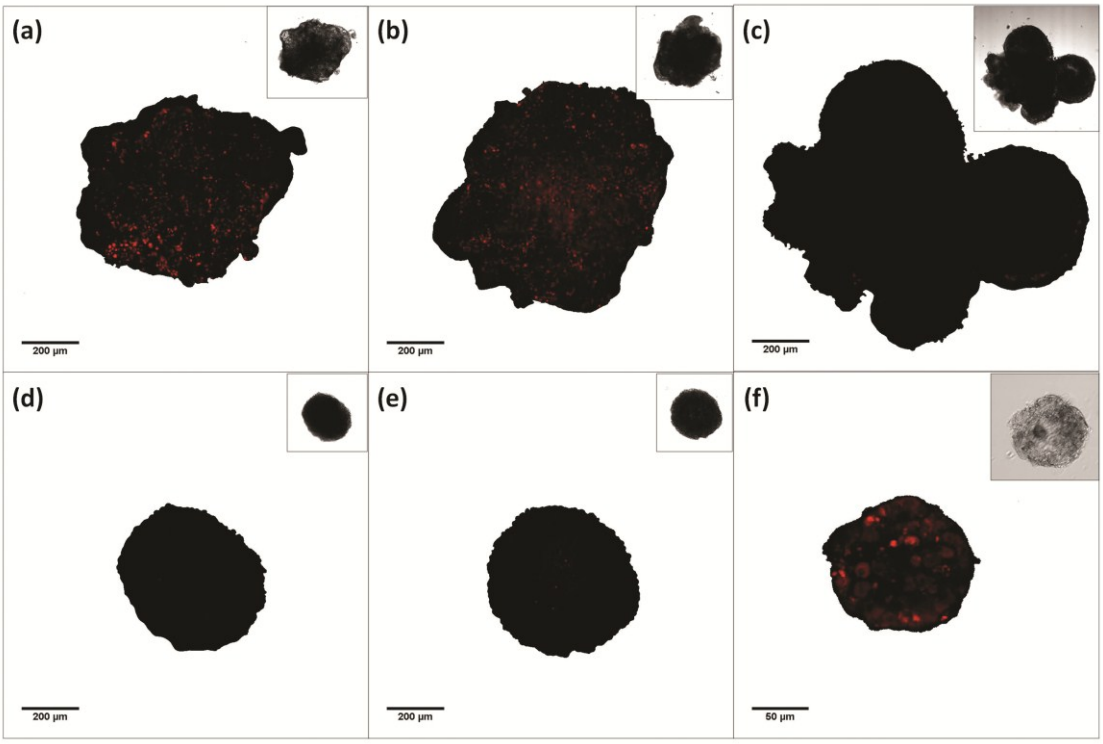

Figure 15: Intracellular accumulation of resorufin due to PROD activity in differentiated aggregates

(a) D20 differentiated aggregates after treatment with PB demonstrate PROD activity with higher fluorescence at the exterior of the aggregate. (b) D20 differentiated aggregates without drug treatment similarly demonstrate PROD activity with higher fluorescence at the exterior of the aggregate. (c) Unstained D20 differentiated control of PROD activity without pentoxyresorufin addition demonstrates minimal background fluorescence around aggregate edges. (d,e) Undifferentiated D0 aggregates exhibit minimal background fluorescence either with (d) or without (e) PB drug treatment. (f) Primary hepatocytes cultured as spheroids and treated with PB demonstrate PROD activity at the edges of the spheroid.

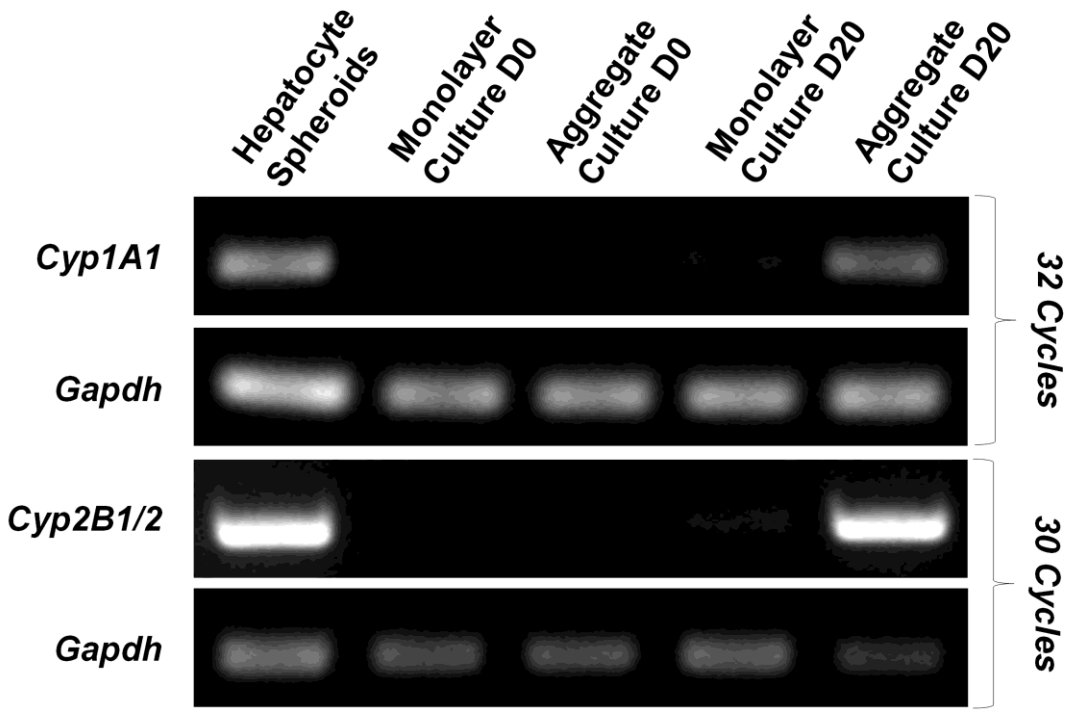

Figure 16: Expression of CYP450 isoforms in differentiated cultures by RT-PCR

The transcript expression levels of *Cyp1A1* and *Cyp2B1/2* isoforms were evaluated via RT-PCR and product separation on a 1.35% agarose gel. The primer sets yielded segment lengths of 331 bp for *Cyp1A1*, 549 bp for *Cyp2B1/2*, and 177 bp for *GAPDH* (loading control). Primary rat hepatocytes were used as a positive control and are shown in Lane 1. Undifferentiated cells in monolayer (Lane 2) or aggregate (Lane 3) cultures did not exhibit any transcript for either isoform. Cells differentiated in aggregate culture (Lane 5) exhibited more intense bands, indicating higher transcript levels, for both *Cyp1A1* and *Cyp2B1/2* than cells differentiated in the monolayer culture. Loading controls indicate equivalent amounts of cDNA product in each lane, and a negative non-template control was performed (not shown) to rule out non-specific amplification.

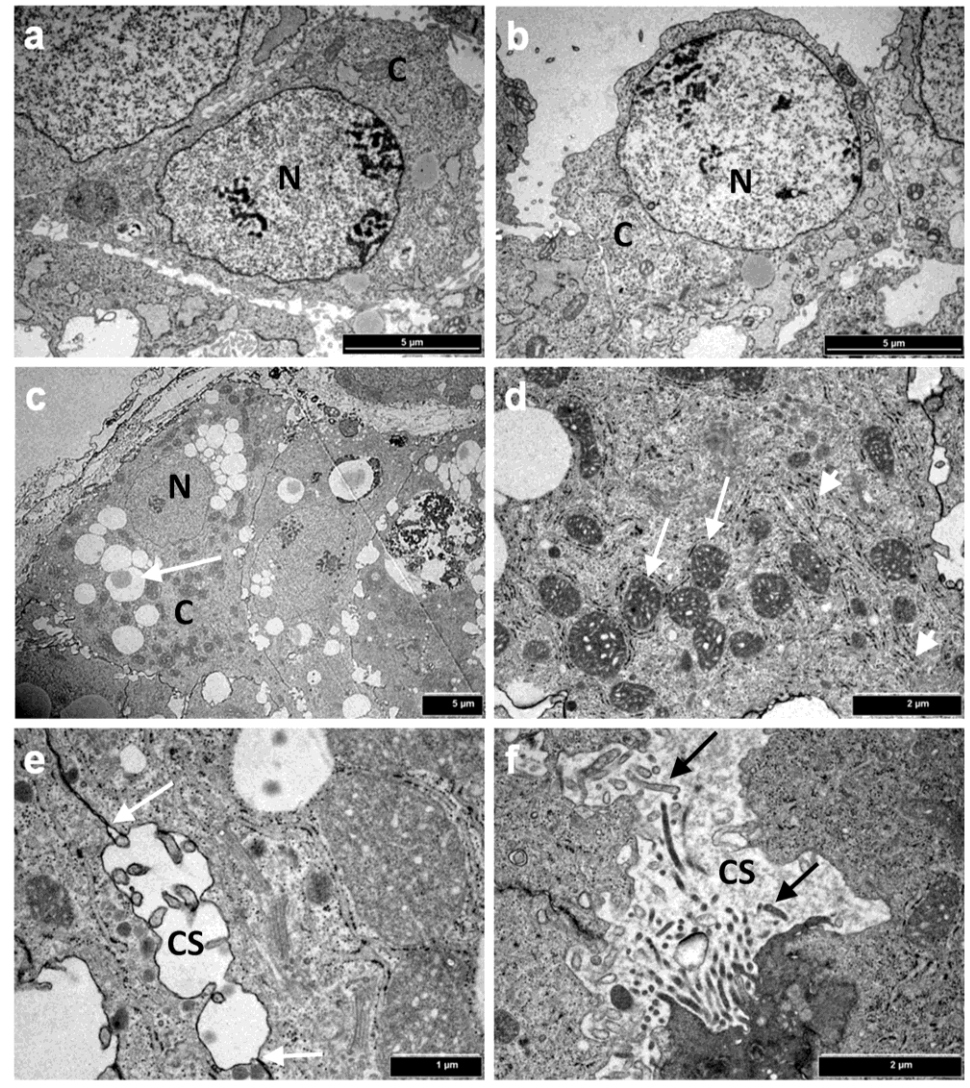

Figure 17: Ultra-structural evaluation of 3D differentiated aggregates

Transmission electron microscopic evaluation of undifferentiated aggregates on D0 (a,b) and fully differentiated aggregates on D20 (c–f) of differentiation. (a,b) Undifferentiated aggregates demonstrate a spindle-like morphology contain a high nucleus (N) to cytoplasm (C) ratio with very few cytoplasmic structures (scale bars 5 µm). (c) Whole-cell micrograph of a differentiated aggregate reveals a polygonal morphology, a significantly reduced nucleus (N) to cytoplasm (C) ratio, and an abundance of cytoplasmic structures including lipid vesicles (arrow) (scale bar 5 µm). (d) Micrograph of a portion of a single cell reveals an abundance of mitochondria (arrows) and rough endoplasmic reticulum (arrowheads) (scale bar 2 µm). (e) Micrograph of a cell-cell border reveals a canaliculus-like structure (CS) between the cells delimited by tight junctions (arrows) (scale bar 1 mm). (f) Micrograph centered on a canaliculus-like structure (CS) reveals microvilli (arrows) protruding into the CS space (scale bar 2 µm).

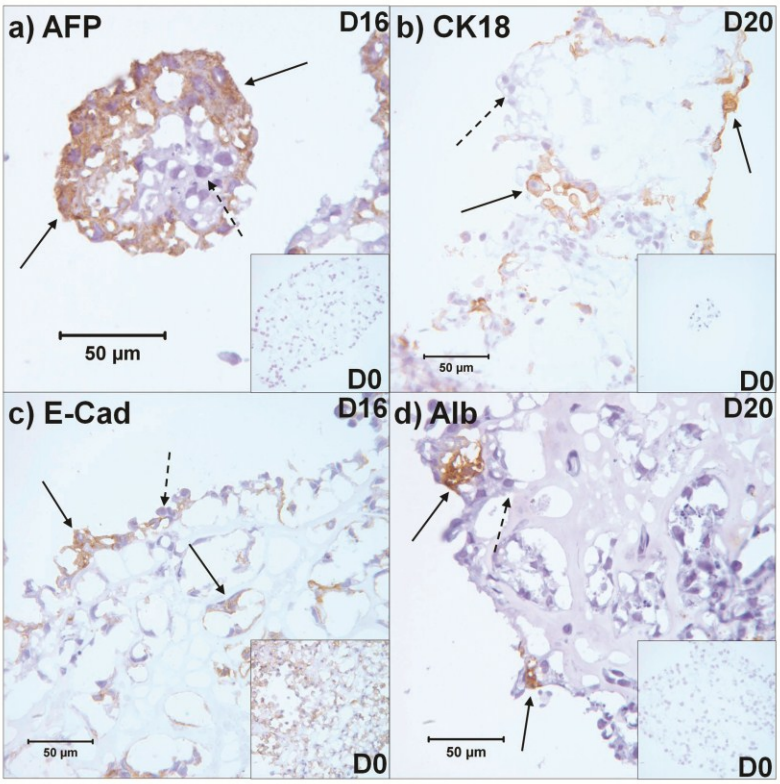

Figure 18: Immunohistochemistry for hepatic protein expression in aggregates

(a) AFP protein expression on D16 of differentiation is observed in the cytoplasm of cells on the exterior of the aggregate, while no AFP protein is observed in the undifferentiated D0 sample (inset); (b) CK18 protein expression on D20 of differentiation is observed in the cytoplasm of cells on the exterior of the aggregate, while no CK18 is observed in the undifferentiated D0 sample (inset); (c) E-Cadherin protein expression is observed on the membrane of cells in both the D0 undifferentiated sample (inset) and the D16 differentiated sample; (d) Albumin protein expression on D20 of differentiation is observed in the cytoplasm of cells on the exterior of the aggregate, while no albumin protein is observed in the undifferentiated D0 sample (inset). Positive stains are indicated with solid arrows while nucleus counterstains are indicated with dashed arrows.

CHAPTER 5: SPHEROID CULTURE FOR ENHANCED DIFFERENTIATION OF HUMAN EMBRYONIC STEM CELLS TO HEPATOCYTE-LIKE CELLS

5.1 Introduction

Early strategies for differentiating human embryonic stem cells (hESCs) to 'hepatocyte-like' cells largely relied on spontaneous differentiation, typically as embryoid bodies (EBs), with more recent approaches involving directed differentiation on adherent matrices as a two-dimensional monolayer (Sancho-Bru, Najimi et al. 2009; Snykers, De Kock et al. 2009). Culture of hESCs on low attachment surfaces results in the formation of EBs with spontaneous differentiation propensity to multiple cell lineages, including the hepatic endoderm; however, this approach is limited by the low efficiency of 'hepatocyte-like' cells obtained (Imamura, Cui et al. 2004). As a result, directed differentiation approaches based on time-dependent treatment of cytokines, growth factors, and hormones mimicking embryonic liver development were adopted with the goal of increasing the efficiency of hepatic endoderm differentiation (Cai, Zhao et al. 2007; Hay, Zhao et al. 2008; Basma, Soto-Gutierrez et al. 2009; Si-Tayeb, Noto et al. 2009; Chen, Tseng et al. 2012; Nakamura, Saeki et al. 2012). Indeed, we recently developed a multistep differentiation protocol for differentiation of pluripotent stem cells towards functional hepatocytes as a two-dimensional (2D) monolayer culture, recapitulating *in vitro* the different stages of liver development during embryogenesis *in vivo* (Roelandt, Pauwelyn et al. 2010).

Despite considerable success in achieving differentiation to an enriched population of cells with characteristics of hepatocytes, current protocols result in a heterogeneous mixture of cells, and the level of mature functions achieved is only a fraction that of primary hepatocytes. Hence, there is still a need for both increased yield and functional maturity of pluripotent stem cell derived hepatocyte-like cells. Further, as the differentiation techniques become more refined to yield higher numbers of hepatocyte-like cells that function at a therapeutic level, there will be a major emphasis on culture

environments capable of sustaining the differentiated phenotype for extended culture times, particularly for applications such as high throughput drug toxicity screening. Our group previously showed that rat primary hepatocytes cultured as three-dimensional cell aggregates, or spheroids, demonstrate enhanced function for a longer time in culture as compared to standard monolayer culture on a tissue culture surface (Peshwa, Wu et al. 1996). Advantages of three-dimensional culture or matrix systems are thought to be imparted by enhanced cell-cell and cell-matrix interactions, cell shape, and the establishment of spatial gradients, which may lead to favorable changes in gene and protein expression and thus provide a conducive and more native 'niche-enviroment' for the cells (Cukierman, Pankov et al. 2001; Griffith and Swartz 2006; Keller, Pampaloni et al. 2006; Pampaloni, Reynaud et al. 2007; Tanimizu, Miyajima et al. 2007). As a result, spheroid culture of differentiated cells such as hepatocytes or hepatic progenitor cells has also found applications in studies related to drug toxicity screening (Ong, Zhao et al. 2009; Toh, Lim et al. 2009), bioartificial liver support (Ijima, Nakazawa et al. 1998), tissue morphogenesis and tumor biology (Debnath and Brugge 2005; Yamada and Cukierman 2007), and as an *in vitro* model for hepatitis C virus infection (Sainz, TenCate et al. 2009).

Thus, we hypothesized that providing a three-dimensional culture environment to the differentiated hepatocyte-like cells may not only improve the yield and phenotype, including expression and function characteristic of primary hepatocytes, but also allow extended culture of the differentiated cells. In the previous chapter, we showed that rMAPC differentiated as three-dimensional aggregates for the twenty day differentiation protocol exhibited enhanced differentiation as compared to the standard monolayer differentiation. However, the aggregate and monolayer differentiations proceeded through the initial stages of definitive endoderm and hepatic endoderm specification with similar efficiencies, with the true enhancement apparent only in the final stage of differentiation. This observation, combined with the unpredictability of beginning a differentiation of hES cells as embryoid bodies, the hES equivalent to our rMAPC aggregates, led us to hypothesize that the hES differentiation may benefit most from carrying out the twenty-day differentiation protocol as a monolayer and then forming

three-dimensional aggregates, in this case termed spheroids, subsequently. In this study, we investigate the formation of 3D spheroids from the spontaneous assembly of differentiated cells at the end of our 2D hepatic differentiation protocol to further enhance and maintain hepatic function suitable for a wide range of clinical applications.

5.2 Results

5.2.1 Optimization of D20 Dissociation Protocol

Human embryonic stem cells, HSF6, differentiated toward the hepatic lineage using a previously described protocol (Roelandt, Pauwelyn et al. 2010) were used as the starting cell population for the subsequent spheroid culture system that we hypothesized would enhance the hepatic differentiation. In order to accurately assess the effects of the three-dimensional spheroid culture system on the hepatic nature of cells, a cell dissociation protocol capable of collecting all cells from the monolayer culture with high viability was desired. Because the bulk population at D20 of differentiation contained a heterogeneous mixture of cell types, including the hepatocyte-like cells of interest, low yield or viability may result in an unintentional enrichment of one or more cell types that differentially survive the dissociation and replating process. Thus, a systematic approach was employed to determine the optimal conditions for cell dissociation from the D20 monolayer culture.

In each condition tested, the D20 monolayer cells were rinsed briefly with PBS followed by incubation in various cell dissociation enzymes according to manufacturers' protocols for incubation temperature and length of treatment. If cells did not dissociate into single-cell solutions with vigorous pipetting, the suspension was further triturated 5-6 times with an 18G syringe. The first iteration of conditions tested were single treatments with the following enzymes or products: 0.1% (w/v) Collagenase Type IV in hES Basal Media, a mixture of 0.1% (w/v) Collagenase Type I and 0.1% (w/v) Collagenase Type IV, 0.05% Trypsin-EDTA, 0.25% Trypsin-EDTA, 0.25% Trypsin without EDTA or Ca2+, Accutase, Tryp-LE, Liberase and Cell Dissociation Buffer. Each of these single

treatments resulted poor viability (<50% by Trypan blue exclusion) and poor yield (less than 200,000 cells per well of a 12-well dish) (data not shown). However, it was noticed that treatment with the collagenase solutions resulted in the monolayer cells lifting off the individual wells as a cell sheet that was only moderately dissociated into smaller sheets with vigorous pipetting. While this did not yield a single-cell solution, the cells within the sheets exhibited strong viability. This treatment then served as a first stage for a second iteration of experiments in which a two-stage dissociation protocol was examined.

In the two-step dissociation protocols, the D20 monolayer cells were treated with 400 µl per well of 0.1% (w/v) Collegenase Type IV in hES Basal Media for 15 min at 37°C, followed by gentle pipetting and collection into a 15-ml conical tube. 600 µl per well collected of PBS was added to the cell suspension prior to centrifugation for 5 min at 1000 rpm. The cell pellet was resuspended in fresh PBS and centrifuged again before being treated with a second enzyme. The cell pellet was resuspended in the second enzyme, and the tube was placed in the 37°C water bath for 10-15 min with pipetting every 2-3 min. After 15 min maximum, cells were triturated with an 18G syringe 5-6 times to produce a single cell suspension. The enzymes tested in this iteration included 0.05% Trypsin-EDTA supplemented with 2% (v/v) chick serum, Accutase, Tryp-LE, 0.25% Trypsin without EDTA and with Ca^{2+}, and Cell Dissociation Buffer. The yield and viability achieved from each of these treatments is presented in Figure 19. Although treatments with Tryp-LE and 0.25% Trypsin without EDTA and with Ca^{2+} both yielded high viability and reasonable cell numbers, treatment with 0.05% Trypsin-EDTA supplemented with 2% chick serum was far superior in terms of both viability and yield to all other conditions. Chick serum was added to promote cell survival during the extended dissociation protocol, as it supports cell viability but does not inactivate trypsin. This optimized protocol was used for all remaining experiments discussed in this chapter.

5.2.2 Three-Dimensional Spheroid Formation

HSF6 cells differentiated to D20 as a monolayer culture were dissociated according to the optimized protocol described in Section 5.2.1. With this protocol, we typically obtained

$4x10^5$ cells/cm^2 from the monolayer culture with high viability (>90%) and distributed 8000 cells/well into U-bottom ultra-low attachment (ULA) culture plates for spheroid formation. With time, cells clustered together, and multiple small clusters progressively agglomerated into larger and fewer spheroids. Six days after seeding (D26), tightly packed compact spheroids were observed (Figure 20).

Viability staining was performed at 0 and 24 hr after seeding into the ULA wells (Figure 21). Although viability immediately after seeding is very high, after 24 hr in the aggregate culture system, single cells were observed to have lost their viability, whereas those in the cell clusters remained viable. The incorporation into cell clusters thus appears essential to cell survival; of course, the possibility that cells which failed to incorporate into clusters were already destined to die, thus lacking the capability to cluster with other cells, cannot be excluded. Timelapse microscopy was also employed to directly observe the early stages of spheroid formation (Video 1, Figure 22). A small fraction (1%) of the cells were labeled with Vybrant DiI membrane dye, allowing observation of individual cells amongst the bulk population as they are or are not incorporated into the forming aggregates. It should be noted that, presumably, there is no bias in labeling, meaning the labeled cell population should represent the same distribution of cell types as the bulk population. Although many labeled cells are incorporated into forming aggregates in proximity to their initial position, a fraction of cells migrate significant distances, sometimes in a seemingly random pattern, before being incorporated into an aggregate. Interestingly, in one case a labeled cell formed a doublet with an unlabeled cell, suggesting they were not in contact with one another during the labeling phase, and the pair migrated significantly before joining with a forming spheroid (Supplementary Video 1). Taken together, these data suggest that incorporation into spheroids is either required for or a consequence of viability and is not random, but may be a function of complementary adhesion molecules between incorporating cells.

5.2.3 Expression of Hepatic Genes in 3D Spheroids

The expression of several hepatic-specific genes was evaluated after spheroid formation (D26) (Figure 23) and compared to the starting population of cells at D20. As a control, cells were also maintained in monolayer, and the change in the transcript levels over the same time period are also shown. The transcript level for the liver specific genes all increased on D26 for 3D spheroids from D20. The transcript level of a*lbumin* increased by about 16-fold in 3D spheroids (D26); in comparison, its level did not change in monolayer culture. The expression level of *UGT1A1*, a gene encoding an enzyme involved in bilirubin conjugation and a mature function mainly observed in the liver, increased by around 30 fold in 3D spheroids as compared to about a 2-fold increase in monolayer. The level of increase was more moderate for other genes, including *arginase 1 (Arg1)*, an enzyme involved in the urea cycle, *hepatocyte nuclear factor 4a (HNF4a)*, a liver enriched transcription factor, *Factor 7 (F7)*, a member of coagulation factor family, and *connexin 32* (CX32), a gap junction protein. Nevertheless, the level of transcript of those genes were all higher than that seen in cells which were maintained in monolayer culture.

The increased level of the transcript level of the hepatic genes in spheroid culture was sustained for at least another ten days as shown in Figure 3. The expression level of most mature hepatic transcripts including *albumin*, *arginase 1*, *UGT1A1*, *HNF4a* and *F7* were maintained till D35 in the 3D spheroid culture (Figure 24). In contrast, the expression levels of these genes in the 2D surface culture were either significantly lower and/or decreased within the same period.

5.2.4 Expression and Secretion of Hepatic Proteins in 3D Spheroids

The expression levels of ASGPR-1 protein (Figure 25) and PEPCK protein (Figure 26) in the 3D spheroids at D26 were evaluated by FACS and compared to the monolayer differentiation at D20. In both cases, the percentage of cells expressing the hepatic-specific proteins were significantly higher in the 3D samples as compared with the monolayer 2D samples. PEPCK protein localization was examined by immunostaining

under confocal imaging and is seen to be distributed diffusely and is abundantly represented in cells located on the exterior of the spheroid (Figure 27). The secretion rate of albumin was quantified by ELISA and found to be 0.45 and 0.53 pg/cell/day in monolayer culture on D26 and D32, respectively, and 4.52 and 12.05 pg/cell/day in the 3D spheroid culture, respectively (Figure 28). Thus, cells in the spheroids express higher levels of ASGPR-1 and PEPCK proteins and secrete albumin at a higher rate than those in the monolayer culture.

5.2.5 Ultra-Structure Characteristics of 3D Spheroids by SEM and TEM

Under scanning electron microscopy, the spheroids appear densely packed; the boundaries of individual cells were nearly indistinguishable (Figure 29a). At higher magnification, typical hepatocyte morphology can be seen on cell clusters on the exterior of the aggregate (Figure 29b): some polygonal cells (Figure 29c) exhibit abundant microvilli on the cell surface (Figure 29d).

Under transmission electron microscopy (Figure 30) cells in the spheroids on D30 displayed the typical polygonal morphology with numerous microvilli. Intercellular bile-canaliculi delimited by tight junctions were also observed. Golgi apparatus, plentiful mitochondria, lipid droplets and endoplasmic reticulum (rough) were all present. Lysosomes and inter-cellular coated vesicles involved in degrading a vast majority of biological materials were also visible.

5.2.6 Cytochrome P450 (CYP) Activity and Other Mature Functions in 3D Spheroids

The maturity of the cells was further evaluated by assessing Cyp1A1/2 and Cyp2B6/7 activities by ethoxyresorufin-O-dealkylation (EROD) and pentoxyresorufin-O-dealkylation (PROD), respectively. The intracellular accumulation of the fluorescent resorufin after the cleavage of ethoxyresorufin or pentoxyresorufin, indicative of EROD (Figure 31a) and PROD (Figure 31c) activities, was seen in the spheroids under confocal microscopy. The spheroids were then treated with β-napthoflavone (BNF) and

Phenobarbital (PB), specific inducers of Cyp1A1 and Cyp2B6/7, respectively. A modest increase in EROD activity after BNF treatment (Figure 31b) was observed, but little change was observed in PROD activity after PB treatment (Figure 31d). These activities were also quantified by measuring the rate of resorufin product released into the media (Figure 32a,b). Consistent with the visualization experiments, resorufin release was after both EROD and PROD activities, and EROD activity increased nearly 5-fold after BNF treatment but not after Rifampicin (Rif) treatment. Likewise, PROD activity increased marginally after treatment with PB but not Rif.

To further interrogate the phenomenon of specific cytochrome P450 activity, the expression of the relevant Cytochrome P450 gene products were evaluated by quantitative PCR with or without drug treatment (Figure 32c,d). Consistent with the activity assays, Cyp1a1 transcript expression increased 24 fold after 24 hr of BNF treatment, while Rif treatment resulted in minimal change in Cyp1a1 expression. Thus, consistent increase was seen in each of the three assays in Cyp1A1/2 expression and activity after BNF treatment, while PB treatment resulted in no significant increase in Cyp2B6/7 expression or activity.

The functional maturity and polarity of the 3D spheroids were investigated by a fluorescein diacetate cleavage and accumulation assay. Fluorescein diacetate can freely diffuse into cells and is converted by the intracellular esterases into fluroescein. In liver cells, fluorescein is known to be secreted into the bile-canaliculi between the cells, and this accumulation can be visualized (Oude Elferink, Meijer et al. 1995; Bravo, Bender et al. 1998). Spheroids were incubated in low concentrations (3 mg/ml) of fluorescein diacetate, and the accumulation of fluorescein in the bile canaliculi was examined by confocal imaging (Figure 33). The fluorescein was observed to accumulate in the spaces between cells, while the space occupied by the cells themselves appears dark, consistent with the accumulation of fluorescein in the intercellular space and indicative of cell polarization.

5.3 Discussion

We previously reported a multi-step directed differentiation protocol capable of guiding hESCs and iPS cells toward the hepatic lineage as a monolayer culture (Roelandt, Pauwelyn et al. 2010). Although the differentiated cells exhibited many characteristics of mature hepatocytes, including gene expression and function, levels of expression and function were not as high as in primary hepatocytes. Further, the cells were among a heterogeneous population of many cell types, and many characteristics of fetal, immature hepatocytes were also present. For stem cell-derived hepatocytes to transition into a technology, further maturation and purification of the differentiated cells must be achieved and a culture system must be established to promote extended survival and function of the cells. In this study, we supplemented our monolayer differentiation culture with a subsequent three-dimensional spheroid culture stage that enhanced the maturity and purity of hepatocyte-like cells derived from hESCs, as determined by increased expression of hepatocyte-specific markers at both the gene expression and protein expression levels along with imaging and functional assays such as albumin expression and cytochrome P450 activity.

As previously discussed, the differentiation of pluripotent stem cells to the hepatic lineage has received much attention in recent years. The hepatocyte-like cells in our three-dimensional spheroid culture system compare favorably to the best of the current reported differentiations. Although assays vary greatly between studies, comparisons can be made based on expression levels of the most markers, such as Afp and Albumin. Multistage differentiations from hES and hiPS based on sequential signaling all yield cells expressing apparently similar levels of Afp and Albumin, assayed by either quantitative PCR or RT-PCR, with levels of Albumin expression similar to or exceeding expression in primary hepatocytes (Asgari, Moslem et al. 2011; Chen, Tseng et al. 2012; Nakamura, Saeki et al. 2012). As Afp is expressed in fetal liver cells but not in primary hepatocytes, the persistent expression of Afp suggests the presence of immature fetal hepatocyte-like cells in the culture. With the expression of exogenous FoxA2 and HNF1a to various differentiation stages, Takayama et al report Albumin expression at levels

equivalent to primary hepatocytes from one hiPS line, although the other two hES lines and four hiPS lines are not able to achieve such high expression, and AFP expression was not discussed (Takayama, Inamura et al. 2012). Similar to these studies, both AFP and Albumin gene expression levels are very high in our spheroid culture system, with Albumin expression increasing approximately 16-fold in comparison to the monolayer differentiation system (Fig 2) and 4-8 fold higher than in adult liver (data not shown). Each of these groups, including us, also reports expression of other hepatocyte-specific markers indicating that the stem cell progeny have adopted some portion of the genetic signature necessary for the primary hepatocyte phenotype.

Although achieving the correct expression profile is important for acquiring the hepatocyte phenotype, the ability of these cells to mimic the in vivo function of primary hepatocytes, including appropriate responses to environmental cues, are paramount for their potential uses as pharmaceutical and clinical cell sources. Each of these studies, like ours, presents a panel of mature liver functions. Perhaps the most clinically relevant are Cyp450 activities, which are largely responsible for drug metabolism and detoxification in the healthy liver. Our three-dimensional spheroid system yielded hepatocyte-like cells that exhibited both Cyp1A1/2 and Cyp2B6/7 activities by EROD and PROD, respectively. However, the ability of primary hepatocytes to upregulate these activities in response to specific inducers is critical to the detoxification process, and any stem cell-derived hepatocytes must exhibit appropriate responses to these environmental cues. In our system, the Cyp1A1/2 activity responded specifically to treatment with the drug β-Napthoflavone (BNF) with increased activity, as evidenced by accumulation of resorufin product within the spheroids (Fig 7), release of resorufin into the media (Supp Fig 1a,b), and expression of the gene transcripts (Sup Fig 1c,d). Although the fold increase of EROD activity was similar to that in primary hepatocytes (data not shown), the absolute levels of the activity still fell short of primary hepatocyte levels. However, the Cyp2B6/7 activity, PROD, did not respond to treatment with the specific inducer Phenobarbital (PB). These results suggest that, although some mature hepatocyte characteristics have been acquired, many are still underdeveloped. Similarly, Asgari et al report significant

increase in Cyp1A2 and Cyp3A4 after induction at the gene expression level and very small increases in Cyp2B6 expression, though all were much lower than primary hepatocytes (Asgari, Moslem et al. 2011); Chen et al report some PROD activity but no measurable increase after PB induction and some Cyp3A4 activity but did not report induction experiments (Chen, Tseng et al. 2012); Takayama et al presented significant increases in Cyp1A2 and Cyp3A4 activities after treatment with BNF and Rifampicin, respectively, but only a marginal increase in Cyp2B6 after PB treatment, and all activities were considerably lower than those exhibited in primary hepatocytes (Takayama, Inamura et al. 2012). Thus, each of the protocols driven by media components, and even one by Takayama et al that includes exogenous transcription factor expressions to drive differentiation farther, still fails to achieve the mature hepatocyte functions necessary for clinical and pharmaceutical applications.

After presumably multiple iterations of differentiation optimizations from multiple groups resulting in similar maturity and expression patterns, it seems unlikely that the current strategy of multi-stage differentiations guided by signaling molecules and media composition will yield fully functional mature hepatocyte-like cells; indeed, these systems must now be combined with other techniques, perhaps including strategies such as exogenous expression of transcription factors, as Takayama et al have begun exploring, or control of metabolism during differentiation. The three-dimensional spheroid culture described in this study is one such strategy that imparts increased hepatic-specific expression and function as compared to the two-dimensional monolayer culture counterpart.

Although the mechanism of increased expression and function in the spheroid system is not yet well characterized, it is likely that the process of self-assembly into spheroids and the associated 3D-niche have major roles in the enhanced hepatic differentiation status. The spheroids were formed and maintained in medium containing hepatocyte growth factor (HGF), insulin-selenium transferrin, and linoleic acid-albumin, all of which have previously been reported to enhance spheroid formation of hepatocytes (Abu-Absi, Friend et al. 2002; Tsuchiya, Heike et al. 2005). Further improvements to this cell-

assembly into higher order structures may include adapting to scalable methods such as rotating well vessel bioreactors (Chang and Hughes-Fulford 2009), the use of scaffolds or matrices (Cheng, Wauthier et al. 2008), or the combination of microfabrication and microcontact printing tools for controlled aggregation of cells (Fukuda and Nakazawa 2005; Fukuda, Sakai et al. 2006).

In addition to enhancing the phenotypic and functional maturity of hepatocyte-like cells from the multi-step differentiation protocol, the 3D spheroid culture system also proved capable of maintaining the differentiated status of the cells for extended culture times. During extended culture for 15 days in the spheroid system, the expression levels of hepatic-specific transcripts were maintained at the level achieved after six days of formation on D26 (Fig 3). The cells in the 3D spheroids further expressed and maintained the levels of expression of ASGPR-1 and PEPCK proteins (Fig 4) and demonstrated hepatocyte-like ultra-structural characteristics (Figs 5 and 6). High cell density environments, such as those in the tightly packed spheroids, have been shown to be conducive to enhanced cell-cell and cell-matrix interactions, increased deposition of ECM proteins, concentration of soluble factors, and spatial polarization (Landry, Bernier et al. 1985; Cukierman, Pankov et al. 2001; Abu-Absi, Friend et al. 2002; Kelm, Timmins et al. 2003; Griffith and Swartz 2006; Keller, Pampaloni et al. 2006). All these factors have been previously reported to contribute towards improved hepatic differentiation and function (Abu-Absi, Friend et al. 2002; Levenberg, Huang et al. 2003; Imamura, Cui et al. 2004; Baharvand, Hashemi et al. 2006; Hanada, Kojima et al. 2007; Kazemnejad, Allameh et al. 2008; Gu, Shi et al. 2009; Okura, Komoda et al. 2009). In contrast, the expression levels of hepatic transcripts in cells that were cultured in 2D surface culture were lower or significantly decreased during the extended culture, highlighting the contribution of the 3D cell-niche not only in enhancing but also in stabilizing the differentiated cells. For *in vitro* drug screening studies with stem cell derived hepatocytes, having a culture platform that facilitates the maintenance of the differentiated phenotype of the cell population for the duration of the screening experiment is a necessity.

In summary, we have developed a simple and reproducible differentiation method consisting of step-wise twenty day 2D adherent monolayer based directed differentiation to the hepatic endoderm followed by a process of natural self-assembly of cells into three-dimensional spheroids. This culture system not only improves the phenotypic and functional maturity of the differentiated cell products, but also offers an additional advantage in more efficient maintenance of the cells for extended culture times. This approach may thus find application in high-throughput drug screening, in bioartificial liver support devices as well as in liver related cell therapy.

Second Step Enzyme	Yield ($x10^6$ cells/well)	Viability
0.05% Trypsin + 2% chick serum	1.0-1.5	> 90%
Accutase	0.3	< 50%
Tryp-LE	1.1	~ 85%
0.25% Trypsin w/out EDTA + Ca^{2+}	0.5	> 90%
Cell Dissociation Buffer	0.2	~ 40%

Figure 19: Yield and viability of cells harvested from D20 monolayer differentiation with different dissociation strategies

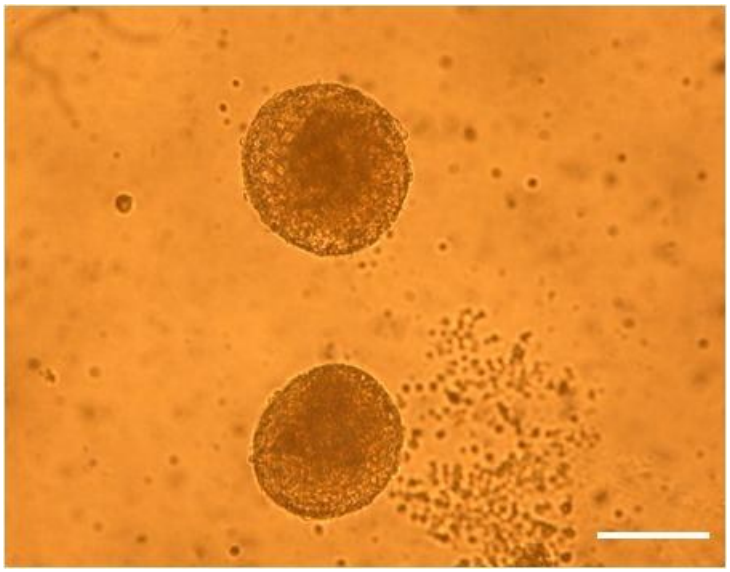

Figure 20: Morphology of hES derived 3D differentiated spheroids (D26; scale bar 200 μm)

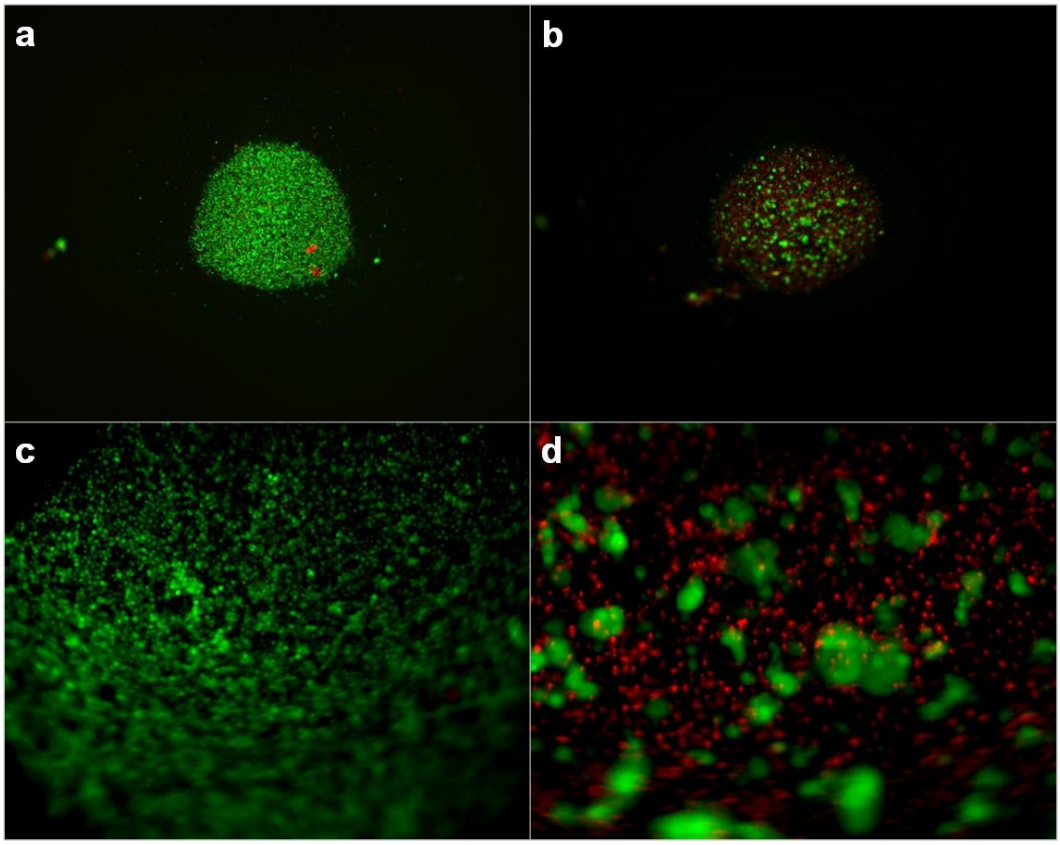

Figure 21: Live-dead viability staining on during spheroid formation

Live-dead viability staining during spheroid formation immediately after seeding on D20 (b, 2.5X; d, 10X) and 24 hr after formation on D21 (c, 2.5X; e, 20X), live, viable cells labeled with green fluorescence and nonviable cells labeled with red fluorescence

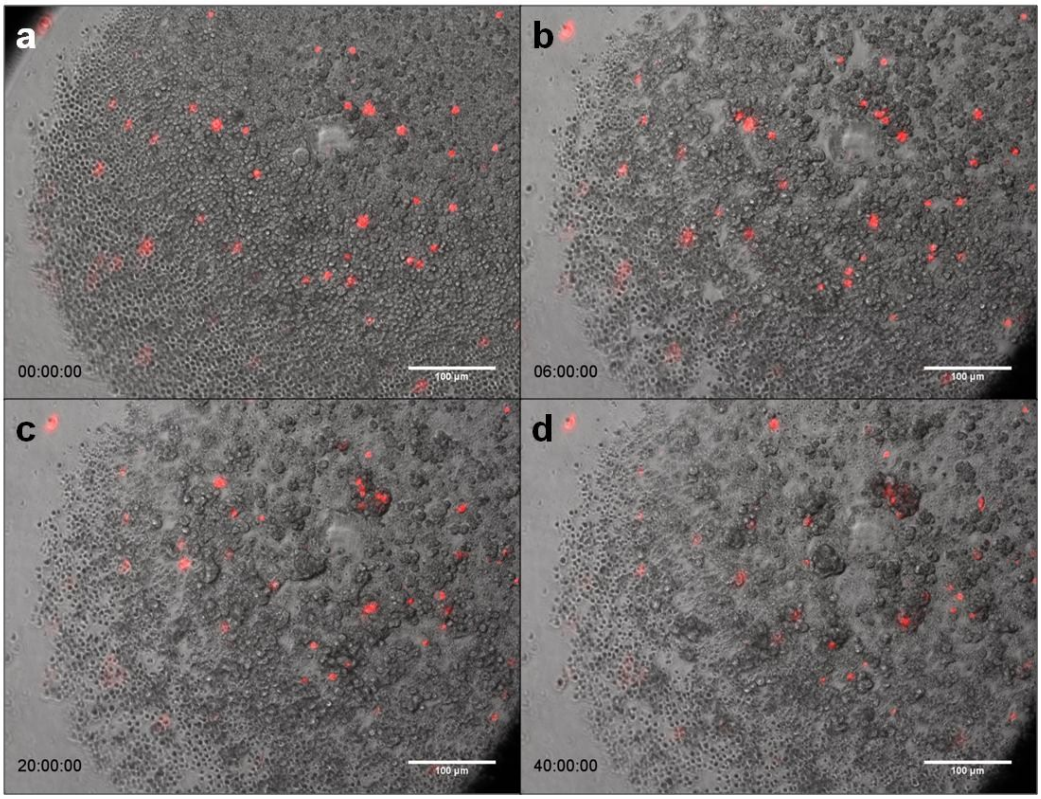

Figure 22: Timelapse images of spheroid formation with 1% of bulk population labeled with DiI membrane stain (scale bars 100 µm)

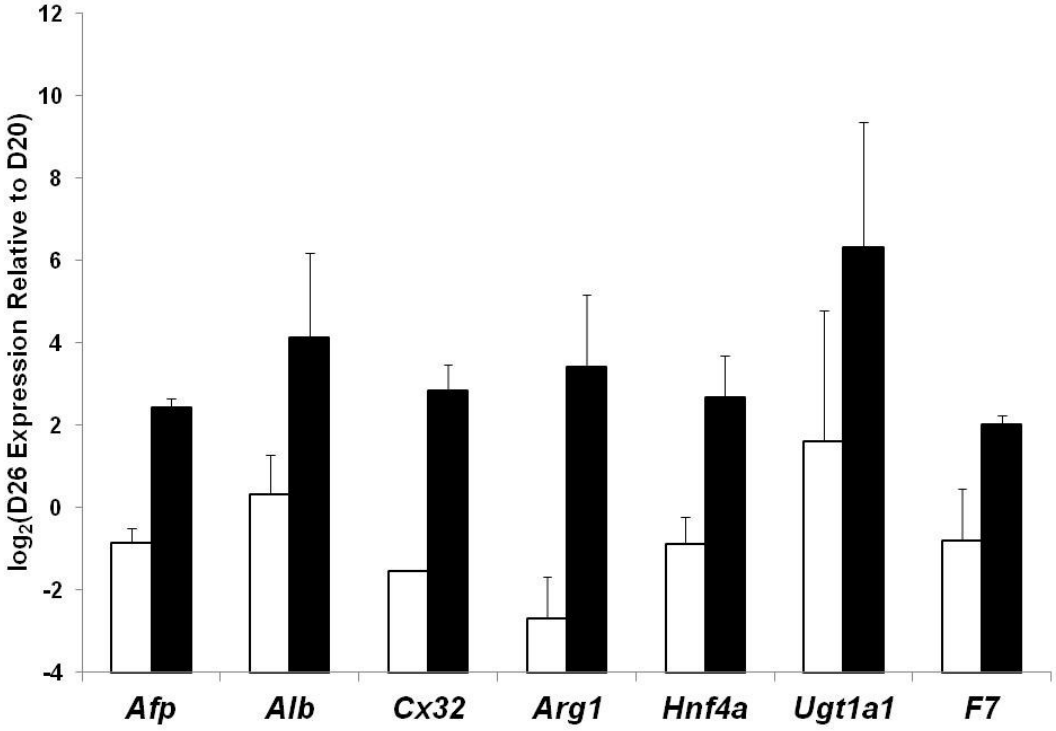

Figure 23: Gene expression on D26 of differentiation by qRT-PCR (average of n=3)

Change in transcript level of liver specific genes on D26 relative to D20 monolayer transcript level in 2D monolayer (□) and 3D spheroid (■) (average of n=3)

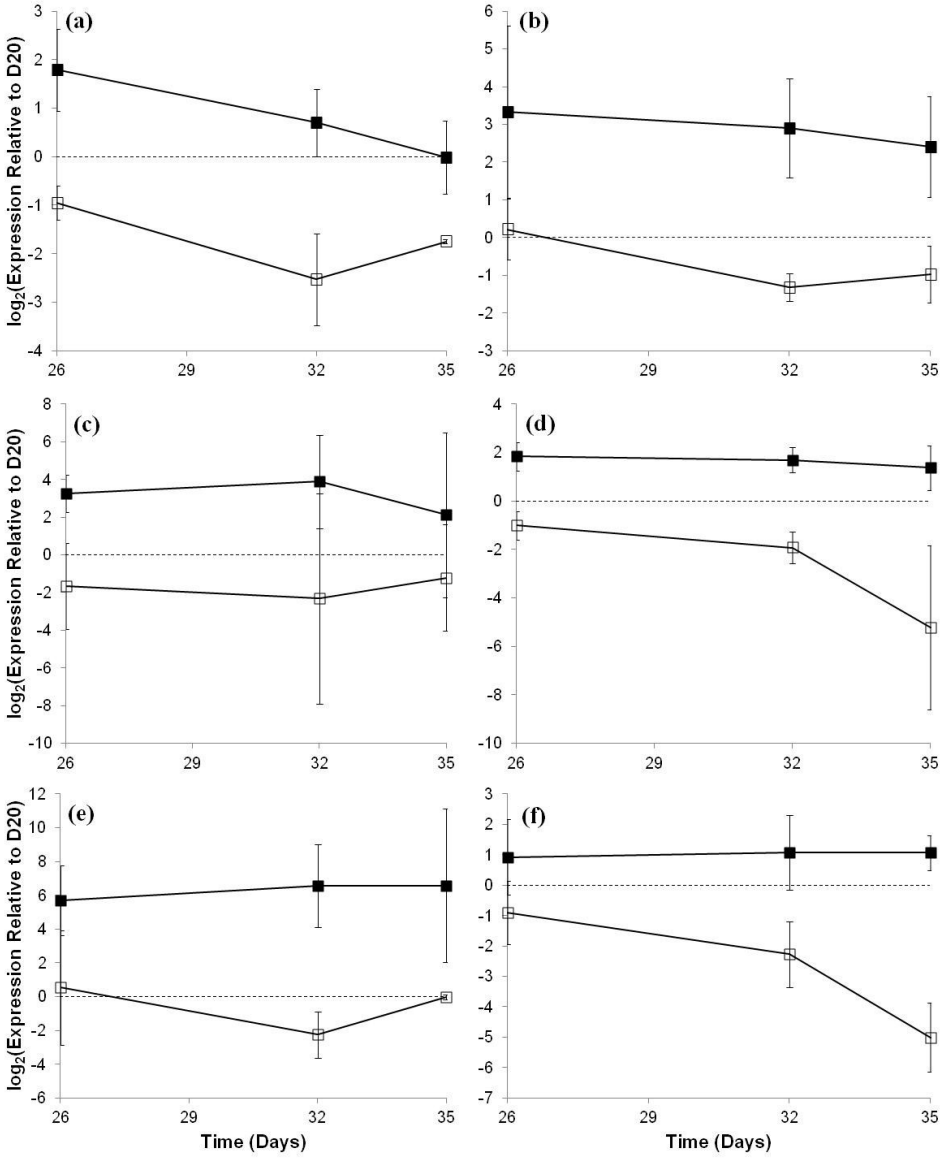

Figure 24: Gene expression in extended differentiation culture by qRT-PCR

Time course of the transcript level of liver specific genes relative to D20 in continued 2D surface differentiation (□) and after transition to 3D spheroid differentiation culture (■) from D26 to D35. (a) *Afp*; (b) *Albumin*; (c) *Arg1*; (d) *Hnf4a*; (e) *Ugt1a1*; (f) *F7*; dashed lines represent no change in expression from D20; average of n=3

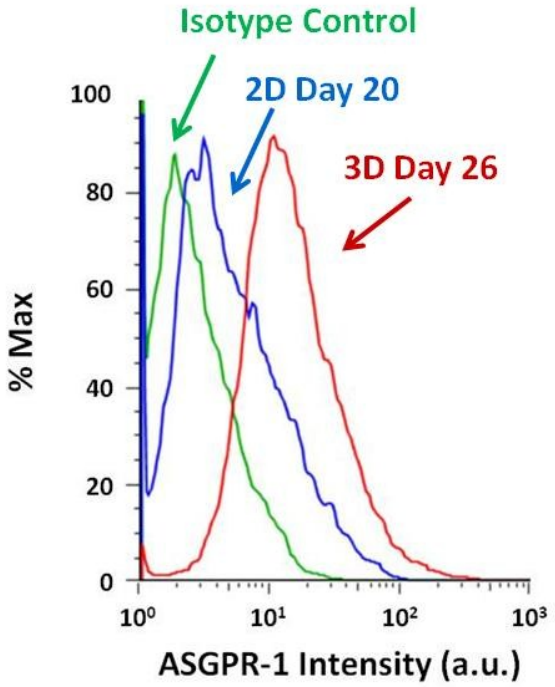

Figure 25: ASGPR-1 expression by FACS analysis

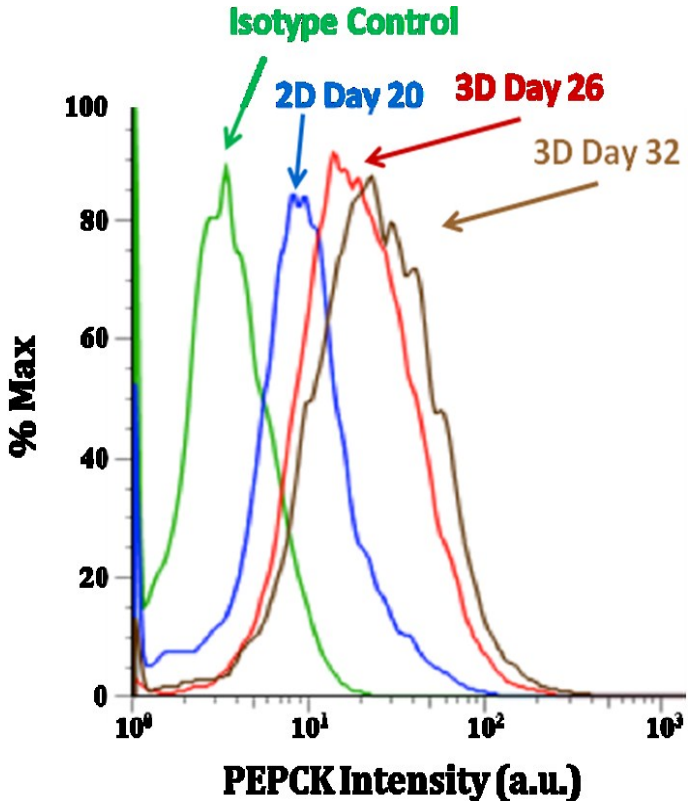

Figure 26: PEPCK expression by FACS analysis

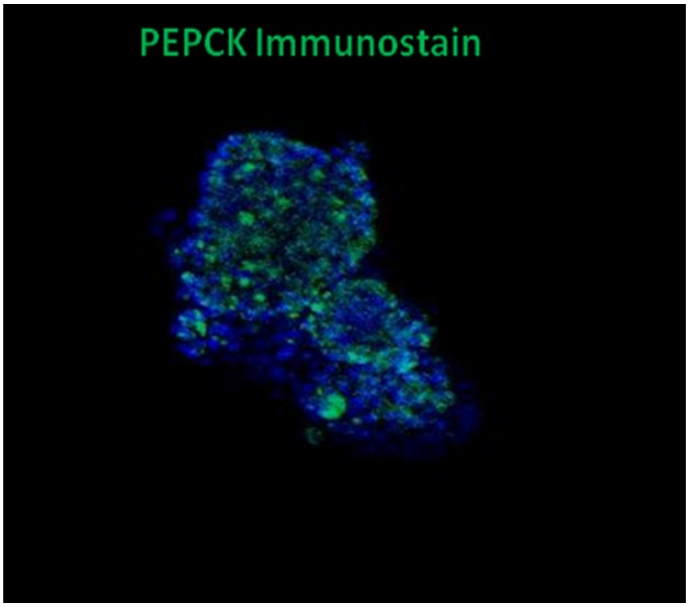

Figure 27: PEPCK immunostaining under confocal microscopy

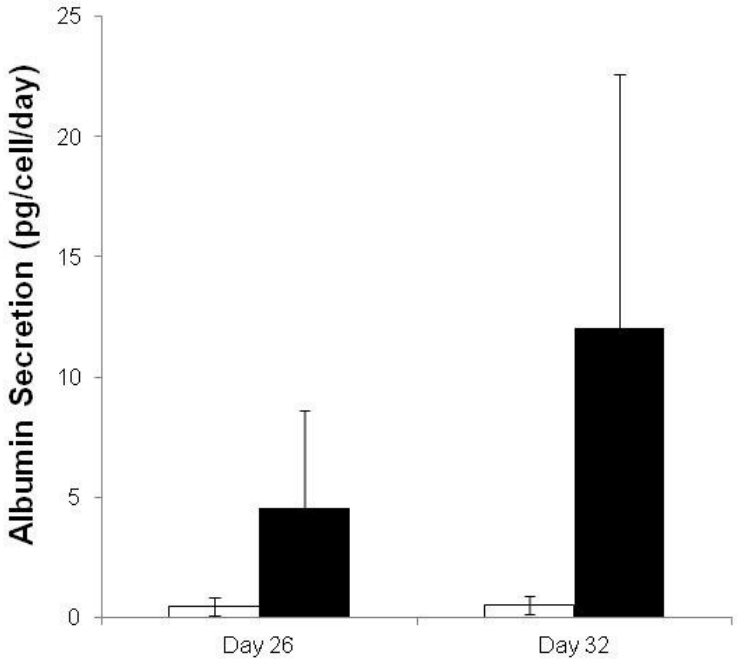

Figure 28: Albumin secretion by ELISA analysis in 2D monolayer (□) and 3D spheroid (■)

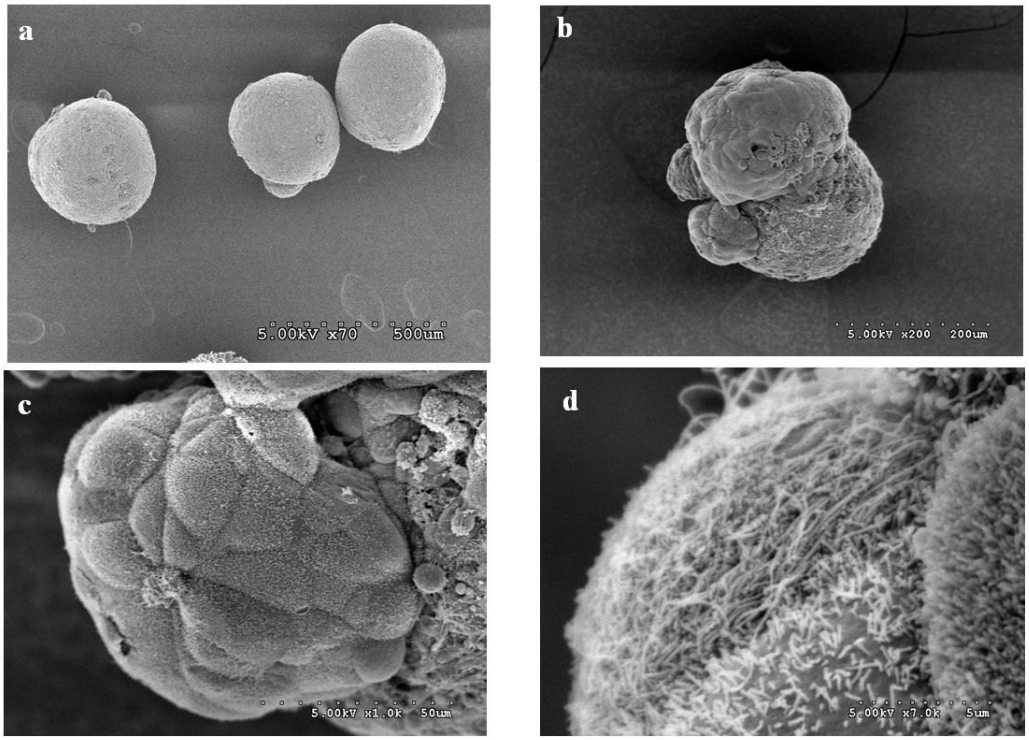

Figure 29: High-power morphology imaging of 3D spheroids

Scanning electron microscopy (SEM) images of representative 3D spheroids on D30 at magnifications of (a) 70X, (b) 200X, (c) 1000X, (d) 7000X

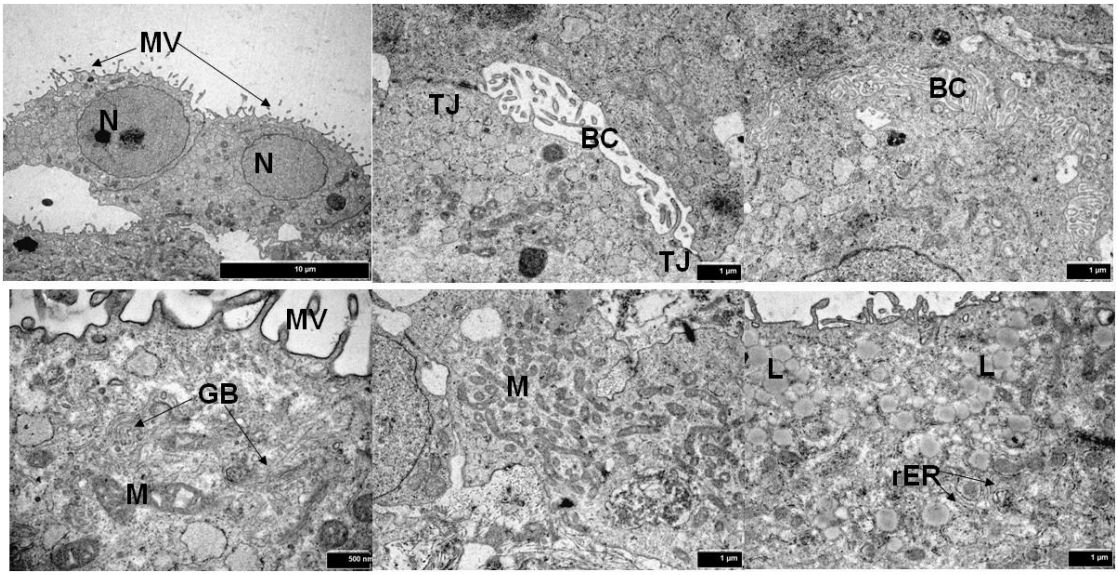

Figure 30: Ultrastructural characterization of 3D spheroids

Transmission electron microscopic (TEM) evaluation of 3D spheroids on D30 demonstrates various ultrastructural features characteristic of hepatocytes apparent and labeled in one or more micrographs: nucleus (N); microvilli (MV); bile-canaliculi (BC); tight junctions (TJ); golgi body (GB); mitochondria (M); (f) lipid droplets (L); and rough endoplasmic reticulum (rER)

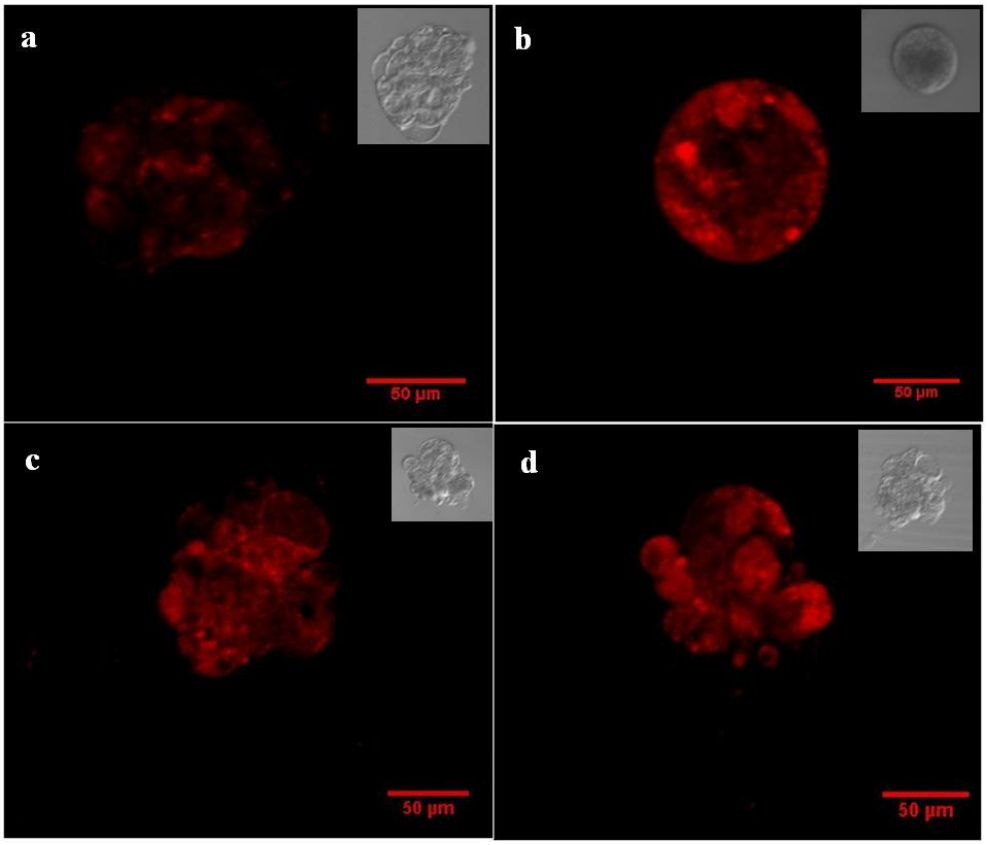

Figure 31: EROD and PROD activity in 3D spheroids

(a,b) EROD activity in 3D spheroids on D32 without (a) or with (b) 24 hours of b-naphthoflavone treatment; **(c,d)** PROD activity in 3D spheroids on D32 without (c) or with (d) 24 hours of Phenobarbital treatment. Insets show transmitted light images of the 3D spheroids collected simultaneously

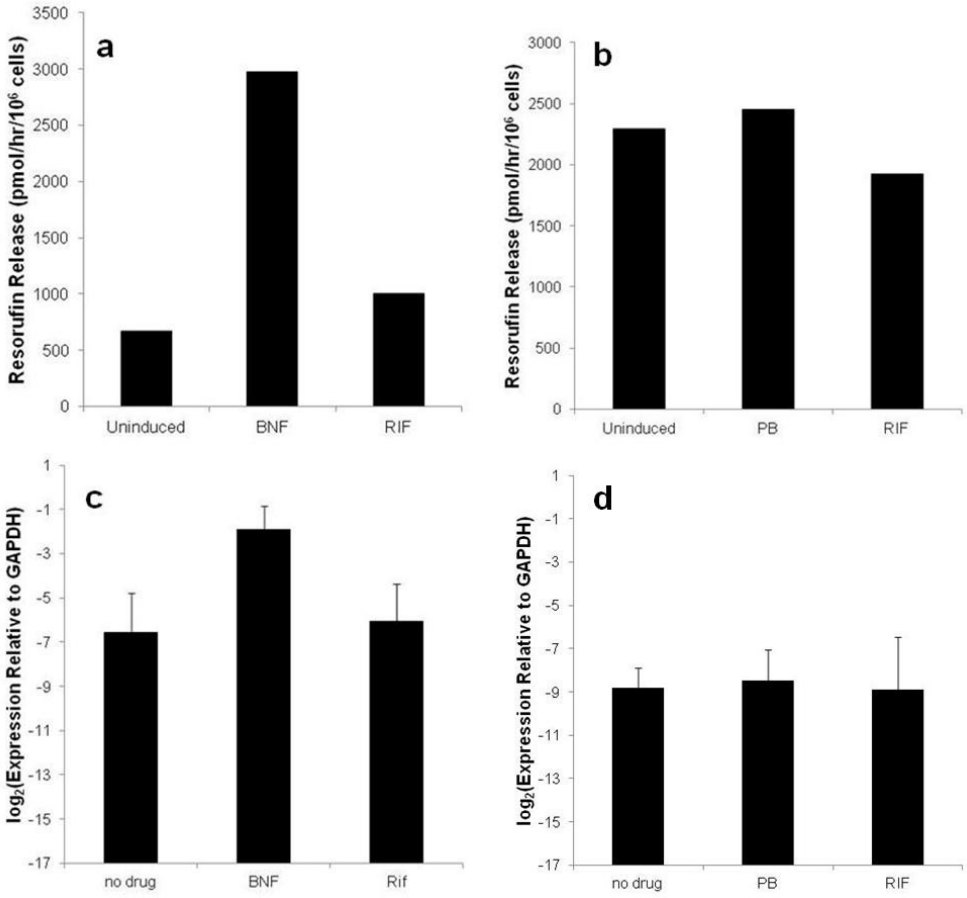

Figure 32: Cytochrome P450 activity and expression in 3D spheroids

(a,b) EROD (a) and PROD (b) activity with no drug or after treatment with BNF or Rifampicin (EROD) or with PB or Rifampicin (PROD); **(c,d)** Expression of Cyp1A1 (a) and Cyp2B6/7 (b) gene transcripts with no drug treatment or after treatment with BNF or Rifampicin (Cyp1A1) or with PB or Rifampicin (Cyp2B6/7)

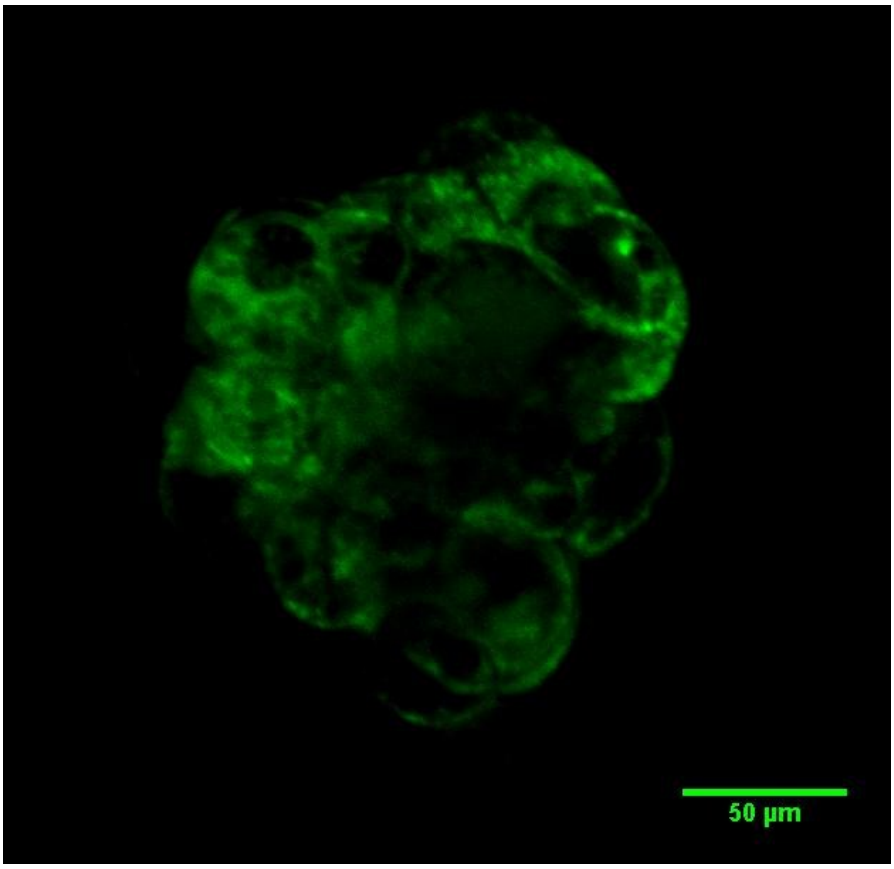

Figure 33: Accumulation of fluorescein after fluorescein diacetate cleavage in 3D spheroids

Confocal imaging visualizing the accumulation of fluorescein in the intercellular space after cleavage of fluorescein diacetate and excretion

CHAPTER 6: COMPARITIVE TRANSCRIPTOME ANALYSIS OF DIFFERENTIATED HUMAN EMBRYONIC STEM CELLS

6.1 Introduction

In the previous chapter, we demonstrated culture as three-dimensional spheroids of human embryonic stem cells differentiated toward the hepatic fate resulted in increased hepatic-specific gene expression, protein expression, morphology, and function as compared to our standard two-dimensional monolayer differentiation culture. However, when comparing our results and recent studies from literature, it is apparent that directed differentiation by soluble factor signaling alone is unlikely to produce the significant increases in function required to enable stem-cell derived hepatocyte-like cells to progress to a technology. Although the field of developmental biology will continue to provide insights into signaling pathways that may be interrogated to further enhance the extents of differentiation, a more robust and ready approach may be to force establishment of relevant transcriptional networks through exogenous expression of relevant factors, similar to reprogramming of somatic cells into iPS cells discussed in Section 2.1.4.

However, a strategy involving exogenous expression to establish the appropriate hepatocyte networks requires a more high-throughput discovery approach, as compared to the specific expression and function interrogation analysis described in the previous two chapters. In other words, in the previous two chapters, generating hepatocyte-like cells by directed differentiation from a starting stem cell population was the objective, and in order to assay the extent of differentiation, functions and expression levels of genes and proteins characteristic of the desired cell type, hepatocytes, were assayed. A high-throughput approach is somewhat opposite in that large numbers of characteristics are simultaneously screened between samples, and comparing the similarities and differences between samples can provide insights and promote discovery. One high-throughput assay that has garnered increasing attention over the past few years is microarray analysis, in which the expression level of large numbers of genes can be

simultaneously quantified by hybridizing a small amount of lysate sample to a microarray chip containing probes for the transcripts of thousands of genes, as described by Schena et al. (Schena, Shalon et al. 1995).

Gene expression analysis, often referred to as transcriptome analysis, is similar to qPCR in concept and in sample processing. Total RNA lysate is obtained from the samples, followed by purification of the mRNA fraction. From this mRNA lysate, complimentary DNA (cDNA) or RNA (cRNA) is generated, which is then amplified and hybrodized to the microarray chip. Although many technologies are currently available for transcriptome analysis, the Illumina HumanHT-12 v4 Expression BeadChip microarray system was used for this analysis. In this system, the oligonucleotide probes (primers) are tethered to microbeads with one probe per bead. cRNA samples are amplified and labeled before hybridization to the microbeads, which are then randomly distributed onto the microarray. Each bead also contains a unique address sequence that is used to identify the location of the bead on the array, which enables reading the plate to accurately determine the expression level of the sequence recognized by each bead-probe pair. The Illumina Human HT-12 v4 Expression BeadChip provides whole-genome gene expression analysis with more than 47,000 probes.

To further investigate the hES differentiation to hepatocyte-like cells discussed in the previous chapter, we probed differentiation samples using the Illumina BeadChip microarray system to obtain a high-throughput whole genome analysis of the gene expression differences between differentiated samples at D20 of monolayer differentiation and at D32 of spheroid differentiation culture. A D0 undifferentiated sample and an adult liver sample were also included for comparison. The objective of this study was to determine which genes and gene families changed from the D20 monolayer differentiation to the D32 spheroid culture. This analysis provided insights into the mechanism of enhanced differentiation in the D32 spheroid culture, as well as potentially providing candidate genes for direct manipulation to promote further maturation of the differentiated hepatocyte-like cells.

6.2 Data Processing

The samples analyzed in this portion of the study included a D0 undifferentiated HSF6 sample (D0), a monolayer differentiated D20 sample (D20), a 3D spheroid sample from D32 of culture (D32), and a standard adult liver mRNA sample (AL). The samples were provided to the Biomedical Genomics Center (BMGC) as mRNA samples, and all sample processing beyond mRNA isolation was performed by BMGC.

The microarray data was received from BMGC as text files either non-normalized or with rank invariant normalization. However, this normalization proved insufficient for this small data set. Because the Illumina Bead Array contained 47,323 genes and cells typically express 10,000-18,000 genes, the majority of genes probed on the array were not expressed, resulting in the negative fraction being heavily weighted in normalization efforts. Thus, alternative means of normalizing were explored. It was decided to manually process the data prior to normalization to obtain a more relevant dataset.

At BMGC, the four samples were processed as three technical replicates each. For each chip, the number of beads representing a particular probe was randomly distributed. The data for each test was therefore received as an average intensity value from all the beads representing the individual probe, a detection p-value, a standard deviation across the multiple beads of the probe, and the number of beads representing that probe. The data for each of the technical replicates was combined by averaging the signal over the total number of beads in all three triplicates and employing a pooled average strategy to determine the pooled standard deviation associated with each probe.

The intensity for each probe in each sample was determined by averaging across the beads, as

$$Int_{samp} = \frac{\sum_{i=1}^{3} Int_{samp,i} \cdot NBEADS_{samp,i}}{\sum_{i=1}^{3} NBEADS_{samp,i}}$$

where Int is the intensity of the sample and NBEADS is the number of beads in each chip. The pooled standard deviation was similarly calculated by accounting for the degrees of freedom in the standard deviations, as

$$\sigma_{samp} = \left[\frac{\sum_{i=1}^{3} \sigma_{samp,i}^{2} \cdot \left(NBEADS_{samp,i} - 1 \right)}{\sum_{i=1}^{3} \left(NBEADS_{samp,i} - 1 \right)} \right]^{\frac{1}{2}}$$

where σ is the standard deviation of the sample.

Because many genes were duplicated with multiple probes, the data set was then condensed by averaging the intensity values from each probe of repeated genes into a single intensity value. The associated standard deviation for the resultant intensity was calculated by the averaging the variances. This condensation was performed in MATLAB. In addition to the condensed data, the MATLAB routine also generates an output file with data from D20 and D32 of the genes with multiple probes. This file allows the user to easily compare the relevant trends across each of the probes to ensure that any observed phenomena are present similarly across multiple probes, as opposed to being biased by an extreme outlier. Another feature of this routine was to remove any genes that are currently unannotated, as for this analysis we wish to focus on genes whose functions and localization are somewhat known. In other words, we wish to focus on genes and networks that may be manipulated or otherwise offer insight to further push differentiation toward functionally mature hepatocytes.

After subjecting the full pooled average data set to the MATLAB routine, the data set was reduced from 47,323 unique probes to 31,430 unique genes. However, this is still a rather large number of genes compared to the expected expression per cell, thereby still imposing bias toward non-expressed genes. The final data reduction step involved removing probes in which the intensity in all four samples fell below a threshold value indicating no expression of that gene within that sample. A number of genes were

inspected that were not expected to be expressed in any of the four samples, and a threshold intensity value of 128 was selected. To be considered in the final data set, at least one of the four samples must have had an average intensity value greater than 128. This exclusion criteria finally reduced the data set to 15,377 which is a reasonably sized data set to investigate the changes during differentiation and from D20 to D32 in spheroid culture.

The reduced data set was then normalized by setting the mean of the middle 96% of intensities in each sample to 500 (arbitrary). Briefly, this was accomplished by sorting the expression within each sample by increasing intensities, removing the top and bottom 2% of intensity values (the 307 lowest and 307 highest values, for 15,377 genes) and computing the mean of the remaining intensities. The individual intensities were then scaled based on this middle mean value by multiplying each intensity by the constant $500/I_{avg}$, where I_{avg} was the mean of the middle 96% of intensities. After data reduction and normalization, the intensity frequency distributions for each sample were compared and are presented in Figure 34.

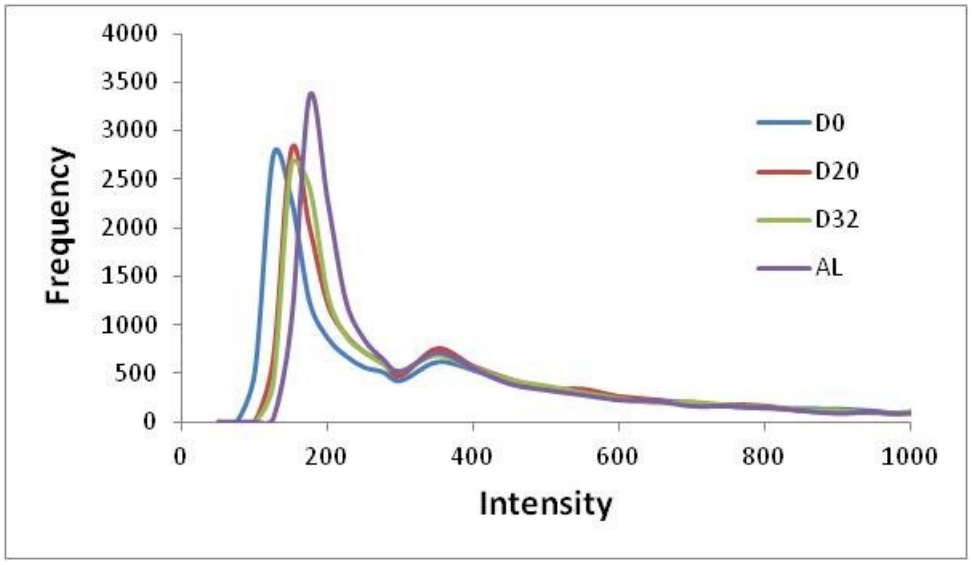

Figure 34: Intensity frequency distribution after data condensation

Finally, the data set was imported into Spotfire DecisionSite for data analysis. The software was used to visualize and identify genes that exhibited increased expression in one sample as compared to another, generally in D32 spheroid sample compared to D20 monolayer sample. K-means clustering was also used to group genes that exhibited similar expression profiles across all four samples.

6.3 Expression Patterns in Known Hepatic Gene Sets

Spotfire DecisionSite was used to explore the processed data from the microarray experiment. Two approaches were taken in examining the data: first, classes of genes known to be important for hepatocyte specification and function were examined; secondly, some individual genes exhibiting marked difference in the spheroid culture as compared to the D20 monolayer sample were investigated in more detail, along with other related gene family members if a number of genes were identified to be changing.

The data were primarily visualized, and are presented in this analysis, as scatter plots with $\log_2$(D32/D20 intensity ratio) on the x-axis with D20 intensity on the y-axis. The positive x-axis, therefore, indicates increased expression in the D32 spheroid sample as compared to the D20 monolayer sample, with higher values indicating higher fold change. In most analyses, genes exhibiting $\log_2$(D32/D20 intensity ratio) > 1 (i.e., those which exhibit a 2-fold increase in expression in the D32 sample) are labeled with their gene symbol on the scatter plots. Although visualizing the data in this manner does not incorporate adult liver (AL) expression data, Spotfire DecisionSite grades the colors the individual points on the scatter plot according to expression in the AL sample; low expression in the AL sample is colored red and the coloration is graded up to blue, indicating high expression in the AL sample. All processed data discussed in this chapter are presented in tables in Appendix including the processed data from all four samples and the $\log_2$(D32/D20 intensity ratio) values.

6.3.1 Hepatocyte Nuclear Factors (HNFs)

Perhaps the most obvious set of genes to investigate in this transcriptome analysis are the hepatocyte nuclear factors (HNFs), which are the transcription factors responsible for establishing and maintaining the transcriptional network defining hepatocytes. The HNFs are not actually a family of related transcription factor, but are rather so named because the set of nine transcription factors are all enriched in the liver. However, members of the four families comprising the HNFs are expressed in myriad tissues, but all four families are expressed simultaneously only in the liver. The HNFs therefore have alternate names based on a more systematic nomenclature. The four families of HNFs and their alternate names are: HNF1 (TCF or MODY); HNF3 (FOXA); HNF4 (HNF4α is also called TCF14 or MODY1, while HNF4γ is also called HNF4g); and HNF6 (ONECUT). Of the 9 HNFs expressed in the adult liver, 8 are represented in the processed data set and are shown in Figure 35 with the intensity values presented in Appendix ,

Table 1. It is noted that HNF4α, which is known to play an important role in embryonic development of and the adult function of the liver, was excluded due to low expression in all four samples, per the processing described in Section 0. However, expression of HNF4a was demonstrated in both D20 and D32 samples in the previous chapter by qPCR, indicating that the probe sets contained in the microarray may be problematic. Nevertheless, the expression profiles of the remaining HNFs in the transcriptome analysis is surprisingly similar across both samples and the adult liver control. Although a majority of the genes are expressed at slightly higher levels in the D32 sample, none are increased by more than 1.5-fold. Additionally, all eight of the HNFs examined exhibit similar expression levels in the D32 and AL samples. These data suggest that the differentiated samples have acquired a similar expression profile of the HNFs to that established in the adult liver. The lower functionality of the spheroid cells described in the previous chapter therefore may be related to other factors that are not fully developed, such as the appropriate combination and expression levels of various cofactors or epigenetic changes affecting the ability of the transcription factors to drive expression on

their downstream targets. Comparative chromatin immunoprecipitation (ChIP) assays against the various HNFs may provide some insight into whether the transcription factors are forming the complexes necessary to bind to downstream targets and may elucidate which cofactors and downstream targets are not being correctly bound.

6.3.2 Cytochrome P450 (CYP) Family

The next approach used in examining the microarray data sets was to probe the expression level of other sets of genes known to be important for hepatocyte function. A major function of the liver of great interest for pharmaceutical applications is drug metabolism and detoxification. Cytochrome P450 (CYP) enzymes are responsible for approximately 75% of drug metabolism in humans. Thus, the expression and correct function of CYP enzymes in differentiated stem cells are necessities for application-ready cell progeny. As we saw in the previous chapters, rMAPC differentiated as 3D aggregates and in hES allowed to form 3D spheroids after monolayer differentiation both exhibit expression and function of some CYP enzymes, including increased expression and function of some enzymes in response to appropriate inducers, but not others. Indeed, cells to be used for drug toxicity screening, bioartificial liver devices, or as transplantation candidates must exhibit levels of expression, function, and response to inducers similar to their *in vivo* counterparts.

The CYP genes remaining after data processing are shown in Figure 36. A total of 39 CYP genes were present in the data set after processing, and of the 39 only 10 exhibited a 2-fold or higher increase in expression level in D32 compared to D20. Included in those was Cyp1A1 (greater than 5-fold increase from D20 to D32) which was examined in the hES spheroids in the previous chapter, Cyp3A5 (greater than 2.5-fold increase from D20 to D32), and Cyp3A7 (3.5-fold increase from D20 to D32). However, Cyp1A1 and Cyp3A7 expression in the D32 spheroid sample is higher than the expression level in the AL sample, while Cyp3A5 is expressed at similarly high levels in both D32 and AL samples. The CYP gene exhibiting the highest increase in expression level between D20 and D32 samples was Cyp4A11, which increased more than 10-fold in the D32 sample;

however, even this expression is only a fraction of the expression level in AL, which was an additional 7-fold higher than in the D32 sample.

Although this analysis does not incorporate response to inhibitors or suppressors, the basal expression levels of differentiated cells should be on the same order as in in vivo hepatocytes, especially those expressed at very high levels. Comparing the expression level in the D32 sample to the most highly expressed CYP enzymes in the AL may give some insight into how close the differentiation protocol is to yielding functional hepatocyte-like cells. Cyp2E1, which is the most highly expressed CYP gene in the AL sample, is not expressed at all in either the D20 or D32 sample. Likewise, Cyp2C8 and Cyp2C9, which are highly expressed in the AL sample, exhibit low levels of expression in D20 and D32 samples. Although Cyp3A5 is expressed in similar levels in D32 and AL, the closely related Cyp3A4 is highly expressed in AL but is not expressed in D20 or D32 samples (intensity values < 128). Even many CYP genes with marked increase in expression from D20 to D32, including Cyp2C18, Cyp2J2, Cyp4A11, Cyp4V2, and Cyp27A1, still exhibit only a fraction of the expression level as compared to the AL sample. These data suggest that, although the drug metabolism enzymes generally increase in expression from D20 monolayer to D32 spheroid culture (33 of 39 genes exhibit $\log_2$(D32/D20 intensity ratio > 0), the drug metabolism network is not yet fully developed. Thus, additional differentiation strategies must include maturation of this class of metabolizing enzymes.

6.3.3 Other Phase I Enzymes

In addition to CYP enzymes, gene expression for other Phase I enzymes of drug metabolism were investigated and are presented in Figure 37, and the intensity values for these genes and their specific Phase I function are given in Appendix , Table 3. There are four major classes of non-CYP Phase I functions represented in these data: alcohol dehydrogenase activity; aldehyde dehydrogenase activity; flavin-containing monooxygenase activity; and monoamine oxide activity.

The alcohol dehydrogenase (ADH) enzymes are members of the Phase I group of enzymes that are responsible for breaking down toxic alcohols and also function in biosynthesis of metabolites involving aldehydes, ketones, and alcohol groups. All seven of the known alcohol dehydrogenases are represented in the processed data set, and of these only two exhibited more than 2-fold increase in expression from D20 to D32: ADH1A increased by more than 14-fold; and ADH4 increased by more than 2.5-fold. However, the expression level of each of these in the D32 sample was much lower than in the AL sample, as ADH1A was 5-fold higher in AL and ADH4 was nearly 11-fold higher in AL. Of the remaining five alcohol dehydrogenases with similar expression between D20 and D32, two were expressed at significantly higher levels in the AL sample (ADH1B was 12.5-fold higher and ADH1C was 21.5-fold higher) while the remaining three, ADH5, ADH6, and ADH7 were expressed at similar levels in D20, D32, and AL samples. These data suggest that the alcohol dehydrogenase activity in the differentiated spheroid cells is partially developed, but must be pushed further to match the expression and, presumably, the activity level demonstrated in adult hepatocytes. However, it should be noted that ADH expression can vary significantly based on age, sex, and ethnicity, and since the source of the AL sample is unknown, these data should be compared across multiple liver samples before conclusions are drawn.

The aldehyde dehydrogenase (ALDH) enzymes are members of the Phase I group of enzymes responsible for oxidizing aldehydes to carboxylic acids, which are secreted from the liver for metabolism in muscle tissues. Of the sixteen aldehyde dehydrogenase genes present in the processed data, only four demonstrate a 2-fold or higher increase in expression in D32 spheroid sample as compared to the D20 monolayer sample. ALDH1A1 exhibits the greatest increase in expression, with a 15-fold increase; however, while the gene is expressed highly in the AL sample, the 3D spheroid sample is 5-fold higher than even the AL sample expression. Another six ALDH genes exhibit 2-fold higher expression in the AL sample than in the D32 sample, indicating overall lower expression of the aldehyde dehydrogenase family of genes in the differentiated samples. Like alcohol dehydrogenases, however, the expression profile of the aldehyde dehydrogenase genes within humans can vary significantly by ethnicity, and since the

source of the AL sample is unknown, these data should be verified across multiple samples before additional conclusions are drawn.

The last two classes of Phase I enzymes investigated in this study are the flavin-containing monooxygenase (FMO) system and the monoamine oxidase (MAO) activity. Although FMO1 expression is nearly 2-fold higher in the D32 sample as compared to the D20 sample, the gene does not exhibit expression in the AL sample; conversely, FMO3, which is highly expressed in the AL sample, is not expressed in either D20 or D32 samples, while FMO5 is expressed at similarly high levels in D20 and D32 samples but not in the AL sample. These data suggest that the FMO expression profile is not similar in either D20 or D32 samples to the AL sample, indicating that this particular Phase I mechanism is likely not functional. However, of the two MAO genes expressed in humans, both are similarly expressed in D32 and AL samples. MAOA is expressed at similar levels in D20, D32, and AL samples, while MAOB exhibits a more than 2-fold increase in expression from D20 to D32, suggesting that the MAO activity may be well-developed in the spheroid samples. However, functional assays should be performed to determine the extent of MOA function within the differentiated cells.

6.3.4 UDP Glucuronosyltransferase (UGT) Family

A second group of enzymes investigated in this transcriptome analysis was the uridine 5'-diphospho-glucuronosyltransfer (UDP-glucuronosyltransferase or UGT) family, which catalyze glucuronidation reactions involving the transfer of a glycosyl group from UTP molecules to hydrophobic molecules. Like the CYP enzymes, the UGT enzymes are important for drug metabolism as one of the primary mechanisms for Phase II detoxication by conjugation. The conjugation of the glucuronosyl group from a UTP derivative onto the functional group, which was added during Phase I of drug metabolism, of the hydrophobic molecule, resulting in a more hydrophilic derivative that can then be more easily excreted by the kidneys. Thus, correct function of the UGT enzymes in stem cell-derived hepatocyte-like cells is paramount to full drug metabolism and detoxification functions in clinical applications.

The 18 UGT genes remaining after data processing are shown in Figure 38, and the intensities for all four samples are given in Appendix , Table 4. Of the 18 UGT genes in the data set, nearly half (8) exhibited more than 2-fold increase from the D20 sample to the D32 sample, and all but 2 exhibited increased expression in the D32 sample. Unlike the CYP gene expression profiles, however, nearly all of the UGT gene enzymes are expressed in the D32 sample at levels similar to the expression level in the AL sample, except UGT2B7 and UGT3A1, which are each about 2-fold higher in the AL sample than in the D32 sample. However, these data overall suggest that the three-dimensional spheroid culture enhances the overall expression of UGT enzymes to levels similar to that seen in the adult liver. Although gene expression does not imply functionality, these data are promising in terms of the potential ability of the cells within the spheroids to perform the conjugation and detoxication steps of drug metabolism.

6.4 Identification of Additional Genes and Gene Sets from Transcriptome Data

After carefully examining the expression profiles in a number of gene sets known to be important for hepatocyte specification and function, the next step in the transcriptome analysis was to evaluate other genes which exhibit changes in expression levels between samples. This method can be useful to identify other sets of genes that may not be as obvious, but which may be important in determining the mechanism of the enhancement of differentiation in the spheroid culture or those which may be further interrogated to promote additional maturation of differentiated cells. The following is a discussion of only two families that exhibited marked increase in expression from D20 to D32. A full list of genes that are either upregulated or downregulated by 4-fold or more from D20 to D32 are presented in Appendix , Table 5 and Table 6, respectively.

6.4.1 Aldo/Keto Reductase (AKR) Superfamily

The aldo/keto reductase (AKR) superfamily is a family of enzymes that catalyze NADPH-dependent redox reactions using myriad carbonyls as substrates and reducing them, typically to either primary or secondary alcohols. Several members of the AKR family of enzymes were identified from analysis of the microarray data, specifically that AKR1B10, AKR1B15, AKR1C1, and AKR1C4 were increased more than 16-fold in D32 samples compared to D20 samples, and AKR1C2 and AKR1C3 were increased more than 4-fold. The log of the ratio of intensity values for D32 and D20 samples for each of the AKR proteins remaining in the data set after processing (Section 0) are shown in Figure 40, and intensity values can be found in Appendix .

6.4.1.1 AKR1A1

In the microarray data set, AKR1A1 is expressed at similar levels in all four samples, although the D20 sample is 1.4-fold lower than the other samples. AKR1A1, commonly referred to as aldehyde reductase, is responsible for the reduction of certain aldehydes and is expressed in nearly all tissues (Barski, Gabbay et al. 1999), although it has a unique role in inositol catabolism, a specific function of the kidney cortex, and is therefore expressed more highly in the kidney (Barski, Papusha et al. 2005). Thus, the expression profile demonstrated in the microarray data set is expected.

6.4.1.2 AKR1B subfamily

The AKR1B subfamily has two enzymes that are well-studied in humans, and each of them exhibited high expression specifically in the D32 sample: AKR1B1, commonly referred to as aldose reductase, is involved in the reduction of the aldehyde form of glucose to sorbitol and is implicated in complications arising from Type 2 diabetes (Yabe-Nishimura 1998); and AKR1B10, which is expressed in multiple tissues including the small intestine, colon, and liver (Cao, Fan et al. 1998), is overexpressed in numerous cancers (Cao, Fan et al. 1998; Fukumoto, Yamauchi et al. 2005; Yoshitake, Takahashi et al. 2007), including hepatic carcinomas. A third member of the AKR1B subfamily,

AKR1B15, also exhibited high expression specifically in the D32 sample. This enzyme has only recently been identified, however, and its expression patterns and function are not yet well understood, although it contains 91% sequence identity with AKR1B10 (Salabei, Li et al. 2011).

The abundant expression of these AKR1B subfamily enzymes specifically in the D32 sample, including a greater than 80-fold increase in AKR1B10 over the D20 sample, suggests that the cells comprising the spheroid may be adopting some characteristic of cancerous cells. Although it is not clear what mechanism is responsible for the increased expression of the AKR1B enzymes, the abundant expression of this subfamily of enzymes must be limited in cells produced for therapeutic purposes, potentially by inclusion of specific inhibitors in the culture media. Further analysis must be performed to determine what role, if any, this family of enzymes are playing in the spheroid cultured cells.

6.4.1.3 AKR1C subfamily

The AKR1C subfamily, commonly known as the 3α-hydroxysteroid dehydrogenases (HSDs), include the four enzymes AKR1C1, AKR1C2, AKR1C3, and AKR1C4, all of which are expressed in the liver where they function in bile acid biosynthesis and the processing of steroids, although only AKR1C4 is uniquely expressed in liver (Penning, Jin et al. 2004). Although AKR1C1 expression was not detected in any samples in this microarray experiments and was therefore excluded from further analysis, AKR1C2, AKR1C3, and AKR1C4 exhibited more than 12-, 8-, and 21-fold increases in expression in D32 sample as compared to D20 sample, and the D32 sample exhibited expression levels similar to those seen in the AL sample. These data suggest that at least portions of the bile acid biosynthesis pathway and the detoxification functions are fairly well established in the spheroid cultured cells, similar to the Cyp450 assays previously discussed (Section 5.2.6). The expression patterns alone are not sufficient to establish functionality, and further analysis should be completed to determine the extent of

function within the spheroids. However, the increase in expression of these enzymes in the spheroid culture to levels similar to those seen in adult liver is encouraging.

6.4.1.4 Other AKR family members

The remaining AKR family members considered in the microarray analysis were AKR1D1, AKR7A2, and AKR7A3, each of which is expressed in the liver. AKR1D1 works in concert with the AKR1C subfamily, specifically AKR1C4, in bile acid biosynthesis and hormone clearance (Lee, Lukacik et al. 2009). The expression levels of AKR1D1 were similar in all four samples, although increased slightly in both D20 and D32 compared to D0, but not as high as in AL, suggesting this component of the pathways may be underdeveloped in the differentiated cells. AKR7A2 and AKR7A3 are both human aflatoxin aldehyde reductases responsible for the detoxification of aflotoxin B1 (Ireland, Harrison et al. 1998; Knight, Primiano et al. 1999). Similar to AKR1D1, AKR7A2 was expressed in all four samples, although it demonstrated slightly increased expression in D20 and D32 samples as compared to D0 samples. However, AKR7A3 was expressed at similarly low levels in each of the differentiation samples D0, D20, and D32, but was highly expressed in the AL sample. These data suggest that the aflotoxin aldehyde reductase activity may not be developed in the differentiated samples, which is further indication that the full functional profile of adult hepatocytes has not yet been achieved in the differentiated samples. Complete maturation of the hepatocyte-like cells should be accompanied by the acquired expression of these and similar functional enzymes.

6.4.2 Metallothionein (MT) family

Metallothionein (MT) is a family of proteins that are cysteine-rich and localized to the Golgi apparatus membrane. Nine members of the protein coding MT family were examined in the microarray analysis, eight of which belong to the subfamily MT1 and the last of which is part of the subfamily MT2 (Figure 41). Each of these exhibited marked increase in expression level in D32 as compared to D20 sample, ranging from a 4-fold increase in MT1B to a 170-fold increase in MT1G. Most of these are also highly

expressed in the adult liver sample, suggesting that abundant expression of these metallothioneins may not be unexpected in differentiated hepatocyte-like cells.

Although the specific physiological functions of MTs are not currently well understood, they have been implicated in regulation of homeostasis through a number of anti-stress mechanisms including metabolism, heavy metal detoxification, and response to environmental stresses such as oxidative stress (Sato and Kondoh 2002). Metallothioneins have also, however, been implicated in the pathology of numerous cancers, potentially as promoters of tumor growth and protection of tumor cells from drug treatments (Krizkova, Fabrik et al. 2009). Thus, the higher levels of expression of some MT genes in D32 as compared to AL, such as MT1E, MT1G, and MT1H, may be of some concern in regards to tumor formation from differentiated cells. Further investigation of the role of the MT protein products in the differentiated cells should be pursued, especially as more information becomes available about the physiological roles of MTs in both normal tissue and in tumor formation and protection.

6.5 Discussion

In the previous chapters, we have shown the ability of three-dimensional culture systems to enhance differentiation toward hepatocyte-like cells as compared with the standard monolayer differentiation. Indeed, culture in these three-dimensional aggregate or spheroid systems resulted in increased expression of transcripts and proteins characteristic of hepatocytes and higher levels of function. Although the differentiated cells exhibited a number of hepatocyte-specific functions, some at physiologically relevant levels, the overall functional profile of cells still remained significantly lower than is required for *in vivo* hepatocytes. Specifically, although some cytochrome P450 activity was observed, only one of the two functions examined in the hES differentiated spheroids responded to a specific inducer by increasing gene expression and function while the other function investigated was unresponsive. Although the three-dimensional spheroid culture system we describe appears capable of maintaining differentiated hepatic expression and function for extended cultures, further maturation of the cells within the

differentiation protocol is necessary before they can be used for drug toxicity screening or for clinical applications.

In order to obtain a more complete picture of the changes between D20 monolayer differentiation and D32 spheroid culture, as well as the shortcomings in the D32 differentiated cells as compared to adult liver, we performed a whole-genome transcriptome analysis on representative samples from D0 (undifferentiated), D20 (monolayer differentiated), and D32 (spheroid culture differentiated) cells along with a representative adult liver standard sample. We first analyzed the expression of a number of families of genes known to be involved in hepatocyte function, including the liver-enriched hepatocyte nuclear factors (HNFs), genes for the Cytochrome P450 enzymes, genes for other Phase I drug metabolism enzyme, and UDP-glucuronosyltransferase (UGT) genes, which are Phase II drug metabolizing enzymes. We observed that the HNFs were all expressed at levels similar to the expression level in the adult liver in the D32 spheroid samples, and these were expressed at only slightly higher levels than in the D20 monolayer sample. However, numerous genes of the other families probed exhibited increased expression in the D32 sample as compared to the D20 sample, although the overall profiles still fell short of expression in adult liver.

We next used the transcriptome analysis to identify other genes that were changing between D20 and D32 that were not necessarily expected to change. We identified two large families of genes that all exhibit higher expression in the D32 sample as compared to the D20 sample: the aldo/keto reductase (AKR) superfamily and the metallothionein (MT) family. A number of other genes demonstrated marked difference between D20 and D32, either increasing or decreasing expression by a large amount. Further anlaysis of these data may yield additional novel transcription factors or signaling pathways that may be manipulated to improve the functional maturity of cells from the directed differentiation culture.

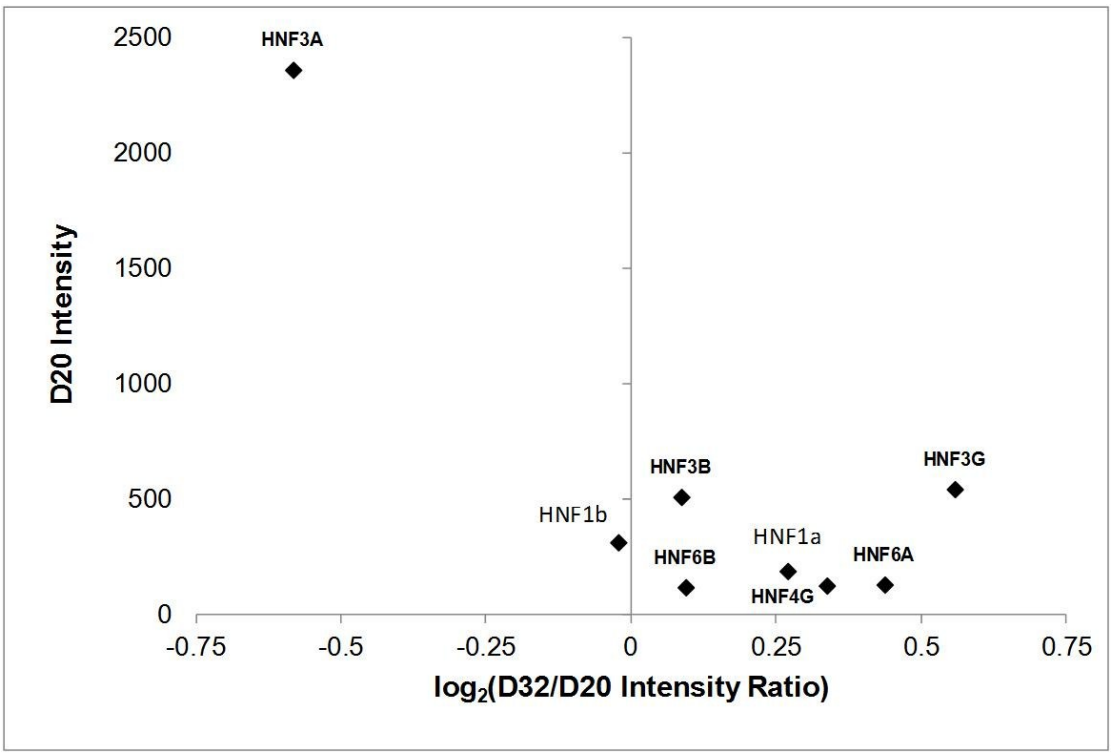

Figure 35: Intensity ratios for hepatocyte nuclear factors in D32 and D20 samples

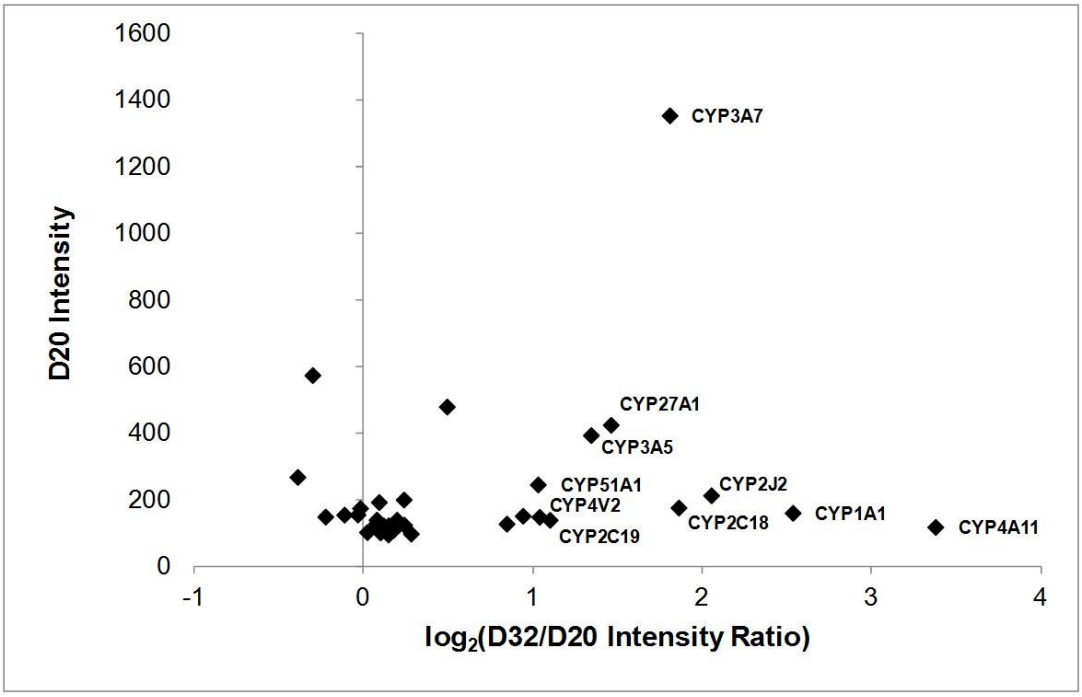

Figure 36: Intensity ratios for CYP450 enzymes in D32 and D20 samples

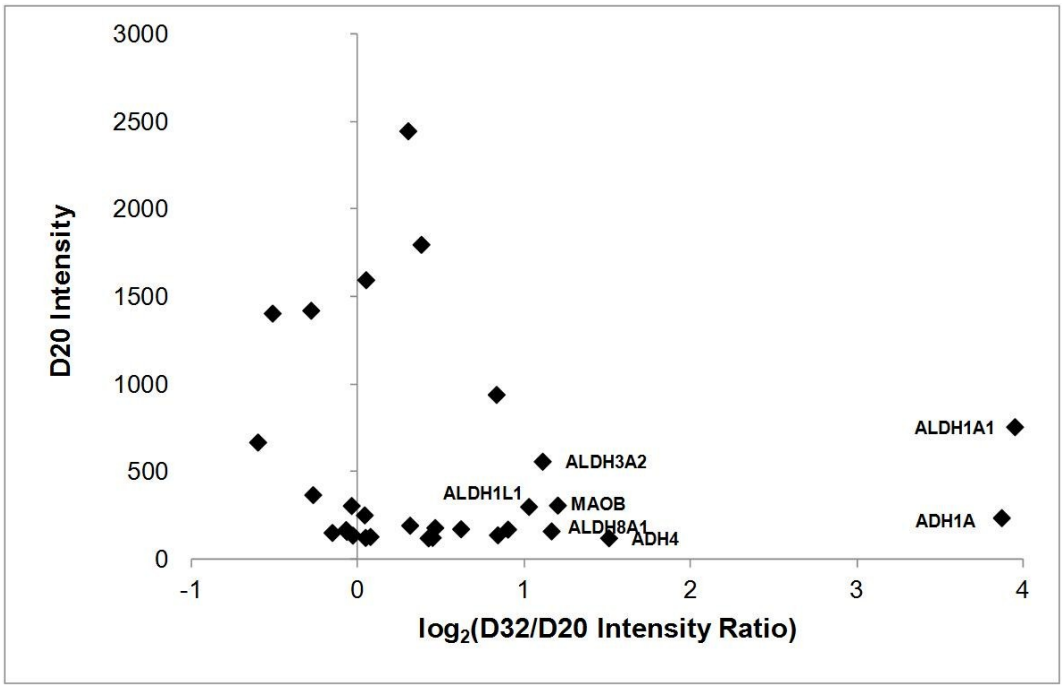

Figure 37: Intensity ratios for non-CYP Phase I enzymes in D32 and D20 samples

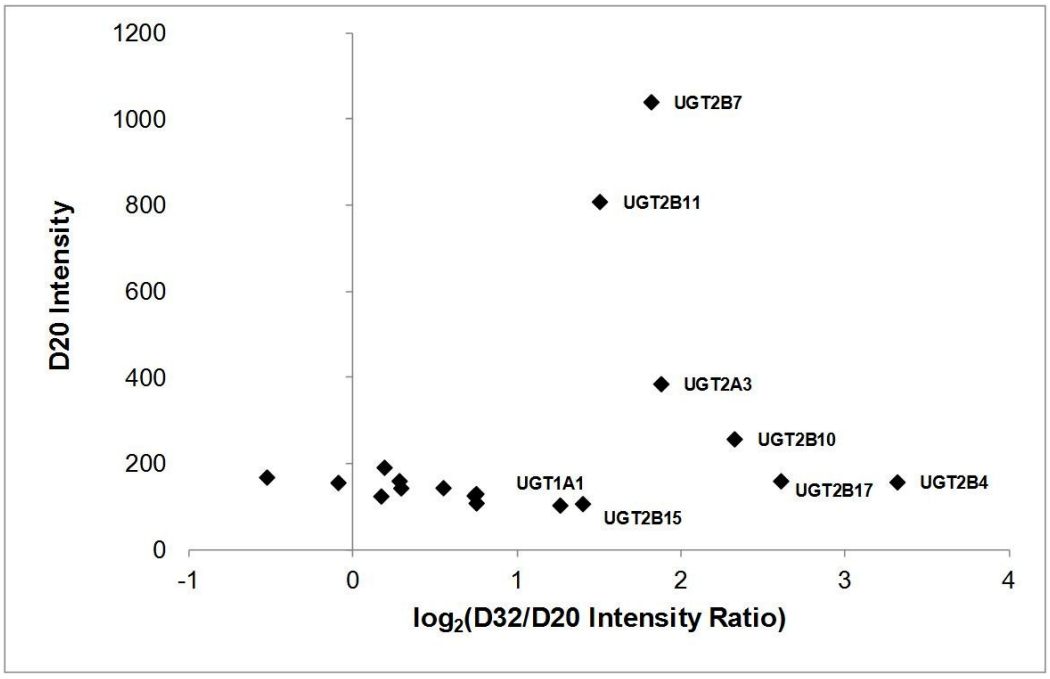

Figure 38: Intensity ratios for UGT enzymes in D32 and D20 samples

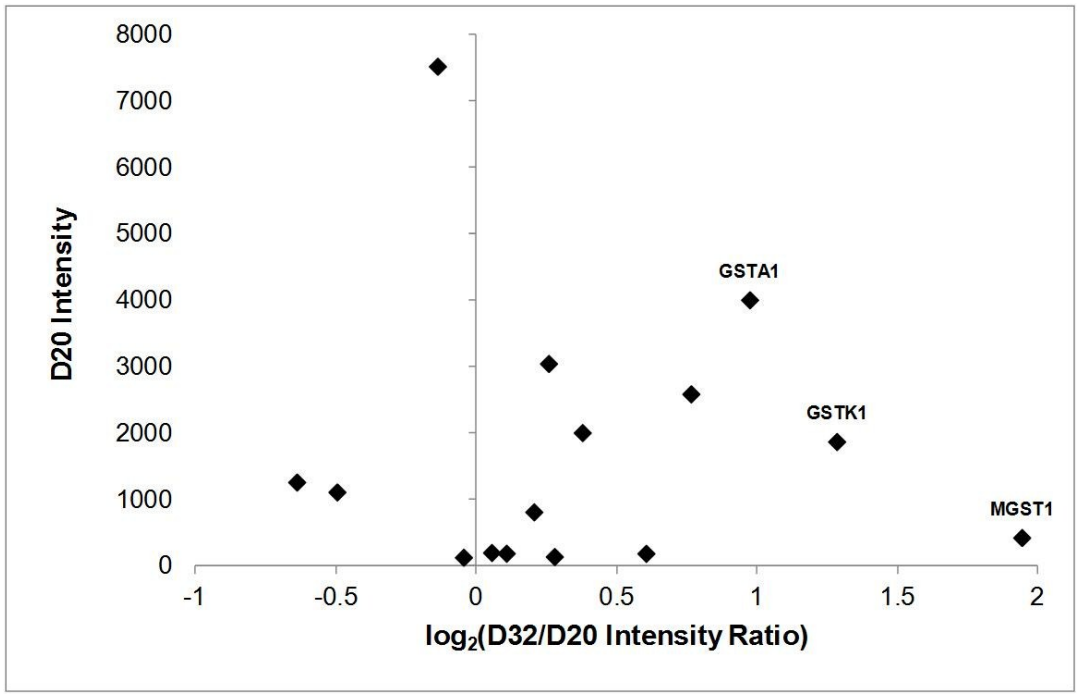

Figure 39: Intensity ratios for GST enzymes in D32 and D20 samples

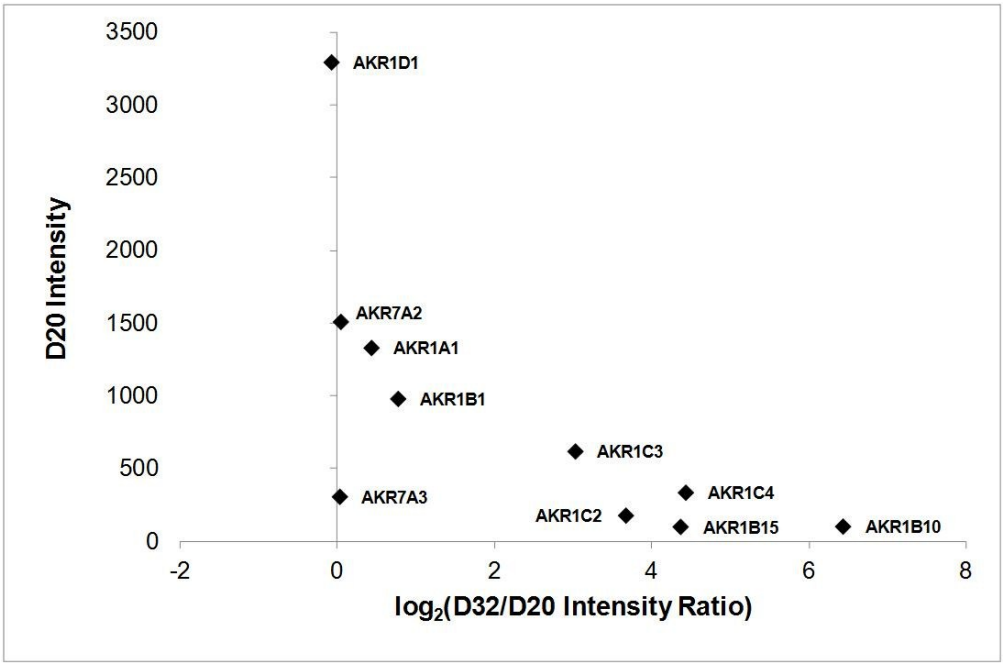

Figure 40: Intensity ratios for AKR superfamily in D32 and D20 samples

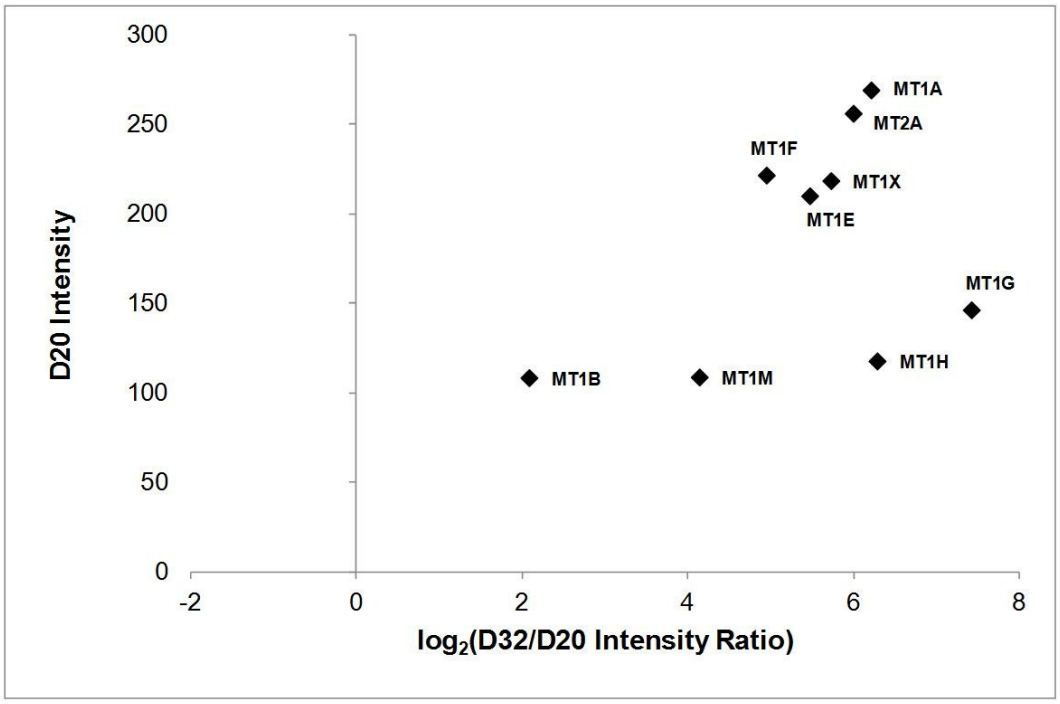

Figure 41: Intensity ratios for MT family in D32 and D20 samples

CHAPTER 7: CONCLUSIONS AND FUTURE DIRECTIONS

The ability of pluripotent stem cells to differentiate into hepatocyte-like cells offers a promising platform for generating large numbers of quality cells for potential applications such as drug discovery, populating a bioartificial liver device, and eventually for therapeutic applications such as a cell source for transplantation for the treatment of end-stage liver disease. In order for this potential to be realized, advancements must be made to all phases of the process with an eye toward efficiency, safety, and scalability. Pluripotent stem cell lines must be established and cultured in the absence of animal products or transgene expression systems, differentiation protocols must be robust and scalable, post-differentiation culture systems must be robust and relevant for the particular application, and tumor-forming cells must be eliminated to a high level of confidence for therapeutic cells. To address these goals, this study involved engineering a three-dimensional culture system capable of enhancing the differentiation of rat multipotent adult progenitor cells and human embryonic stem cells toward the hepatic fate. The objectives of this study were thus: (i) to engineer a three-dimensional culture system for the enhancement of differentiation from rat multipotent adult progenitor cells to a hepatocyte-like cell (Chapter 4); (ii) to engineer a three-dimensional culture system for the enhancement of differentiation from human embryonic stem cells to a hepatocyte-like cell and to maintain the differentiated state for extended culture (Chapter 5); (iii) to use whole genome expression data to explore the changes in expression of genes in classes relevant to the hepatocyte fate and to discover genes or families of genes as candidates for investigation into the mechanisms of the differentiation enhancement (Chapter 6).

7.1 Aggregate differentiation of rMAPC cells

Rat multipotent adult progenitor cells (rMAPC) offer many advantages as a potent stem cell population to use as a readily adaptable model for human systems. Primary rat hepatocytes, because of the ease of isolation and the well-studied cultured methods and drug responsiveness, are routinely used for high-throughput substitutes in lieu of the

scarce human hepatocytes. Indeed, our multistep differentiation hepatic protocol was optimized using rMAPC as a model system, and the optimized protocol was readily extended to human embryonic stem (hES) and induced pluripotent stem (iPS) cells with minimal alterations (Roelandt, Pauwelyn et al. 2010). We had also previously demonstrated the ability of rMAPC to self-assemble into tightly packed three-dimensional aggregates under low-attachment culture conditions and proliferate without losing their potency or self-renewal capacity (Subramanian, Park et al. 2011). Thus, we hypothesized that carrying out the directed four-step differentiation protocol toward hepatic cells on rMAPC aggregates may enhance the yield and maturity of hepatocyte-like cells after differentiation.

To test this hypothesis, we compared differentiation of rMAPC as three-dimensional aggregates to the standard monolayer differentiation culture. We showed that differentiation in the aggregate culture system resulted in significantly higher expression of liver-specific transcripts, including an increased *albumin* mRNA level, and higher levels of albumin and urea secretion. This coincides with the presence of significantly more cells that express intracellular albumin at levels found in primary hepatocytes. The differentiated cell aggregates exhibited cytochrome P450 mediated ethoxyresorufin-O-dealkyation (EROD) and pentoxyresorufin-O-dealkylation (PROD) activity. Consistent with these increased mature functions, cells within the aggregates were shown to have many ultrastructural features of mature hepatocytes by transmission electron microscopy. With the scalability of the aggregate culture system and the enhanced differentiation capability, this system may facilitate translation of generating hepatocytes from stem cells to technology.

7.2 Spheroid culture of differentiation hES cells

Human embryonic stem (hES) cells are the quintessential pluripotent cell type, with the ability to generate all cell types of the adult organism. Furthermore, they are the benchmark for determining the pluripotent cell fate of induced pluripotent stem (hiPS) cells. Although hiPS cells exhibit expanded versatility for applications, with the ability to

readily generate hiPS cells with myriad genetic backgrounds and disease states, hES cells remain an important cell type for studying the mechanisms of pluripotency and differentiation, especially since most techniques developed for hES cells, including differentiation protocols, should be readily extended to hiPS with minimal modifications. Additionally, as there are still myriad safety issues with the establishment of hiPS cells, hES cells may yield clinically relevant progeny in the shorter term. Nevertheless, the ability to generate a renewable source of functional hepatocyte-like cells from hES cells holds great potential for drug toxicity screening and therapeutic applications. After our success with a three-dimensional aggregate system for enhancing differentiation in the rMAPC model, we next applied a similar concept to the HSF6 differentiation culture. However, as the enhancement in the rMAPC differentiation was observed primarily in the final stage of differentiation, we hypothesized that culturing hES progeny in a three-dimensional culture system after the 20 day monolayer differentiation may similarly enhance the hepatic phenotype of the differentiated cells.

To apply this three-dimensional culture system, we first differentiated the HSF6 hES cells for 20 days as a monolayer according to our standard protocol. We then optimized a cell dissociation protocol by investigating the effectiveness of several commonly used cell dissociation enzymes or solutions either in a single stage or in a combination of two dissociation steps. The optimized protocol involved removing the differentiated cells from the Matrigel-covered culture dish as a layer by treatment with collagenase followed by dissociation into single cells by treatment with trypsin supplemented with chick serum. The resulting protocol yielded approximately $1.5x10^6$ million cells per well of a 12-well tissue culture dish with >90% viability. The single cells were then distributed into low-attachment culture dishes and centrifuged to initiate the three-dimensional spheroid culture. Cells self-assembled into three-dimensional spheroids over time, first as small groups of cells and coming together into fewer and larger spheroids by D6 of spheroid culture. By viability staining after 24 hours of spheroid culture, we showed that only those cells being incorporated into the forming aggregates maintained viability over time, while the rest perished, indicating that either agglomeration promotes survival or a

fraction of the cells were already fated to die by the time they were seeded into the 3D culture system.

After six days of formation, higher expression of a number of hepatocyte-specific gene transcripts were observed in the spheroid cultured cells but not in the monolayer cells, including genes such as *Albumin*, *Cx32*, *Arg1*, *Hnf4a*, and *F7*. Additionally, cells in the spheroids maintained this higher expression for an additional two weeks of culture while cells maintained in the monolayer culture system exhibited loss of expression of many of these genes. We also demonstrated larger fractions of cells expressing ASGPR-1 and PEPCK protein by fluorescence-activated cell sorting and PEPCK expression localized to the exterior of the spheroids by immunofluorescence. Ultrastructural characteristics of hepatocytes were observed in cells within the spheroids by electron microscopy. Additionally, cells in the spheroids exhibited some mature functions, such as EROD and PROD activity, which are Cyp1A1 and Cyp2B6/7 activities, respectively. Although the cells responded to treatment with β-napthoflavone (BNF) by increased EROD activity and expression of Cyp1A1 transcript, treatment with Phenobarbital (PB) did not result in increases in PROD activity or Cyp2B6/7 expression, indicating that cells in the spheroid are capable of responding appropriately to some external stimulations but not others. Finally, cells in the spheroid exhibited biliary excretion and accumulation of fluorescein diacetate metabolite, demonstrating polarity of cells within the spheroids.

These data suggest that the spheroid culture system is capable of bestowing significant enhancement of the hepatic differentiation from hES cells and maintaining that differentiated state for extended culture. However, the function of cells within the spheroids still fell short of the level exhibited by primary hepatocytes, indicating that further optimization is necessary to promote differentiation to more mature hepatocytes.

7.3 Whole-genome transcriptome analysis of differentiated cells

Although our three-dimensional spheroid culture system exhibited enhanced differentiation of hES cells to the hepatic cell fate, the levels of function of the

differentiated progeny still falls short of clinically relevant levels exhibited by primary hepatocytes. In surveying recent literature, in which a number of groups have all independently optimized differentiation strategies to generate hepatocyte-like cells from hES or hiPS cells, it appears that virtually all strategies are currently yielding cells of approximately the same level of mature function and heterogeneity with fetal hepatocyte characteristics and other cell types. Thus, other strategies may be more successful at this stage in the technology than further optimization of directed differentiation by signaling molecules in a traditional differentiation assay, especially in the final maturation stage of differentiation. Direct manipulation of the transcriptional networks responsible for establishing and maintaining the hepatocyte phenotype may prove useful in overcoming this barrier to producing mature hepatocytes. To identify individual genes and families of genes which may be important for the hepatocyte phenotype, and also to identify genes which are changing and may be partially responsible for the enhanced differentiation in the spheroid culture system, we performed a whole-genome transcriptome comparison on undifferentiated HSF6, D20 monolayer differentiated cells, D32 spheroid culture differentiated cells, and an adult liver standard sample.

We first examined the trends in the expression of a number of families of genes known to be important for the hepatocyte phenotype or function. Such families include the liver-enriched hepatocyte nuclear factors (HNFs), genes for the Cytochrome P450 enzymes, genes for other Phase I drug metabolism enzyme, and UDP-glucuronosyltransferase (UGT) genes, which are Phase II drug metabolizing enzymes. We observed that the HNFs were all expressed at levels similar to the expression level in the adult liver in the D32 spheroid samples, and these were expressed at only slightly higher levels than in the D20 monolayer sample. However, numerous genes of the other families probed exhibited increased expression in the D32 sample as compared to the D20 sample, although the overall profiles still fell short of expression in adult liver. We next used the transcriptome analysis to identify other genes that were changing between D20 and D32 that were not necessarily expected to change. We identified two large families of genes that all exhibit higher expression in the D32 sample as compared to the D20 sample: the aldo/keto reductase (AKR) superfamily and the metallothionein (MT) family. A number of other

genes demonstrated marked difference between D20 and D32, either increasing or decreasing expression by a large amount. Further anlaysis of these genes may yield novel transcription factors that may be manipulated to improve the functional maturity of cells from the directed differentiation culture.

7.4 Future Directions

The applications for stem cell derived hepatocytes discussed throughout this thesis include serving as model cells for high-throughput drug toxicity screening, populating bioartificial liver devices, and as transplantable cells for the treatment of end-stage liver disease. Although each of these applications has different requirements in terms of function and safety, they all potentially require high-quality, functionally mature hepatocytes or hepatocyte-like cells.

Stem cell-derived hepatocytes for drug toxicity screening obviously requires that the full panel of drug metabolism and detoxification systems to not only function at a basal level, but also to demonstrate the correct physiological response to specific inducers and inhibitors. Since it is impossible to test all possible combinations of inducers, inhibitors, and substrates on a single batch of differentiated cells to validate functionality, stem cell isolation, culture, and differentiation strategies established to generate the cells must be robust and reproducible. Additionally, criteria must be developed to quickly validate batches of differentiated cells with a small sample, likely in a high-throughput manner such as transcriptome or proteome analysis or even single-cell or single-colony/spheroid activity assays to quickly assess function.

Additional safety concerns, in addition to function, must be addressed before stem cell-derived hepatocytes can be themselves used as a product, as for populating a bioartificial liver device or for transplantation. Not only must the hepatocyte-like cells be functionally mature, but they must also be highly purified; any cell types remaining must be very well characterized for their safety. In addition to assessing the functions native to hepatocytes, these applications also require that no extra-hepatic functions with potentially adverse

effects have been acquired during culture or differentiation. This question will likely require high-throughput transcriptome and proteome analyses in combination with animal studies, and will ultimately require confidence in the robustness of the culture and differentiation protocols.

A final consideration that must be addressed for transplantation therapies is determining what cell type is actually best for transplantation. In other words, the terminally differentiated hepatocytes may not ultimately be the best candidates. It is indeed likely, as has been demonstrated in preliminary studies in pancreatic β-cell transplants, that a progenitor cell population, such as the bipotential hepatoblasts, may actually promote better engraftment, *in vivo* expansion, and terminal differentiation to the functional cell type. These studies may also involve priming the in vivo environment to accept and promote engraftment, proliferation, and differentiation of the transplanted cells by drug treatment or potentially by surgical manipulation prior to transplant, which may successfully prime the organ for engraftment by eliciting the injury and regeneration responses.

It is indeed an exciting time in the stem cell field as understanding and control of pluripotency and cell fate decisions are growing exponentially through collaborative research and knowledge sharing across myriad disciplines. Stem cells and their progeny are on the move toward becoming a true technology, and the next 5-10 years will be pivotal in realizing the potential impact of these cells in pharmaceutical and clinical applications.

REFERENCES

Abu-Absi, S. F., J. R. Friend, et al. (2002). "Structural polarity and functional bile canaliculi in rat hepatocyte spheroids." Exp Cell Res **274**(1): 56-67.

Abu-Absi, S. F., L. K. Hansen, et al. (2004). "Three-dimensional co-culture of hepatocytes and stellate cells." Cytotechnology **45**(3): 125-140.

Aranguren, X. L., A. Luttun, et al. (2007). "In vitro and in vivo arterial differentiation of human multipotent adult progenitor cells." Blood **109**(6): 2634-2642.

Asgari, S., M. Moslem, et al. (2011). "Differentiation and Transplantation of Human Induced Pluripotent Stem Cell-derived Hepatocyte-like Cells." Stem Cell Rev.

Auernhammer, C. J., C. Bousquet, et al. (2000). "SOCS proteins: modulators of neuroimmunoendocrine functions. Impact on corticotroph LIF signaling." Ann N Y Acad Sci **917**: 658-664.

Avilion, A. A., S. K. Nicolis, et al. (2003). "Multipotent cell lineages in early mouse development depend on SOX2 function." Genes Dev **17**(1): 126-140.

Avital, I., D. Inderbitzin, et al. (2001). "Isolation, characterization, and transplantation of bone marrow-derived hepatocyte stem cells." Biochem Biophys Res Commun **288**(1): 156-164.

Baharvand, H., S. M. Hashemi, et al. (2006). "Differentiation of human embryonic stem cells into hepatocytes in 2D and 3D culture systems in vitro." Int J Dev Biol **50**(7): 645-652.

Bakre, M. M., A. Hoi, et al. (2007). "Generation of multipotential mesendodermal progenitors from mouse embryonic stem cells via sustained Wnt pathway activation." J Biol Chem **282**(43): 31703-31712.

Barski, O. A., K. H. Gabbay, et al. (1999). "Characterization of the human aldehyde reductase gene and promoter." Genomics **60**(2): 188-198.

Barski, O. A., V. Z. Papusha, et al. (2005). "Developmental expression and function of aldehyde reductase in proximal tubules of the kidney." Am J Physiol Renal Physiol **289**(1): F200-207.

Basma, H., A. Soto-Gutierrez, et al. (2009). "Differentiation and transplantation of human embryonic stem cell-derived hepatocytes." Gastroenterology **136**(3): 990-999.

Besley, M. J. and A. K. Pavlou (2005). "Marketspace: Leading therapeutic recombinant protein sales forecast and analysis to 2010." Journal of Commercial Biotechnology **12**: 69-73.

Bodnar, M. S., J. J. Meneses, et al. (2004). "Propagation and maintenance of undifferentiated human embryonic stem cells." Stem Cells Dev **13**(3): 243-253.

Boeuf, H., C. Hauss, et al. (1997). "Leukemia inhibitory factor-dependent transcriptional activation in embryonic stem cells." J Cell Biol **138**(6): 1207-1217.

Boiani, M. and H. R. Scholer (2005). "Regulatory networks in embryo-derived pluripotent stem cells." Nat Rev Mol Cell Biol **6**(11): 872-884.

Brambrink, T., R. Foreman, et al. (2008). "Sequential expression of pluripotency markers during direct reprogramming of mouse somatic cells." Cell Stem Cell **2**(2): 151 - 159.

Bravo, P., V. Bender, et al. (1998). "Efficient in vitro vectorial transport of a fluorescent conjugated bile acid analogue by polarized hepatic hybrid WIF-B and WIF-B9 cells." Hepatology **27**(2): 576-583.

Breyer, A., N. Estharabadi, et al. (2006). "Multipotent adult progenitor cell isolation and culture procedures." Exp Hematol **34**(11): 1596-1601.

Burdon, T., C. Stracey, et al. (1999). "Suppression of SHP-2 and ERK signalling promotes self-renewal of mouse embryonic stem cells." Dev Biol **210**(1): 30-43.

Cai, J., Y. Zhao, et al. (2007). "Directed differentiation of human embryonic stem cells into functional hepatic cells." Hepatology **45**(5): 1229-1239.

Cao, D., S. T. Fan, et al. (1998). "Identification and characterization of a novel human aldose reductase-like gene." J Biol Chem **273**(19): 11429-11435.

Chang, T. T. and M. Hughes-Fulford (2009). "Monolayer and spheroid culture of human liver hepatocellular carcinoma cell line cells demonstrate distinct global gene expression patterns and functional phenotypes." Tissue Eng Part A **15**(3): 559-567.

Chase, L. G. and M. T. Firpo (2007). "Development of serum-free culture systems for human embryonic stem cells." Curr Opin Chem Biol **11**(4): 367-372.

Chen, Y. F., C. Y. Tseng, et al. (2012). "Rapid generation of mature hepatocyte-like cells from human induced pluripotent stem cells by an efficient three-step protocol." Hepatology **55**(4): 1193-1203.

Cheng, N., E. Wauthier, et al. (2008). "Mature human hepatocytes from ex vivo differentiation of alginate-encapsulated hepatoblasts." Tissue Eng Part A **14**(1): 1-7.

Chinzei, R., Y. Tanaka, et al. (2002). "Embryoid-body cells derived from a mouse embryonic stem cell line show differentiation into functional hepatocytes." Hepatology **36**(1): 22-29.

Cukierman, E., R. Pankov, et al. (2001). "Taking cell-matrix adhesions to the third dimension." Science **294**(5547): 1708-1712.

D'Amour, K. A., A. G. Bang, et al. (2006). "Production of pancreatic hormone-expressing endocrine cells from human embryonic stem cells." Nat Biotechnol **24**(11): 1392-1401.

D'Ippolito, G., S. Diabira, et al. (2004). "Marrow-isolated adult multilineage inducible (MIAMI) cells, a unique population of postnatal young and old human cells with extensive expansion and differentiation potential." J Cell Sci **117**(Pt 14): 2971-2981.

Dalgetty, D. M., C. N. Medine, et al. (2009). "Progress and future challenges in stem cell-derived liver technologies." Am J Physiol Gastrointest Liver Physiol **297**(2): G241-248.

Dasgupta, A., R. Hughey, et al. (2005). "E-cadherin synergistically induces hepatospecific phenotype and maturation of embryonic stem cells in conjunction with hepatotrophic factors." Biotechnol Bioeng **92**(3): 257-266.

Debnath, J. and J. S. Brugge (2005). "Modelling glandular epithelial cancers in three-dimensional cultures." Nat Rev Cancer **5**(9): 675-688.

Deutsch, G., J. Jung, et al. (2001). "A bipotential precursor population for pancreas and liver within the embryonic endoderm." Development **128**(6): 871-881.

Dvir-Ginzberg, M., T. Elkayam, et al. (2004). "Ultrastructural and functional investigations of adult hepatocyte spheroids during in vitro cultivation." Tissue Eng **10**(11-12): 1806-1817.

Enns, G. M. and M. T. Millan (2008). "Cell-based therapies for metabolic liver disease." Mol Genet Metab **95**(1-2): 3-10.

Evans, M. J. and M. H. Kaufman (1981). "Establishment in culture of pluripotential cells from mouse embryos." Nature **292**(5819): 154-156.

Fearon, E. R. and C. V. Dang (1999). "Cancer genetics: tumor suppressor meets oncogene." Curr Biol **9**(2): R62-65.

Fukuda, J. and K. Nakazawa (2005). "Orderly arrangement of hepatocyte spheroids on a microfabricated chip." Tissue Eng **11**(7-8): 1254-1262.

Fukuda, J., Y. Sakai, et al. (2006). "Novel hepatocyte culture system developed using microfabrication and collagen/polyethylene glycol microcontact printing." Biomaterials **27**(7): 1061-1070.

Fukumoto, S., N. Yamauchi, et al. (2005). "Overexpression of the aldo-keto reductase family protein AKR1B10 is highly correlated with smokers' non-small cell lung carcinomas." Clin Cancer Res **11**(5): 1776-1785.

Gage, F. H. (2000). "Mammalian neural stem cells." Science **287**(5457): 1433-1438.

Gilbert, S. F. (2006). Developmental Biology, Eighth Edition, Sinauer Associates, Inc.

Griffith, L. G. and M. A. Swartz (2006). "Capturing complex 3D tissue physiology in vitro." Nat Rev Mol Cell Biol **7**(3): 211-224.

Grompe, M. (2001). "Liver repopulation for the treatment of metabolic diseases." J Inherit Metab Dis **24**(2): 231-244.

Gu, J., X. Shi, et al. (2009). "Heterotypic interactions in the preservation of morphology and functionality of porcine hepatocytes by bone marrow mesenchymal stem cells in vitro." J Cell Physiol **219**(1): 100-108.

Gupta, S., C. Verfaillie, et al. (2006). "Isolation and characterization of kidney-derived stem cells." J Am Soc Nephrol **17**(11): 3028-3040.

Haegele, L., B. Ingold, et al. (2003). "Wnt signalling inhibits neural differentiation of embryonic stem cells by controlling bone morphogenetic protein expression." Mol Cell Neurosci **24**(3): 696-708.

Hanada, S., N. Kojima, et al. (2007). "Soluble Factor-Dependent In Vitro Growth and Maturation of Rat Fetal Liver Cells in a Three-Dimensional Culture System." Tissue Eng.

Hanna, J., M. Wernig, et al. (2007). "Treatment of sickle cell anemia mouse model with iPS cells generated from autologous skin." Science **318**(5858): 1920-1923.

Haouzi, D., S. Baghdiguian, et al. (2005). "Three-dimensional polarization sensitizes hepatocytes to Fas/CD95 apoptotic signalling." J Cell Sci **118**(Pt 12): 2763-2773.

Haridass, D., N. Narain, et al. (2008). "Hepatocyte transplantation: waiting for stem cells." Curr Opin Organ Transplant **13**(6): 627-632.

Hay, D. C., D. Zhao, et al. (2008). "Efficient differentiation of hepatocytes from human embryonic stem cells exhibiting markers recapitulating liver development in vivo." Stem Cells **26**(4): 894-902.

Horslen, S. P. and I. J. Fox (2004). "Hepatocyte transplantation." Transplantation **77**(10): 1481-1486.

Horslen, S. P., T. C. McCowan, et al. (2003). "Isolated hepatocyte transplantation in an infant with a severe urea cycle disorder." Pediatrics **111**(6 Pt 1): 1262-1267.

Humphrey, R. K., G. M. Beattie, et al. (2004). "Maintenance of pluripotency in human embryonic stem cells is STAT3 independent." Stem Cells **22**(4): 522-530.

Ijima, H., K. Nakazawa, et al. (1998). "Formation of a spherical multicellular aggregate (spheroid) of animal cells in the pores of polyurethane foam as a cell culture substratum and its application to a hybrid artificial liver." J Biomater Sci Polym Ed **9**(7): 765-778.

Imamura, T., L. Cui, et al. (2004). "Embryonic stem cell-derived embryoid bodies in three-dimensional culture system form hepatocyte-like cells in vitro and in vivo." Tissue Eng **10**(11-12): 1716-1724.

Ireland, L. S., D. J. Harrison, et al. (1998). "Molecular cloning, expression and catalytic activity of a human AKR7 member of the aldo-keto reductase superfamily: evidence that the major 2-carboxybenzaldehyde reductase from human liver is a homologue of rat aflatoxin B1-aldehyde reductase." Biochem J **332 (Pt 1)**: 21-34.

Jensen, J., J. Hyllner, et al. (2009). "Human embryonic stem cell technologies and drug discovery." J Cell Physiol **219**(3): 513-519.

Jiang, J., N. Kojima, et al. (2004). "Efficacy of engineered liver tissue based on poly-L-lactic acid scaffolds and fetal mouse liver cells cultured with oncostatin M, nicotinamide, and dimethyl sulfoxide." Tissue Eng **10**(9-10): 1577-1586.

Jiang, Y., D. Henderson, et al. (2003). "Neuroectodermal differentiation from mouse multipotent adult progenitor cells." Proc Natl Acad Sci U S A **100 Suppl 1**: 11854-11860.

Jiang, Y., B. N. Jahagirdar, et al. (2002). "Pluripotency of mesenchymal stem cells derived from adult marrow." Nature **418**(6893): 41-49.

Jiang, Y., B. Vaessen, et al. (2002). "Multipotent progenitor cells can be isolated from postnatal murine bone marrow, muscle, and brain." Exp Hematol **30**(8): 896-904.

Johnson, B. V., J. Rathjen, et al. (2006). "Transcriptional control of pluripotency: decisions in early development." Curr Opin Genet Dev **16**(5): 447-454.

Jung, J., M. Zheng, et al. (1999). "Initiation of mammalian liver development from endoderm by fibroblast growth factors." Science **284**(5422): 1998-2003.

Kazemnejad, S., A. Allameh, et al. (2008). "Functional hepatocyte-like cells derived from human bone marrow mesenchymal stem cells on a novel 3-dimensional biocompatible nanofibrous scaffold." Int J Artif Organs **31**(6): 500-507.

Keller, P. J., F. Pampaloni, et al. (2006). "Life sciences require the third dimension." Curr Opin Cell Biol **18**(1): 117-124.

Kelm, J. M., N. E. Timmins, et al. (2003). "Method for generation of homogeneous multicellular tumor spheroids applicable to a wide variety of cell types." Biotechnol Bioeng **83**(2): 173-180.

Khurana, S., A. K. Jaiswal, et al. (2010). "Hepatocyte nuclear factor-4alpha induces transdifferentiation of hematopoietic cells into hepatocytes." J Biol Chem **285**(7): 4725-4731.

Khurana, S. and A. Mukhopadhyay (2008). "In vitro transdifferentiation of adult hematopoietic stem cells: an alternative source of engraftable hepatocytes." J Hepatol **49**(6): 998-1007.

Kinsella, K. G. (1992). "Changes in life expectancy 1900-1990." Am J Clin Nutr **55**(6 Suppl): 1196S-1202S.

Knight, L. P., T. Primiano, et al. (1999). "cDNA cloning, expression and activity of a second human aflatoxin B1-metabolizing member of the aldo-keto reductase superfamily, AKR7A3." Carcinogenesis **20**(7): 1215-1223.

Kogler, G., S. Sensken, et al. (2004). "A new human somatic stem cell from placental cord blood with intrinsic pluripotent differentiation potential." J Exp Med **200**(2): 123-135.

Koide, N., K. Sakaguchi, et al. (1990). "Formation of multicellular spheroids composed of adult rat hepatocytes in dishes with positively charged surfaces and under other nonadherent environments." Exp Cell Res **186**(2): 227-235.

Krizkova, S., I. Fabrik, et al. (2009). "Metallothionein--a promising tool for cancer diagnostics." Bratisl Lek Listy **110**(2): 93-97.

Kucia, M., M. Halasa, et al. (2007). "Morphological and molecular characterization of novel population of CXCR4+ SSEA-4+ Oct-4+ very small embryonic-like cells purified from human cord blood: preliminary report." Leukemia **21**(2): 297-303.

Kucia, M., R. Reca, et al. (2006). "A population of very small embryonic-like (VSEL) CXCR4(+)SSEA-1(+)Oct-4+ stem cells identified in adult bone marrow." Leukemia **20**(5): 857-869.

Kyrmizi, I., P. Hatzis, et al. (2006). "Plasticity and expanding complexity of the hepatic transcription factor network during liver development." Genes Dev **20**(16): 2293-2305.

Landry, J., D. Bernier, et al. (1985). "Spheroidal aggregate culture of rat liver cells: histotypic reorganization, biomatrix deposition, and maintenance of functional activities." J Cell Biol **101**(3): 914-923.

Lazaro, C. A., E. J. Croager, et al. (2003). "Establishment, characterization, and long-term maintenance of cultures of human fetal hepatocytes." Hepatology **38**(5): 1095-1106.

Lee, W. H., P. Lukacik, et al. (2009). "Structure-activity relationships of human AKR-type oxidoreductases involved in bile acid synthesis: AKR1D1 and AKR1C4." Mol Cell Endocrinol **301**(1-2): 199-204.

Lemaigre, F. P. (2003). "Development of the biliary tract." Mech Dev **120**(1): 81-87.

Levenberg, S., N. F. Huang, et al. (2003). "Differentiation of human embryonic stem cells on three-dimensional polymer scaffolds." Proc Natl Acad Sci U S A **100**(22): 12741-12746.

Li, F., P. Liu, et al. (2010). "Hepatoblast-like progenitor cells derived from embryonic stem cells can repopulate livers of mice." Gastroenterology **139**(6): 2158-2169 e2158.

Lowe, L. A., S. Yamada, et al. (2001). "Genetic dissection of nodal function in patterning the mouse embryo." Development **128**(10): 1831-1843.

Miki, T., A. Ring, et al. (2011). "Hepatic differentiation of human embryonic stem cells is promoted by three-dimensional dynamic perfusion culture conditions." Tissue Eng Part C Methods **17**(5): 557-568.

Murphy, S. L., J. Xu, et al. (2012). "Deaths: Preliminary Data for 2010." National Vital Statistics Report **60**(4).

Nakamura, N., K. Saeki, et al. (2012). "Feeder-free and serum-free production of hepatocytes, cholangiocytes, and their proliferating progenitors from human pluripotent stem cells: application to liver-specific functional and cytotoxic assays." Cell Reprogram **14**(2): 171-185.

Navarro-Alvarez, N., A. Soto-Gutierrez, et al. (2009). "Stem cell research and therapy for liver disease." Curr Stem Cell Res Ther **4**(2): 141-146.

Ng, E. S., R. P. Davis, et al. (2005). "Forced aggregation of defined numbers of human embryonic stem cells into embryoid bodies fosters robust, reproducible hematopoietic differentiation." Blood **106**(5): 1601-1603.

Nichols, J., B. Zevnik, et al. (1998). "Formation of pluripotent stem cells in the mammalian embryo depends on the POU transcription factor Oct4." Cell **95**(3): 379-391.

Ogawa, S. and S. Miyagawa (2009). "Potentials of regenerative medicine for liver disease." Surg Today **39**(12): 1019-1025.

Ogawa, S., Y. Tagawa, et al. (2005). "Crucial roles of mesodermal cell lineages in a murine embryonic stem cell-derived in vitro liver organogenesis system." Stem Cells **23**(7): 903-913.

Okura, H., H. Komoda, et al. (2009). "Properties of Hepatocyte-like Cell Clusters Derived from human adipose tissue-derived mesenchymal stem cells." Tissue Eng Part C Methods.

Olsen, S. K. and R. S. Brown, Jr. (2008). "Live donor liver transplantation: current status." Curr Gastroenterol Rep **10**(1): 36-42.

Ong, S. M., Z. Zhao, et al. (2009). "Engineering a scaffold-free 3D tumor model for in vitro drug penetration studies." Biomaterials.

Ong, S. Y., H. Dai, et al. (2006). "Inducing hepatic differentiation of human mesenchymal stem cells in pellet culture." Biomaterials **27**(22): 4087-4097.

Oude Elferink, R. P., D. K. Meijer, et al. (1995). "Hepatobiliary secretion of organic compounds; molecular mechanisms of membrane transport." Biochim Biophys Acta **1241**(2): 215-268.

Pampaloni, F., E. G. Reynaud, et al. (2007). "The third dimension bridges the gap between cell culture and live tissue." Nat Rev Mol Cell Biol **8**(10): 839-845.

Peignon, G., S. Thenet, et al. (2006). "E-cadherin-dependent transcriptional control of apolipoprotein A-IV gene expression in intestinal epithelial cells: a role for the hepatic nuclear factor 4." J Biol Chem **281**(6): 3560-3568.

Penning, T. M., Y. Jin, et al. (2004). "Structure-function of human 3 alpha-hydroxysteroid dehydrogenases: genes and proteins." Mol Cell Endocrinol **215**(1-2): 63-72.

Peshwa, M. V., F. J. Wu, et al. (1996). "Mechanistics of formation and ultrastructural evaluation of hepatocyte spheroids." In Vitro Cell Dev Biol Anim **32**(4): 197-203.

Pevny, L. H. and R. Lovell-Badge (1997). "Sox genes find their feet." Curr Opin Genet Dev **7**(3): 338-344.

Reubinoff, B. E., M. F. Pera, et al. (2000). "Embryonic stem cell lines from human blastocysts: somatic differentiation in vitro." Nat Biotechnol **18**(4): 399-404.

Reya, T., S. J. Morrison, et al. (2001). "Stem cells, cancer, and cancer stem cells." Nature **414**(6859): 105-111.

Reyes, M., A. Dudek, et al. (2002). "Origin of endothelial progenitors in human postnatal bone marrow." J Clin Invest **109**(3): 337-346.

Rivera-Perez, J. A. and T. Magnuson (2005). "Primitive streak formation in mice is preceded by localized activation of Brachyury and Wnt3." Dev Biol **288**(2): 363-371.

Roelandt, P., K. A. Pauwelyn, et al. (2010). "Human embryonic and rat adult stem cells with primitive endoderm-like phenotype can be fated to definitive endoderm, and finally hepatocyte-like cells." PLoS One **5**(8): e12101.

Ross, J. J., Z. Hong, et al. (2006). "Cytokine-induced differentiation of multipotent adult progenitor cells into functional smooth muscle cells." J Clin Invest **116**(12): 3139-3149.

Rossi, J. M., N. R. Dunn, et al. (2001). "Distinct mesodermal signals, including BMPs from the septum transversum mesenchyme, are required in combination for hepatogenesis from the endoderm." Genes Dev **15**(15): 1998-2009.

Sainz, B., Jr., V. TenCate, et al. (2009). "Three-dimensional Huh7 cell culture system for the study of Hepatitis C virus infection." Virol J **6**: 103.

Salabei, J. K., X. P. Li, et al. (2011). "Functional expression of novel human and murine AKR1B genes." Chem Biol Interact **191**(1-3): 177-184.

Sancho-Bru, P., M. Najimi, et al. (2009). "Stem and progenitor cells for liver repopulation: can we standardise the process from bench to bedside?" Gut **58**(4): 594-603.

Santoro, A., E. Mancini, et al. (2007). "Liver support systems." Contrib Nephrol **156**: 396-404.

Sartipy, P., P. Bjorquist, et al. (2007). "The application of human embryonic stem cell technologies to drug discovery." Drug Discov Today **12**(17-18): 688-699.

Sato, M. and M. Kondoh (2002). "Recent studies on metallothionein: protection against toxicity of heavy metals and oxygen free radicals." Tohoku J Exp Med **196**(1): 9-22.

Sato, N., L. Meijer, et al. (2004). "Maintenance of pluripotency in human and mouse embryonic stem cells through activation of Wnt signaling by a pharmacological GSK-3-specific inhibitor." Nat Med **10**(1): 55-63.

Sato, N., I. M. Sanjuan, et al. (2003). "Molecular signature of human embryonic stem cells and its comparison with the mouse." Dev Biol **260**(2): 404-413.

Schena, M., D. Shalon, et al. (1995). "Quantitative monitoring of gene expression patterns with a complementary DNA microarray." Science **270**(5235): 467-470.

Schwartz, R. E., J. L. Linehan, et al. (2005). "Defined conditions for development of functional hepatic cells from human embryonic stem cells." Stem Cells Dev **14**(6): 643-655.

Schwartz, R. E., M. Reyes, et al. (2002). "Multipotent adult progenitor cells from bone marrow differentiate into functional hepatocyte-like cells." J Clin Invest **109**(10): 1291-1302.

Seaman, D. S. (2001). "Adult living donor liver transplantation: current status." J Clin Gastroenterol **33**(2): 97-106.

Seglen, P. O. (1976). "Preparation of isolated rat liver cells." Methods Cell Biol **13**: 29-83.

Sekhon, S. S., X. Tan, et al. (2004). "Fibroblast growth factor enriches the embryonic liver cultures for hepatic progenitors." Am J Pathol **164**(6): 2229-2240.

Sekiya, S. and A. Suzuki (2011). "Direct conversion of mouse fibroblasts to hepatocyte-like cells by defined factors." Nature **475**(7356): 390-393.

Semler, E. J., A. Dasgupta, et al. (2005). "Cytomimetic engineering of hepatocyte morphogenesis and function by substrate-based presentation of acellular E-cadherin." Tissue Eng **11**(5-6): 734-750.

Serls, A. E., S. Doherty, et al. (2005). "Different thresholds of fibroblast growth factors pattern the ventral foregut into liver and lung." Development **132**(1): 35-47.

Shen, C. N., M. E. Horb, et al. (2003). "Transdifferentiation of pancreas to liver." Mech Dev **120**(1): 107-116.

Shi, X. L., Y. Zhang, et al. (2009). "Coencapsulation of hepatocytes with bone marrow mesenchymal stem cells improves hepatocyte-specific functions." Transplantation **88**(10): 1178-1185.

Si-Tayeb, K., F. K. Noto, et al. (2009). "Highly efficient generation of human hepatocyte-like cells from induced pluripotent stem cells." Hepatology.

Smith, A. G. (2001). "Embryo-derived stem cells: of mice and men." Annu Rev Cell Dev Biol **17**: 435-462.

Snykers, S., J. De Kock, et al. (2009). "In vitro differentiation of embryonic and adult stem cells into hepatocytes: state of the art." Stem Cells **27**(3): 577-605.

Subramanian, K., M. Geraerts, et al. (2010). "Isolation procedure and characterization of multipotent adult progenitor cells from rat bone marrow." Methods Mol Biol **636**: 55-78.

Subramanian, K., Y. Park, et al. (2011). "Scalable Expansion of Multipotent Adult Progenitor Cells as Three-Dimensional Cell Aggregates." Biotechnol Bioeng **108**(2): 364-375.

Subramanian, K., Y. Park, et al. (In Press). "Scalable Expansion of Multipotent Adult Progenitor Cells as Three-Dimensional Cell Aggregates." Biotechnol Bioeng.

Suzuki, A., Y. Zheng, et al. (2000). "Flow-cytometric separation and enrichment of hepatic progenitor cells in the developing mouse liver." Hepatology **32**(6): 1230-1239.

Takahashi, K., K. Tanabe, et al. (2007). "Induction of pluripotent stem cells from adult human fibroblasts by defined factors." Cell **131**(5): 861-872.

Takahashi, K. and S. Yamanaka (2006). "Induction of pluripotent stem cells from mouse embryonic and adult fibroblast cultures by defined factors." Cell **126**(4): 663-676.

Takayama, K., M. Inamura, et al. (2012). "Generation of metabolically functioning hepatocytes from human pluripotent stem cells by FOXA2 and HNF1alpha transduction." J Hepatol.

Tam, P. P., D. A. Loebel, et al. (2006). "Building the mouse gastrula: signals, asymmetry and lineages." Curr Opin Genet Dev **16**(4): 419-425.

Tanimizu, N., A. Miyajima, et al. (2007). "Liver progenitor cells develop cholangiocyte-type epithelial polarity in three-dimensional culture." Mol Biol Cell **18**(4): 1472-1479.

Thomson, J. A., J. Itskovitz-Eldor, et al. (1998). "Embryonic stem cell lines derived from human blastocysts." Science **282**(5391): 1145-1147.

Toh, Y. C., T. C. Lim, et al. (2009). "A microfluidic 3D hepatocyte chip for drug toxicity testing." Lab Chip **9**(14): 2026-2035.

Tsuchiya, A., T. Heike, et al. (2005). "Long-term extensive expansion of mouse hepatic stem/progenitor cells in a novel serum-free culture system." Gastroenterology **128**(7): 2089-2104.

Tzanakakis, E. S., D. J. Waxman, et al. (2002). "Long-term enhancement of cytochrome P450 2B1/2 expression in rat hepatocyte spheroids through adenovirus-mediated gene transfer." Cell Biol Toxicol **18**(1): 13-27.

Ulloa-Montoya, F., B. L. Kidder, et al. (2007). "Comparative transcriptome analysis of embryonic and adult stem cells with extended and limited differentiation capacity." Genome Biol **8**(8): R163.

Ulloa-Montoya, F., C. M. Verfaillie, et al. (2005). "Culture systems for pluripotent stem cells." J Biosci Bioeng **100**(1): 12-27.

Weissman, I. L. (2000). "Translating stem and progenitor cell biology to the clinic: barriers and opportunities." Science **287**(5457): 1442-1446.

Wells, J. M. and D. A. Melton (1999). "Vertebrate endoderm development." Annu Rev Cell Dev Biol **15**: 393-410.

Wobus, A. M., H. Holzhausen, et al. (1984). "Characterization of a pluripotent stem cell line derived from a mouse embryo." Exp Cell Res **152**(1): 212-219.

World Health Organization, W. (2001). "Smallpox." Fact Sheets Retrieved August 2012.

Wu, F. J., J. R. Friend, et al. (1999). "Enhanced cytochrome P450 IA1 activity of self-assembled rat hepatocyte spheroids." Cell Transplant **8**(3): 233-246.

Yabe-Nishimura, C. (1998). "Aldose reductase in glucose toxicity: a potential target for the prevention of diabetic complications." Pharmacol Rev **50**(1): 21-33.

Yamada, K. M. and E. Cukierman (2007). "Modeling tissue morphogenesis and cancer in 3D." Cell **130**(4): 601-610.

Ying, Q. L., J. Nichols, et al. (2003). "BMP induction of Id proteins suppresses differentiation and sustains embryonic stem cell self-renewal in collaboration with STAT3." Cell **115**(3): 281-292.

Yoshitake, H., M. Takahashi, et al. (2007). "Aldo-keto reductase family 1, member B10 in uterine carcinomas: a potential risk factor of recurrence after surgical therapy in cervical cancer." Int J Gynecol Cancer **17**(6): 1300-1306.

Yu, J., M. A. Vodyanik, et al. (2007). "Induced pluripotent stem cell lines derived from human somatic cells." Science **318**(5858): 1917-1920.

Yuan, H., N. Corbi, et al. (1995). "Developmental-specific activity of the FGF-4 enhancer requires the synergistic action of Sox2 and Oct-3." Genes Dev **9**(21): 2635-2645.

Zaret, K. S. and M. Grompe (2008). "Generation and regeneration of cells of the liver and pancreas." Science **322**(5907): 1490-1494.

Zhou, X., H. Sasaki, et al. (1993). "Nodal is a novel TGF-beta-like gene expressed in the mouse node during gastrulation." Nature **361**(6412): 543-547.

Appendix A: Tables of Microarray Data (Processed)

Table 1: Normalized intensities and alternate names of hepatocyte nuclear factors

Symbol	Alternate Symbol	Normalized Intensities				log(D32/D20)
		D0	D20	D32	AL	
HNF3A	FOXA1	103	2363	1577	1138	-0.58
HNF3B	FOXA2	130	513	545	884	0.09
HNF3G	FOXA3	253	547	805	912	0.56
HNF1α		105	193	232	242	0.27
HNF1β		98	317	312	245	-0.02
HNF4G		96	130	164	224	0.34
HNF6A	ONECUT1	126	134	181	208	0.44
HNF6B	ONECUT2	101	122	130	261	0.09

Table 2: Normalized intensities of Cytochrome P450 family gene expression

SYMBOL	Normalized Intensities				log(D32/D20)
	D0	D20	D32	AL	
CYP1A1	97	162	936	136	2.53
CYP1A2	88	103	110	1806	0.10
CYP1B1	275	575	466	303	-0.30
CYP2A6	82	100	121	1612	0.28
CYP2A7	99	113	125	635	0.14
CYP2B6	97	113	124	237	0.13
CYP2B7P1	92	111	120	208	0.11
CYP2C18	108	178	644	2101	1.86
CYP2C19	107	141	301	165	1.10
CYP2C8	100	194	207	11959	0.09
CYP2C9	93	153	293	2849	0.94
CYP2D6	102	125	132	1084	0.08
CYP2D7P1	108	131	138	659	0.07
CYP2E1	108	124	134	34336	0.12
CYP2J2	102	215	889	2413	2.05
CYP2R1	216	270	206	215	-0.39
CYP2S1	513	129	232	144	0.84
CYP2U1	144	157	153	189	-0.04
CYP3A4	86	107	119	3799	0.16
CYP3A5	110	395	1000	1099	1.34
CYP3A7	99	1355	4731	440	1.80
CYP4A11	91	120	1239	8660	3.37
CYP4F11	94	111	125	690	0.17
CYP4F12	94	104	105	587	0.02
CYP4F2	108	126	149	624	0.24
CYP4F22	85	97	107	429	0.14
CYP4F3	108	129	136	957	0.07
CYP4V2	111	150	308	2183	1.04
CYP8B1	88	481	675	7487	0.49
CYP11A1	153	176	173	203	-0.02

CYP20A1	189	202	238	271	0.23
CYP21A2	97	113	126	305	0.16
CYP26A1	1143	151	129	155	-0.23
CYP26B1	124	141	149	179	0.07
CYP27A1	212	426	1170	2844	1.46
CYP27C1	126	141	161	185	0.19
CYP39A1	104	125	138	224	0.15
CYP46A1	103	156	144	164	-0.12
CYP51A1	245	247	503	385	1.03

Table 3: Normalized intensities of non-CYP Phase I enzyme gene expression

Symbol	Phase I Function	Normalized Intensities				log(D32/D20)
		D0	D20	D32	AL	
ADH1A	Alcohol Dehydrogenase	109	238	3476	17336	3.87
ADH1B	Alcohol Dehydrogenase	97	125	171	2136	0.45
ADH1C	Alcohol Dehydrogenase	108	125	129	2767	0.04
ADH4	Alcohol Dehydrogenase	96	123	349	3744	1.51
ADH5	Alcohol Dehydrogenase	445	307	299	212	-0.04
ADH6	Alcohol Dehydrogenase	95	140	250	465	0.84
ADH7	Alcohol Dehydrogenase	121	131	137	167	0.07
ALDH16A1	Aldehyde Dehydrongenase	274	195	242	352	0.31
ALDH18A1	Aldehyde Dehydrongenase	639	670	441	625	-0.60
ALDH1A1	Aldehyde Dehydrongenase	104	757	11685	2233	3.95
ALDH1A2	Aldehyde Dehydrongenase	118	154	138	168	-0.16
ALDH1A3	Aldehyde Dehydrongenase	162	369	306	168	-0.27
ALDH1B1	Aldehyde Dehydrongenase	298	182	250	569	0.46
ALDH1L1	Aldehyde Dehydrongenase	111	302	614	2435	1.02
ALDH2	Aldehyde Dehydrongenase	307	942	1674	6044	0.83

ALDH3A2	Aldehyde Dehydrongenase	562	560	1207	814	1.11
ALDH3B1	Aldehyde Dehydrongenase	95	123	164	154	0.42
ALDH4A1	Aldehyde Dehydrongenase	154	175	268	1420	0.62
ALDH5A1	Aldehyde Dehydrongenase	133	254	260	356	0.04
ALDH6A1	Aldehyde Dehydrongenase	301	1406	983	3033	-0.52
ALDH7A1	Aldehyde Dehydrongenase	2016	1423	1168	1750	-0.28
ALDH8A1	Aldehyde Dehydrongenase	106	162	363	981	1.16
ALDH9A1	Aldehyde Dehydrongenase	3553	2448	3011	5349	0.30
FMO1	Flavin-Containing Monoxygenase	112	172	321	172	0.90
FMO2	Flavin-Containing Monoxygenase	120	160	152	230	-0.07
FMO3	Flavin-Containing Monoxygenase	99	138	135	1377	-0.03
FMO4	Flavin-Containing Monoxygenase	101	170	161	420	-0.07
FMO5	Flavin-Containing Monoxygenase	103	1597	1648	645	0.05
MAOA	Monoamine Oxidase	219	1799	2338	2796	0.38
MAOB	Monoamine Oxidase	102	310	710	845	1.20

Table 4: Normalized intensities of UGT family gene expression

SYMBOL	Normalized Intensities				log(D32/D20)
	D0	D20	D32	AL	
UGT1A1	90	105	251	548	1.26
UGT1A3	127	162	196	278	0.28
UGT1A4	107	126	142	417	0.17
UGT1A6	94	110	185	242	0.75
UGT1A7	114	145	212	207	0.55
UGT1A9	118	132	221	202	0.75
UGT1A10	103	127	212	202	0.74
UGT2A3	111	387	1418	181	1.87
UGT2B4	102	159	1578	1822	3.31
UGT2B7	102	1042	3661	6580	1.81
UGT2B10	86	259	1293	1572	2.32
UGT2B11	109	810	2290	2735	1.50
UGT2B15	94	109	286	211	1.40
UGT2B17	104	162	982	1286	2.60
UGT2B28	87	193	220	227	0.19
UGT3A1	110	158	148	244	-0.09
UGT3A2	190	170	118	132	-0.53
UGT8	117	145	177	151	0.29

Table 5: Normalized intensities of genes expressed 4-fold or more higher in D32 sample as compared to D20 sample

Symbol	Normalized Intensities				log(D32/D20)
	D0	D20	D32	AL	
MT1G	1062	146	25048	16865	7.42
AKR1B10	88	105	9048	219	6.43
MT1H	393	118	9158	2100	6.28
MT1A	5133	269	19886	30731	6.21
MT2A	3838	256	16309	25048	5.99
MT1X	4819	219	11543	25600	5.72
MT1E	2373	210	9292	5924	5.47
MT1F	2161	222	6821	2507	4.94
SAA4	90	129	3702	24606	4.85
MTE	680	115	3119	3436	4.77
AKR1C4	122	338	7270	4199	4.43
AKR1B15	92	103	2118	149	4.36
MT1M	338	109	1912	6135	4.13
TFF1	86	105	1681	128	4.00
C20orf127	516	142	2241	1288	3.98
S100P	88	203	3187	146	3.97
ALDH1A1	104	757	11685	2233	3.95
HAMP	119	208	3168	14775	3.93
APCS	88	103	1527	16689	3.89
ADH1A	109	238	3476	17336	3.87
CTSE	112	140	2018	166	3.85
AKR1C2	111	181	2291	2130	3.66
AADAC	110	256	3024	1772	3.56
TSPAN8	111	149	1759	343	3.56
CCL20	99	222	2544	169	3.52
SPP1	1066	186	2087	405	3.49
BAAT	88	289	3113	5294	3.43
ORM1	107	1465	15484	26643	3.40

ARG1	106	193	2035	8930	3.40
AFM	87	344	3565	3574	3.37
CYP4A11	91	120	1239	8660	3.37
LOC644844	116	147	1512	168	3.36
GATM	140	480	4830	2613	3.33
UGT2B4	102	159	1578	1822	3.31
APOC2	119	596	5915	11479	3.31
HKDC1	107	337	3091	178	3.20
CDH17	110	162	1422	172	3.13
GCNT3	83	130	1120	124	3.11
AKR1C3	213	621	5043	9721	3.02
TFF2	104	168	1318	167	2.97
PEG10	261	295	2293	157	2.96
IL32	149	232	1758	3846	2.92
UBD	113	326	2462	194	2.91
CIDEC	99	162	1178	252	2.86
FBP1	133	283	1971	7305	2.80
ORM2	103	610	4165	32854	2.77
ANXA10	110	157	1057	733	2.75
PTGR1	801	1932	12143	2744	2.65
NQO1	409	373	2273	242	2.61
UGT2B17	104	162	982	1286	2.60
VSIG1	116	169	1017	152	2.59
BHMT	122	403	2354	3179	2.55
INHBE	169	237	1378	2638	2.54
HMGCS2	91	2054	11903	3461	2.53
GAL	2193	105	608	131	2.53
CYP1A1	97	162	936	136	2.53
OKL38	112	205	1147	1123	2.49
NUPR1	110	155	849	823	2.46
IGFBP1	109	177	967	1528	2.45
GPX2	111	216	1177	10816	2.45
LYZ	98	120	648	322	2.44
LOC441019	184	122	651	1374	2.41

A2M	87	899	4790	9330	2.41
ABCC2	94	172	913	626	2.41
SQSTM1	1365	2111	11127	4823	2.40
ALDOB	97	1522	8010	18888	2.40
SERPINA3	109	2722	14280	27163	2.39
LGALS4	89	150	772	486	2.37
GC	96	4304	21939	29342	2.35
LOC728811	106	445	2222	4595	2.32
UGT2B10	86	259	1293	1572	2.32
CA2	240	936	4555	1577	2.28
GBP2	96	145	703	627	2.28
TXNIP	856	153	740	3488	2.28
TXNRD1	601	368	1755	568	2.26
LCT	99	115	522	151	2.18
ISG15	400	339	1521	318	2.17
RNF113A	289	447	2001	464	2.16
SRXN1	370	358	1580	904	2.14
F12	251	248	1093	5561	2.14
LOC653879	121	280	1225	7966	2.13
OTC	107	321	1393	947	2.12
RENBP	221	205	886	290	2.11
SERPINA6	86	141	610	522	2.11
SLC40A1	113	333	1427	1979	2.10
SULT2A1	108	364	1560	5430	2.10
FTH1	654	678	2880	565	2.09
MIR1974	893	3025	12824	695	2.08
MT1B	93	108	458	138	2.08
SLC2A2	86	117	489	2385	2.07
HABP2	83	539	2242	2429	2.06
HIST1H1C	304	626	2594	1049	2.05
CYP2J2	102	215	889	2413	2.05
FAM65B	157	216	891	189	2.05
IDI1	755	495	2033	625	2.04
MOCOS	157	141	575	965	2.02

SDCBP2	100	157	636	170	2.01
LBP	101	528	2131	20302	2.01
LOC729009	1189	933	3754	1283	2.01
FGL1	116	522	2083	10157	2.00

Table 6: Normalized intensities of genes expressed 4-fold or more higher in D20 sample as compared to D32 sample

Symbol	Normalized Intensities				log(D32/D20)
	D0	D20	D32	AL	
SLC2A3	15118	11819	709	351	-4.06
NPPB	230	2956	234	149	-3.66
LIN28	5817	1264	112	132	-3.50
IGDCC3	498	1467	150	131	-3.29
SLN	105	1934	223	166	-3.11
IRX3	395	1308	178	278	-2.88
GABRP	111	1768	248	181	-2.83
SCGB2A1	91	4301	613	147	-2.81
CRABP2	1422	1482	234	208	-2.66
CRABP1	1632	2856	462	168	-2.63
CDH3	362	814	140	142	-2.53
SLC2A1	5025	5153	973	219	-2.40
HAND1	91	3118	595	138	-2.39
VTCN1	93	857	166	139	-2.37
SNORA12	158	1130	230	297	-2.29
LOC391045	1009	747	155	159	-2.27
DEFB1	107	1659	361	3691	-2.20
MDK	1029	1134	252	145	-2.17
IGFBP5	353	3553	794	2070	-2.16
WNT3A	88	755	169	135	-2.16
H19	115	19247	4338	1309	-2.15
FRZB	233	765	176	160	-2.12
MYLIP	427	1329	308	233	-2.11
LEPREL1	1458	1603	373	219	-2.10
MYCN	954	654	157	170	-2.06
LCN15	134	1291	313	149	-2.04
FSTL1	1104	1998	485	318	-2.04
LGI4	96	781	191	130	-2.03
PXDN	1520	1437	353	249	-2.03

DSCR6	217	1017	250	139	-2.02
IGFBP3	133	1412	348	1761	-2.02
CDH11	125	732	181	148	-2.02
LOX	121	1906	476	136	-2.00